Hans-Otto Carmesin

The Electroweak Interaction Explained by and Derived from Gravity and Relativity

Book, Book chapter as: published version (Version of Record)

DOI of this document*(secondary publication): https://doi.org/10.26092/elib/2659

Publication date of this document: 11/01/2024

* for better findability or for reliable citation

Recommended Citation (primary publication/Version of Record) incl. DOI:

The Electroweak Interaction Explained by and Derived from Gravity and Relativity

This text has also been published in the form of a printed book and is available in book trading companies or book stores since March 16^{th} 2022.

author: Hans-Otto Carmesin

title: The Electroweak Interaction Explained by and Derived from Gravity and Relativity

ISBN: 978-3-96831-032-9

ISSN: 2629 - 1525

Please cite this text as follows:

Carmesin, Hans-Otto (March 16^{th} 2022): The Electroweak Interaction Explained by and Derived from Gravity and Relativity. Verlag Dr. Köster, Berlin.

Berlin: Verlag Dr. Köster

Book Series: Universe: Unified from Microcosm to Macrocosm, Volume 8

Hans-Otto Carmesin

b

Electromagnetic interactions are omnipresent in everyday life. These are part of the electroweak interactions, including the Higgs mechanism. However, the nature and microscopic structure thereof were a mystery. That mystery is solved in this book.

We derive the observed charges and masses of the electroweak interaction from the equivalence principles, gravity and relativity, by analyzing the vacuum.

We derive and clarify the origin of electroweak interactions:

• Vacuum forming since the Big Bang constitutes space, time and cosmic phase transitions with a large scale energy spectrum.

• That spectrum causes electroweak charges and masses.

• Thereby, two-dimensional charge space forms.

• Hereby, the electric charge, the weak angle, a non-electric charge, a hypercharge, an isospin charge and isospin form.

• Electroweak masses originate from transitions at the large scale spectrum.

Using the local principles of the formation of vacuum, we derive general relativity and results beyond: the density of vacuum, quantum physics, cosmic phase transitions as well as the electroweak interactions, charges and masses. Our results are in precise accordance with observation, whereby we do not execute any fit.

Invited to discover the nature of electromagnetic and weak interactions are classes from grade 10 or higher, courses, research clubs, enthusiasts, observers, experimentalists, mathematicians, natural scientists, researchers ...

c

Physics Archive, Physik Archive, Verlag Dr. Köster, Berlin

PD Dr. Hans-Otto Carmesin (March 16 2022): The Electroweak Interaction Explained by and Derived from Gravity and Relativity; ISBN 978-3-96831-032-9

PD Dr. Hans-Otto Carmesin (February 11 2022): Quantum Physics Explained by Gravity and Relativity; ISBN 978-3-96831-028-2

PD Dr. Hans-Otto Carmesin (October 2021). The Elementary Charge Explained by Quantum Gravity; ISBN 978-3-86831-023-7

Prof. Dr. Peter Möller (2021): Warum es Leben im Universum gibt; ISBN 978-3-96831-019-0

PD Dr. Hans-Otto Carmesin (August 2021): Cosmological and Elementary Particles Explained by Quantum Gravity; ISBN 978-3-96831-018-3

PD Dr. Hans-Otto Carmesin (March 2021): Quanta of Spacetime Explain Observations, Dark Energy, Graviton and Nonlocality; ISBN 978-3-96831-008-4

PD Dr. Hans-Otto Carmesin (September 2020): The Universe Developing from Zero-Point Energy - Discovered by Making Photos, Experiments and Calculations; ISBN 978-3-89574-993-3

PD Dr. Hans-Otto Carmesin (March 2020): Wir entdecken die Geschichte des Universums mit eigenen Fotos und Experimenten; ISBN 978-3-89574-973-5

Prof. Dr. Peter Möller (2020): Corona - Zahlen richtig verstehen; ISBN 978-3-96831-005-3

Dr. Gerold O. Schellstede (2020): Über nichtlineare Effekte in den Elektrodynamiken der Plebanskiklasse; ISBN S78-3-89574-968-1

PD Dr. Hans-Otto Carmesin (2019): Die Grundschwingungen des Universums - The Cosmic Unification; ISBN 978-3-89574-961-2

Prof. Dr. Peter Möller (2010): Geheimnisse des Universums - Relativitätstheorie, Quantenmechanik und schwarze Löcher; ISBN 978-3-89574-959-9

PD Dr. Hans-Otto Carmesin (November 2018): Entstehung der Raumzeit durch Quantengravitätion - Theory for the Emergence of Space, Dark Matter, Dark Energy and Space-Time; ISBN 978-3-89574-951-3

PD Dr. Hans-Otto Carmesin (July 2018): Entstehung dunkler Energie durch Quantengravitation - Universal Model for Dynamics of Space, Dark Matter and Dark Energy; ISBN 978-3-89574-944-5

PD Dr. Hans-Otto Carmesin (May 2018): Entstehung dunkler Materie durch Gravitation - Model for the Dynamics of Space and the Emergence of Dark Matter; ISBN 978-3-89574-939-1

PD Dr. Hans-Otto Carmesin (2017): Vom Big Bang bis heute mit Gravitation - Model for the Dynamics of Space; ISBN 978-3-89574-899-8 d

The Electroweak Interaction Explained by and Derived from Gravity and Relativity

Berlin: Verlag Dr. Köster

Book Series: Universe: Unified from Microcosm to Macrocosm, Volume 8

Hans-Otto Carmesin

March 23, 2022

Contents

Chapter 1

Introduction

1.1 Great concepts of the microcosm

Physical theories are based on great fundamental concepts of the microcosm.

1.1.1 Atoms

Leukippos (fifth century BC) and his student Democritos (460-370 BC) proposed that objects are constituted by smallest indivisible particles, see e.g. Tsoucalas et al. (2013), Oldershaw (1998). They proposed an essential argument: These particles constitute the phase gas, the phase fluid and the phase solid including the corresponding phase transitions. Dalton (1808) established the modern concept of the atom, Fig. (1.1). However, an atom is not indivisible, as it consists of a nucleus and one or more electrons, see e.g. Millikan (1911).

1.1.2 Elementary particles

A nucleus consists of nucleons, these are protons or neutrons, see e.g. Rutherford (1911). Moreover, a nucleon consists of quarks, see e.g. Gell-Mann (1964). Today, electrons and quarks are regarded as elementary particles, many other elementary particles have been discovered, and these are described by the **standard model of elementary particles, SMEP**, see e.g.

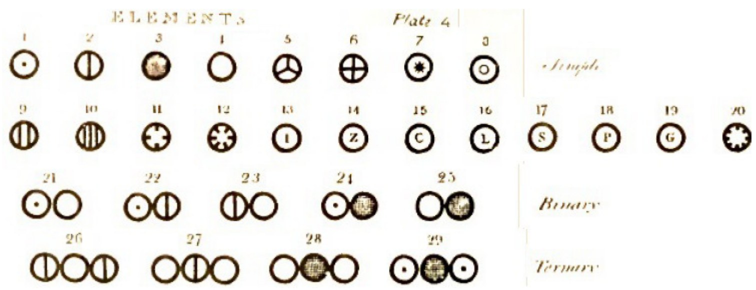

Figure 1.1: Dalton (1808) discovered the molecules and their constituents, the atoms. For instance, one molecule of carbon monoxide (25) consists of one atom of carbon (3) and one atom of oxygen (4), whereas one molecule of carbon dioxide (28) consists of one atom of carbon (3) and two atoms of oxygen (4).

Griffiths (2008), Tanabashi et al. (2018), Zyla (2020). However, the SMEP requires many parameters that have been determined by observation only. So the explanation and derivation of these parameters is an open problem of the SMEP, see (Zyla, 2020, p. 507, line 37-41).

1.1.3 Elementary interactions

The elementary particles interact with each other by elementary interactions. Hereby, the electromagnetic interaction, the weak interaction and the strong interaction are especially effective.

1.1.3.1 The essential source of electromagnetism

Coulomb (1785) discovered the law of electric force, it shows that the electric charge is the essential source of electromagnetism. Oersted (1820) discovered electromagnetism. Faraday (1852) introduced the concept of fields that transfer that force from one location to another, moreover he discovered electromagnetic induction.

Maxwell (1865) unified the results about electromagnetic fields, and using these, he derived the concept of electromagnetic waves. Millikan (1911) measured the essential quantum of electricity: the **elementary charge** e. That charge essentially corresponds to the coupling constant of electrodynamics. Indeed, Feynman (1985) wrote that the corresponding **coupling constant of electrodynamics** *'... has been a mystery ever since it was discovered ...'*. With our theory, the elementary charge is now derived and explained, see Carmesin (2021f).

1.1.4 Electroweak unification

The electromagnetic and weak interaction have been unified. So the **standard model of the electroweak interaction, SMEWI**, has been introduced, Pich (2007). However, the SMEWI requires parameters such as the elementary electric charge $\tilde{e}$, the couplings g and g' and the weak angle Θ[1]. So the explanation and derivation of these parameters is an open problem of the SMEWI, see (Zyla, 2020, p. 507, line 37-41).

1.1.5 Quantum physics

Planck (1900) discovered the quantization of objects in nature, introduced quantum physics, **QP**, including the universal constant h. Quantum physics is essential for the SMEP and SMEWI. However, Feynman (1967) wrote *'I think I can safely say that no one understands quantum mechanics'*. Accordingly, a clarification is necessary.

1.2 Great cosmic concepts

Physical theories are based on great fundamental cosmic concepts, describing the microcosm as well as the macrocosm.

1.2.1 Heavenly objects move according to gravity

In the geocentric concept, Earth formed the center, and nearby, there were some heavenly bodies. Aristarchos discovered the

[1]Coupling constants, such as g and g', are often named couplings, see e.g. Weinberg (1996), Pich (2007), Griffiths (2008), Zyla (2020).

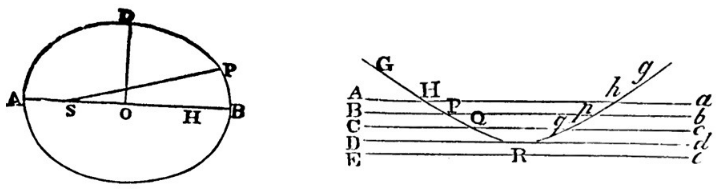

Figure 1.2: Newton (1686) discovered the $1/r^2$-law of gravity. With it, he derived elliptic and hyperbolic motions of planets, moons and comets.

heliocentric concept, described by Archimedes (287-212 BC), see e.g. (Archimedes, 1897, Chap. The Sand-Reckoner). In the heliocentric concept, there was a very huge space. In that space, the planets move around the sun, and the stars are very far away. Using that concept, Brahe (1588) and Kepler (1627) developed the basic observation and analysis (Kepler (1619)) of gravity, while Newton (1686) developed the law of gravity including the universal constant G, measured by Cavendish (1798), see also Carmesin et al. (2021) and Fig. (1.2). While Newton combined his theory of gravity and mechanics with assumptions about space and time, see e.g. Carmesin (2022), Gauss (1809) isolated the essential mechanism of the gravitational source providing an $1/r^2$-law of gravity. So he introduced **Gaussian gravity, GG**, see section (2.4).

1.2.2 Equivalence principle

Galileo (1638) analyzed gravity of falling balls, Fig. (1.3). Thereby, he discovered that two bodies fall equally fast, if friction can be neglected, see section (2.4). Accordingly, the two bodies exhibit the same acceleration $\vec{a} = d\vec{v}/dt$, which is equal to the gravitational field G^*. This example of a motion turns out to be prototypical for a wide class of motions in the universe, and there is a set of **principles of free fall, PFF**, see chapter (2) or Carmesin (2022).

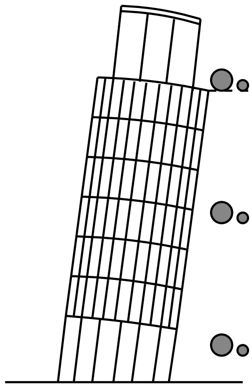

Figure 1.3: Galileo analyzed experiments with different falling objects at the tower in Pisa, see Galileo (1638), Schlichting (1999). If two bodies with different masses are started at the top at the same time, then they arrive at the same time in the middle and near the bottom. This fact holds in the ideal case of zero friction.

1.2.3 Space and time evolve according to relativity

Einstein (1905) applied the invariance of the velocity of light c, in order to derive the special relativity, **SR**. That invariance can be confirmed by an observation of appropriate binary stars, see Fig. (1.4) or section (2.4). Moreover, that invariance can be derived by a thought experiment about freely propagating radio waves, see section (2.1.3.1). Correspondingly, we name the invariance of the propagation of light the **principle of free propagation, PFP**, alternatively, see section (2.1.3.1).

Moreover, Einstein (1915a) proposed a curvature of space-time. With it, he elaborated a theory of general relativity, **GR**. Using GR, we can partially explain the continuous **expansion of space** since the Big Bang, see Einstein (1917), Wirtz (1922), Hubble (1929) or Carmesin (2020e), Carmesin (2021a) as well as Carmesin (2021d)).

The expansion of space corresponds to an increase of the volume, which is physically caused by an increase of the amount of vacuum, see for instance Carmesin (2018c), Carmesin (2018b), Carmesin (2019a), Carmesin (2021d), Carmesin (2021a). Accordingly, we remind the discovery of the vacuum by Guericke (1672) next.

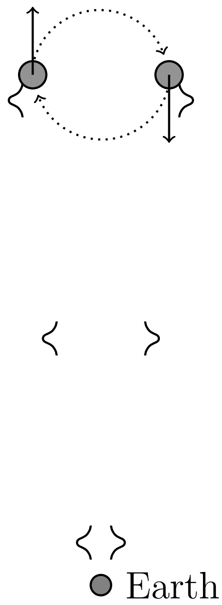

Figure 1.4: Binary star: two stars rotate around their center of mass. For instance, when the stars have the same distance to Earth, they emit one light signal each. These signals arrive at Earth simultaneously, though the emitting stars move in opposite directions. Such observations confirm that light propagates at a constant velocity relative to an observer, irrespective of the velocity of the light emitting source relative to the observer, see e.g. de Sitter (1913), Carmesin (2006).

1.2.4 Vacuum

Guericke (1672) invented pumps for the evacuation of objects with an internal isolated volume. With it, he discovered relations between the atmosphere and the vacuum, Fig. (1.5). Einstein (1917) introduced a cosmological constant Λ in GR that attributes a density or energy density to the vacuum. However, that constant cannot be determined within GR. Perlmutter et al. (1998), Riess et al. (2000), Spergel et al. (2007), Smoot (2007) and many others, see e.g. in Carmesin (2021c), discovered a density ρ_Λ or energy density of the vacuum. That density

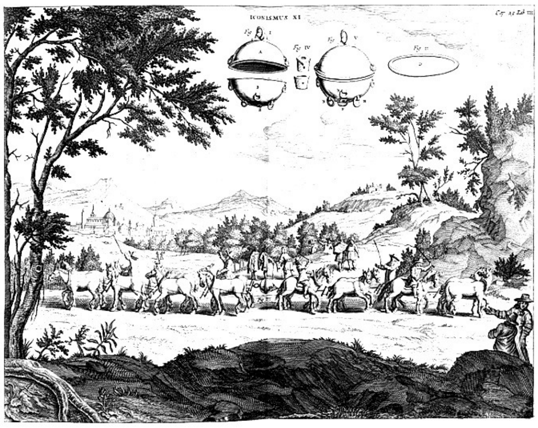

Figure 1.5: Guericke (1672) invented a vacuum pump and discovered relations between the atmosphere and the vacuum. In one of his experiments, more than ten horses were not strong enough in order to separate to half spheres that enclosed an evacuated volume.

ρ_Λ amounts to approximately 68 % to 75 % of the energy of the universe, see e.g. Planck-Collaboration (2020), Riess et al. (2021). In fact, that density ρ_Λ has been explained and derived, see e.g. Carmesin (2018c), Carmesin (2018b), Carmesin (2019a), Carmesin (2021d), Carmesin (2021a). Altogether, this shows that vacuum forms physically, and it has a density ρ_Λ and a volume. We name this essential fact of nature the **formation of vacuum, FV**.

1.2.5 Spacetime quadruple, SQ

We summarize the four fundamental concepts as a quadruple, we call it the **spacetime-quadruple, SQ**, see Carmesin (2022):

1. Principles of free fall, principles of free fall, PFF.
2. Gaussian gravity, GG.
3. Principle of free propagation, PFP, as a basis for SR. Here we apply SR for the case of non-quantized objects, as quantization is derived therefrom, see Carmesin (2022).

4. Formation of vacuum, FV, with a corresponding volume, see for instance Fig. (1.6) or Carmesin (2021d), Carmesin (2021a), Carmesin (2021f).

$$\text{spacetime} - \text{quadruple}, \text{SQ} = \{PFF, GG, PFP, FV\} \quad (1.1)$$

The four fundamental concepts, SQ, essentially represent gravity and relativity[2].

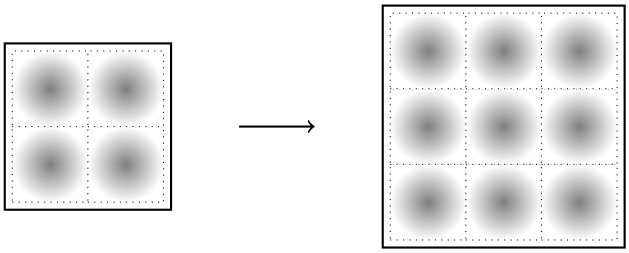

Figure 1.6: The expansion of space (solid line) is caused by an increase of the amount of vacuum (dotted). More realistically, vacuum propagates freely at c. The dynamics of vacuum is derived in our theory, see e.g. Carmesin (2021d).

1.2.6 Organization of the book

In chapter (2), we summarize the basic theory of gravity, relativity and vacuum. With it, we explain useful traditional theories of physics in Chap. (3). You will find the aim of this book in Chap. (4), while we will derive these aims in chapters (5, 6, 7, 8, 9). The results will be discussed in Chap. (10). You can find useful tables and a glossar in the appendix.

[2]We derive general relativity, GR, in Chap. (9). We do not apply GR, see e.g. Einstein (1915a), Carmesin (1996), Hobson et al. (2006), as it is incomplete, see e.g. (Carmesin, 2021a, 2.4) or (Carmesin, 2020e, Fig. 5.7). Moreover, GR is mesoscopic, see e.g. Carmesin (2022), Carmesin (2018b).

Chapter 2

Basic Theory

In this chapter, we summarize the basic theory of the vacuum. That basic theory is fundamental for general relativity, GR, and for quantum physics, QP.

Moreover, that theory has been published since Carmesin (2017b). Furthermore, that theory has been published in a series of books at the publisher Dr. Köster, Berlin: Carmesin (2018d), Carmesin (2018c), Carmesin (2018b).

Thereby, these books became a scientific book series starting with Carmesin (2019d), Carmesin (2020f), Carmesin (2020e), Carmesin (2021d). Hereby, essential basic results about elementary particles, see Carmesin (2021a), Carmesin (2021f), and about quantum physics have been derived, see Carmesin (2022).

Additionally, that basic theory has been published in scientific journals, Carmesin (2018a), Sprenger and Carmesin (2018).

See also Carmesin and Carmesin (2018a), Carmesin (2019f), Carmesin and Carmesin (2018b), Carmesin (2019b), Carmesin (2019a), see e.g. Carmesin (2020b), Heeren et al. (2020).

See e.g. Carmesin and Carmesin (2020), or Schöneberg and Carmesin (2020b), Lieber and Carmesin (2021), see additionally Carmesin (2021c), Schöneberg and Carmesin (2021a), Sawitzki and Carmesin (2021), Carmesin (2021g), Carmesin (2021b).

Simultaneously, the theory has been presented at scientific conferences, see e. g. Carmesin (2017a), Carmesin and Brüning

(2018), Carmesin (2019e), Carmesin (2019c), Carmesin (2020c), Carmesin (2020d), Schöneberg and Carmesin (2020a), Herren et al. (2020), Carmesin (2020a), Carmesin (2021e), Schöneberg and Carmesin (2021b).

2.1 Introduction of SQ

The basic theory can be derived from four basic principles: the principles of free fall (PFF), Gaussian gravity (GG), the principle of free propagation (PFP), and the formation of vacuum, see Carmesin (2022).

These four principles can be conformed by observation in a very precise manner. Moreover, these four principles can be conformed by thought experiments. According to this twofold foundation, these four principles exhibit an especially convincing evidence, and additionally, these principles imply the basic theory, which in turn implies very important theories such as quantum physics, quantum gravity and essential findings of the SMEP and SMEWI. As the set of these four principles characterizes spacetime, essentially corresponding to gravity and relativity, we name that set the spacetime-quadruple, SQ, see Carmesin (2022).

In this section, we elaborate the foundation of the spacetime-quadruple, SQ.

2.1.1 Principles of free fall

In this section, we treat principles that hold for a freely falling object or system.

2.1.1.1 Galileo's equivalence principle, GEP

Galileo (1638) provided a first principle of free fall, see section (1.2.2). However, there are more interesting principles inherent to free fall.

2.1.1.2 Einstein equivalence principle, EEP

(Einstein, 1911, p. 898-899) used Galileo's equivalence principle and extended it by the following statement: A local observer in a frame K at rest in a gravitational field $\vec{G}^*$ experiences the same laws of physics as a local observer in a frame K' at an acceleration $\vec{a}'$ with $\vec{a}' = -\vec{G}^*$, see Fig. (2.1). In particular, the inertial mass and the gravitational mass are equal.

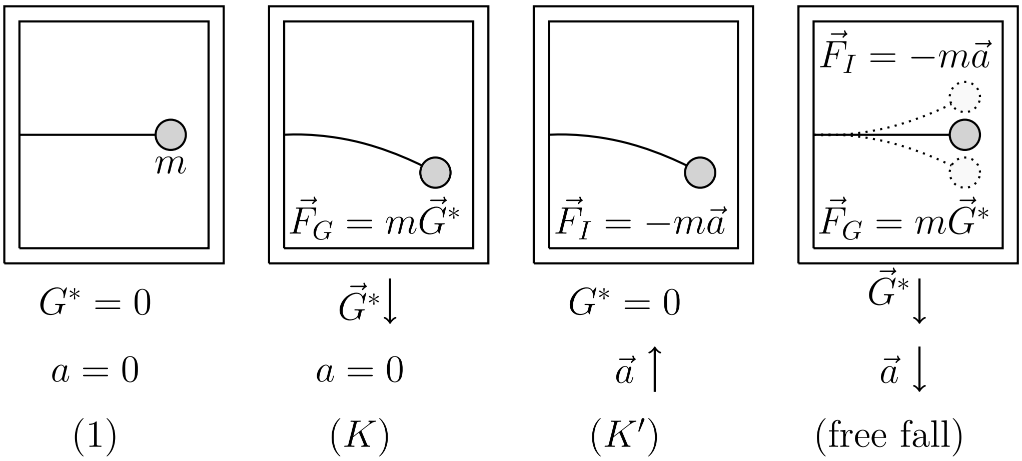

Figure 2.1: Frame with a mass m at a flat spring in four cases:
(1) Zero field $\vec{G}^* = 0$, zero acceleration $\vec{a} = 0 \rightarrow$ zero force.
(K) Field $\vec{G}^*$ downwards, $\vec{a} = 0 \rightarrow$ force $\vec{F}_G$ downwards.
(K') $\vec{G}^* = 0$, $\vec{a}$ upwards $\rightarrow$ inertial force $\vec{F}_I$ downwards.
(free fall) $\vec{G}^*$ downwards, $\vec{a}$ downwards, whereby $|\vec{G}^*| = |\vec{a}| \rightarrow$ gravitational force $\vec{F}_G$ downwards, inertial force $\vec{F}_I$ upwards, and zero resulting force $\vec{F} = 0$.

In particular, we consider a frame with a mass m at a flat spring, see Fig. (2.1). If such a frame falls freely, then the mass m experiences the gravitational force $\vec{F}_G = m\vec{G}^*$ and an inertial force $\vec{F}_I = -m\vec{a}$, whereby the sum of these two forces is zero as a result of the free fall:

$$\vec{F}_G + \vec{F}_I = m\vec{G}^* - m\vec{a} = 0 \tag{2.1}$$

We solve for the acceleration:

$$\vec{a} = \vec{G}^* \tag{2.2}$$

Thus, the Einstein equivalence principle, EEP, includes the Galileo's equivalence principle. Also the EEP has been confirmed by many experiments, see e. g. Will (2014).

2.1.1.3 Principle of energy conservation at free fall

Energy conservation is a very general principle of nature. However, the calculated value of energy depends on the chosen frame. For instance, if you ride on your bicycle on a road, then your kinetic energy in the frame of the bicycle is zero, whereas your kinetic energy is nonzero in the frame of the road. This example shows that the principle of conservation of energy makes sense only in a particular frame.

In what frame is the energy conserved, if a mass or dynamical m falls freely towards a mass or dynamical mass M? According to the local nature of the principles of the SQ, an appropriate frame is the local frame of the field generating mass M.

This energy conservation includes the case of an isotropically distributed mass M interacting with itself, see e.g. Carmesin (2022).

2.1.1.4 Summarized principles of free fall, PFF

In the following, we combine Galileo's equivalence principle, Einstein's equivalence principle and the principle of energy conservation at free fall to the **principles of free fall, PFF**:

$$PFF = \{GEP, EEP, \text{energy conservation at free fall}\} \tag{2.3}$$

2.1.2 On Gaussian gravity

The first essential theory of gravity is Newton's gravity, NG, see e. g. Newton (1686). We identify four essential parts of

NG: Firstly, according to Newton, (Newton, 1686, p. 78), space is absolute and at absolute rest. Secondly, Newton (Newton (1686)) used Euclidean geometry, which presumes flat space, see e. g. Euklid (C325). Thirdly, Newton presumed absolute time that goes on at a constant rate and in the same manner everywhere in space, see (Newton, 1686, p. 79). Fourthly, a mass is the source of gravity, see (Newton, 1686, p. 397) and Gauss (1809).

The third part about time has been generalized in special relativity, SR. The first and second part about space have been generalized in general relativity, GR. The fourth part has been generalized only slightly by the fact that mass is equivalent to energy and both (mass and energy) are sources of gravity. However, the essential part of gravity did not change: there are sources of gravity, these are mass as well as energy.

Accordingly, we will use that fourth part of NG, whereby we include energy as an additional source of gravity. We denote that fourth part of NG by *Gaussian gravity, GG.*

The idea of Gaussian gravity is simple and robust: A mass M generates a gravitational field $\vec{G}^*$, spreading uniformly in the vicinity. For an illustration see figure (2.2). We apply GG locally in a freely falling system, so it is applicable without any loss of generality. Accordingly, the field G^* generated by a mass M at a distance r is as follows:

$$|\vec{G}^*| = \frac{G \cdot M}{r^2} \tag{2.4}$$

Hereby G denotes the gravitational constant (Sect. 11.1).

Gaussian gravity was discovered on the basis of the motions of the planets as follows: Tycho Brahe observed the motions of the planets, see Brahe and Kepler (1627). Analyzing these results, Kepler (1619) discovered the Kepler laws of planetary motions. Huygens (1673) discovered the law of radial force. Newton (1686) combined the radial force with Kepler's laws of planetary motions and discovered Newton's law of gravitation.

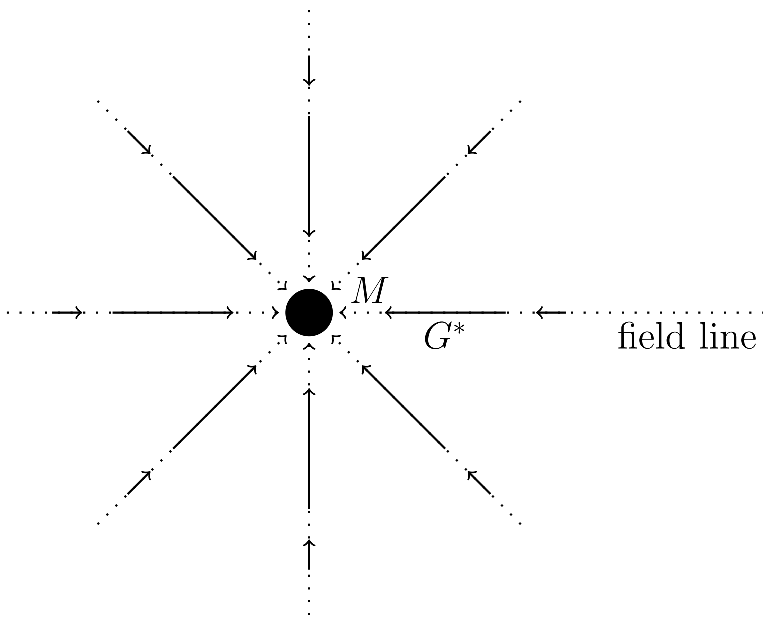

Figure 2.2: Mass M with field lines (dotted) and vectors (solid) of the gravitational field $\vec{G}^*$.

Note that this combination can be derived at a single page, see e. g. (Carmesin et al., 2021, p. 108-109). Gauss (1809) elaborated the essence of the generation of gravity by sources such as masses.

2.1.2.1 Field G^* as a function of the radial coordinate r

In this section, we derive the field[1] in the vicinity of a mass M. Thereby, the field is a function of the radial coordinate r, whereby M is at the coordinate $r = 0$. In general, the space can be elongated in the radial direction. Thereby, a coordinate difference dr may be elongated to a length dL, as a function of r. In the following we show that this has no effect on the function $G^*(r)$.

[1] Usually, we emphasize a field generating mass by a large letter M. Of course, all masses are in principle equal in physics. The distinction between a field generating mass and a probing mass is just a method of the analysis. It can easily be avoided by considering both masses as field generating masses and probing masses simultaneously. The above distinction may be appropriate, when one mass is relatively large compared to the other. Whenever a high accuracy is essential, then this distinction is not appropriate, of course.

There is no gravity in the horizontal direction, by definition. Therefore there is no spatial elongation in this direction. Thus a circle with a radius r and with its center at a field-generating mass M at the **radial coordinate** $r = 0$ has the following circumference U:

$$U = 2\pi \cdot r \tag{2.5}$$

Likewise, a sphere with the center at $r = 0$ and with the **radial coordinate** r has the following surface A:

$$A = 4\pi \cdot r^2 \tag{2.6}$$

With it we derive G^*:

$$\boxed{G^*(r) = -\frac{G \cdot M}{r^2}} \tag{2.7}$$

2.1.2.2 Local measurements in curved spacetime

In this section, we derive physical quantities that can be measured locally in the vicinity of a mass M. In particular, the field can be measured. An object at a coordinate r can be investigated in the object's own frame: In particular, a local observer localized at the object can measure the **radius** r, the 'object's own time' $d\tau$, the velocity $v = \frac{dr}{d\tau}$ relative to the mass M, the acceleration $a = \frac{dv}{d\tau}$ and the mass M as elaborated in Fig. (2.3). We summarize our results:

$$v = \frac{dr}{d\tau} \text{ and } a = \frac{dv}{d\tau} \text{ can be measured locally in GR} \tag{2.8}$$

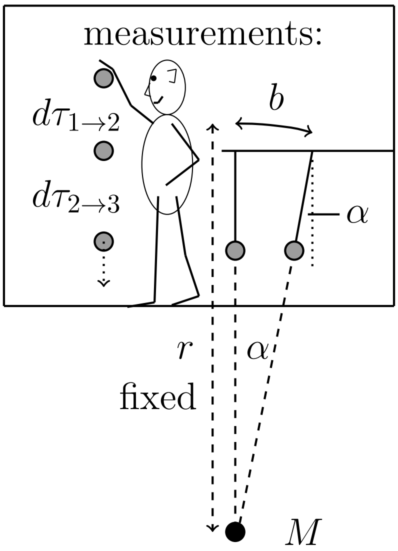

evaluation:

$$r = \frac{b}{\alpha}$$

for $j = 1$ and $j = 2$:

$$dr_{j \to j+1} = r_{j+1} - r_j$$

$$v_{j \to j+1} = \frac{dr_{j \to j+1}}{d\tau_{j \to j+1}}$$

$$dv = v_{2 \to 3} - v_{1 \to 2}$$

$$d\tau = \frac{d\tau_{1 \to 2}}{2} + \frac{d\tau_{2 \to 3}}{2}$$

$$a = \frac{dv}{d\tau} = G^*$$

$$M = -\frac{G^* \cdot r^2}{G}$$

Figure 2.3: A local observer localized at an object at r measures: Two hand leads provide the angle α and the arc length b. A falling ball yields time intervals in the observer's frame $d\tau_{j \to j+1}$. Therefrom r, v, a, G^* and M are evaluated.

2.1.3 On special relativity

Einstein (1905) introduced special relativity, SR, in order to describe **non-quantized objects** that move at relatively high velocity v and $v \leq c$. (see also Hobson et al. (2006), Carmesin et al. (2022), Straumann (2013), Moore (2013), or Carmesin (2020e)).

Einstein (1905) introduced the **special relativity theory, SR**, in order to describe objects with high velocity in various **inertial frames**, these are frames that are not accelerated. Thereby, Einstein assumed that the velocity of light c is an invariant. This has been confirmed, for instance by de Sitter (1913) or by Will (2014), see Fig. (1.4). As a consequence, space and time are no longer invariant, instead they form a four dimensional **spacetime**, see e. g. Einstein (1905) or Carmesin (2020f), Carmesin (2020e).

For instance, if two events occur within an object resting in its **own inertial frame**, then the time interval Δt beginning at the first event and ending at the second event depends on the inertial frame measuring Δt. The shortest Δt is measured in the own frame of the object, while the corresponding intervals are longer in external frames moving at a velocity v relative to the object:

$$\Delta t_{own} \leq \Delta t_{external} = \Delta t_{own} \cdot \gamma \text{ with } \gamma = \frac{1}{1 - v^2/c^2} \tag{2.9}$$

Thereby γ is called **Lorentz factor**, and v is the corresponding velocity.

2.1.3.1 SR fully based on a thought experiment

In this section, we derive the invariance of the velocity of light c by a thought experiment. To each star in Fig. (1.4), we add an orbiting satellite with a radio transmitter emitting radio waves. The corresponding frequency is f_1, for the 1^{st} transmitter, and f_2, for the 2^{nd} transmitter. In the region $R_{binary-Earth}$ between the binary and Earth, the frequencies are modified according to the Doppler effect, so that f_1 becomes f_1', and f_2 becomes f_2'.

These transmitters are controlled so that in $R_{binary-Earth}$, the waves have the same frequencies $f_1' = f_2'$, phases and directions (of polarization and of propagation). That is possible, as f_1 and f_2 can be chosen small compared to the frequencies of electronics and since radio waves can be described by classical waves.

Altogether, in $R_{binary-Earth}$, the two waves have the same frequencies, phases and directions. Hence the two waves form common fields $\vec{E}$ and $\vec{B}$ in $R_{binary-Earth}$. Thence the two waves or the common wave have the same velocity of propagation in $R_{binary-Earth}$. We call this fact the **principle of free propagation, PFP: If two waves propagate in a homogeneous region and have the same physical quantity constituting the amplitude, the same frequencies, phases and directions (of polarization and propagation), then these**

waves exhibit the same velocity of propagation. So the velocity of the radio waves is invariant, irrespective of the motion of the radio transmitters. Thus c is invariant. This implies SR, see e. g. Carmesin (2020e). Indeed, thought experiments provide the PFF, PFP and GG.

2.1.4 On general relativity

Einstein (1915a) introduced general relativity, in order to describe acceleration and gravity, in addition to special relativity (see also Hobson et al. (2006), Carmesin (1996), Carmesin et al. (2022), Straumann (2013), Moore (2013)).

2.1.4.1 General relativity is mesoscopic

The usual theory of GR is based on curvature. In general, curvature can be measured in terms of radii of curvature, see figure (2.4). For it, at least three smallest regions are necessary. In this sense, the usual theory of GR is mesoscopic.

As GR is mesoscopic, while we derive a theory of elementary objects, we do not use results of GR here. However, we use the essential concept of GR that spacetime is modified by mass and energy. If we need results in GR, we derive these results on our own.

In fact, we derive the mesoscopic curvature of spacetime on the basis of our microscopic description of the vacuum, see e. g. Carmesin (2021d) or section (2.1.5). So we confirm that spacetime is curved at a mesoscopic level.

2.1.5 Formed vacuum

We realized that the curvature of GR is a mesoscopic concept, see figure (2.4). Accordingly, we need a really microscopic concept. For it, we realize that vacuum is permanently formed, according to the expansion of space since the Big Bang. Accordingly, we use the volume δV of the formed vacuum at one

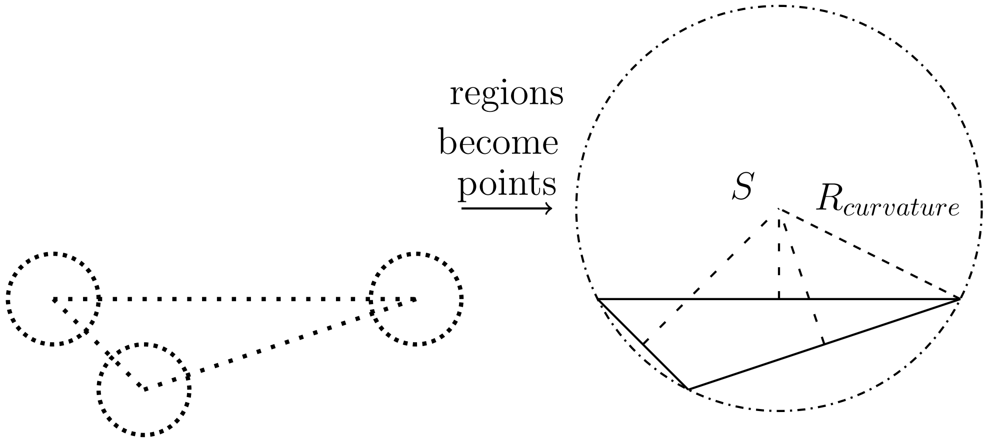

Figure 2.4: Three smallest regions are marked by three balls (dotted) and form a triangular construct (loosely dotted). The circumcircle (dashdotted) with its circumcentre S and the circumradius $R_{curvature}$ can be constructed. That curvature can be used as a radius of curvature. In that manner, a radius of curvature can be measured by using three smallest regions.

microscopic location per time δt and per existing volume dV. Carmesin (2021d) proposed and analyzed that concept.

Thereby, formed vacuum with its corresponding volume δV can be added and integrated. This fact is very deeply founded: Volume can be added. An independent foundation of the addition of vacua is the addition of energies, in particular of the dark energy, which is the energy of the vacuum. Correspondingly, the principle of linear superposition holds for formed vacuum and for formed volume.

Moreover, the formed vacuum propagates at the velocity of light c, for the following reason: If the formed vacuum would propagate at a smaller velocity $v_{vac} < c$, then it would be possible to measure a velocity $v < c$ of an object relative to the vacuum. However, such a velocity $v < c$ relative to the vacuum cannot be measured, according to SR. According to SR, non-quantized objects do not exhibit velocities $v > c$.

2.1.6 Thought experiment on formed vacuum

In this section, we show that the concept that vacuum forms in nature can be derived on the basis of the PFF, SR and GG via a thought experiment. For it we use the fact that the triple (PFF, SR, GG) can be used in order to derive the Friedmann-Lemaître equation about the expansion of space, see Friedmann (1922), Lemaitre (1927), Carmesin (2018b), Carmesin (2020e). However, if the space expands, then the volume increases. So the amount of vacuum increases. Thus there must be a permanent net formation of new vacuum.

2.1.7 Spacetime-quadruple, SQ

Altogether, we summarize the basics of gravity and relativity by four principles, see section (1.2.5). Thereby, each of these four principles is based on two mutually independent foundations: observation and thought experiment. Thus these four principles have an exceptionally well tested, clear and evident foundation.

2.1.8 On the structure of time

In this section, we analyze the structure of time in the SQ.

We realize that the SQ does not assume any global structure of time. Instead, the following local properties of time are inherent to the SQ:

According to the PFF, the local time derivative of the velocity is equal to the gravitational field, see Eq. (2.2).

According to the PFP, the velocity of light is an invariant, irrespective of a possible velocity of the considered frame, for an underlying thought experiment see Fig. (1.4). This implies the time dilation in SR, and transformations among frames correspond to linear transformations in spacetime. Note that time dilation in accelerated frames have been derived therefrom, see e.g. Carmesin (2021d).

According to the formation of vacuum FV, the amount of vacuum increases in an expanding universe.

Thus, we confirm that the SQ does not presume any global concept of time or space. Instead, the SQ describes the formation of vacuum, as a consequence, time dilation has been derived, see e.g. Carmesin (2020e), Carmesin (2021d). If desired, these results of the SQ can be described in terms of models of spacetime or of space and time.

Moreover, we note that the SQ includes two great special cases: For the case of smooth transformations of spacetime, general relativity has been derived from the SQ, see chapter (9). For the case of a far distance limit, quantum physics, QG, has been derived from the SQ, see Carmesin (2022). Accordingly, the SQ includes quantum gravity, SQ.

Theorem 1 Properties of the SQ

The spacetime-quadruple, SQ, has the following properties, see section (1.2.5 or Eq. (1.1):

(1) **The SQ has a twofold foundation***:*

(1.1) The four principles of the SQ are empirically founded.

(1.2) The four principles of the SQ are theoretically founded by thought experiments.

(2) **The SQ does not suffer from usual restrictions***:*

(2.1) The SQ does not assume absolute time or space, in contrast to Newton's gravity, NG, see Newton (1686).

(2.2) The SQ does not assume any continuous concept such as curvature, in contrast to general relativity, GR, see e.g. Einstein (1915a).

(2.3) The SQ does not assume a semiclassical concept such as the principle of stationary action, PGA. That restriction is inherent to GR, according to the Einstein-Hilbert action, see e.g.

Hilbert (1915), Hobson et al. (2006).

(2.4) The SQ is not restricted to classical physics. Instead, the SQ implies quantum physics, see Carmesin (2022).

(2.5) The SQ is not restricted to gravity and spacetime. Instead, the SQ implies quantum gravity, QG, as the SQ includes gravity and implies quantum physics, QP, see Carmesin (2022).

(2.6) The SQ is not restricted to three-dimensional space. Instead, in the SQ, the dimension $D \geq 3$ of space has been derived by five mutually independent methods, see e.g. Carmesin (2017b), Carmesin (2018b), Carmesin (2021d), Carmesin and Schöneberg (2022).

(3) **The SQ implies essential physical theories***:*

(3.1) For the case of spacetime transformations that can be described by Riemann curvature, the SQ implies the Einstein field equation, EFE, see chapter (9). Accordingly, the SQ implies GR, see e.g. Einstein (1915a), Hilbert (1915).

(3.2) The SQ implies the fact of quantization. Accordingly, the SQ implies implies quantum physics, QP, see Carmesin (2022).

(3.3) The SQ implies the elementary electric charge e, including electromagnetism, see Carmesin (2021f).

(3.4) The SQ implies the couplings g and g', the masses M_W and M_Z, as well as the Lagrangians of the electroweak interaction, see chapters (7, 5, 6, 8).

(4) **The SQ generalizes essential physical theories***:*

(4.1) The SQ solves cases of incompleteness of GR, chapter (9).

(4.2) The SQ solves a mystery of quantum electrodynamics: the origin of the elementary electric charge, (Feynman, 1985, p. 129). For details see Carmesin (2021f).

(4.3) The SQ solves essential assumptions of the standard model of the electroweak interaction, SMEWI, see (Weinberg, 1996,

p. 307,308): the Higgs mechanism, the weak angle and the couplings g, g'. For details see chapters (7, 5, 6, 8).

(5) **Local principles of SQ imply global structures***:*

(5.1) The four principles of the SQ are local rules. In particular, the structure of spacetime is not assumed neither with respect to dimension, nor with respect to continuous curvature, nor with respect to discontinuous processes such as phase transitions.

(5.2) The SQ implies the formation of the vacuum, including the density $\rho_{\Lambda,c.,h.}$ of possible constant and homogeneous vacuum, see e.g. (Carmesin, 2022, chapter 4):

$$\rho_{\Lambda,c.,h.} = \frac{1}{4\pi G \cdot t_H^2} = \frac{c^2}{4\pi G \cdot R_H^2} \tag{2.10}$$

Hereby, G is Newton's constant of gravitation, t_H is the Hubble constant, and R_H is the Hubble radius.

(5.3) The SQ implies the formation of the vacuum, including the density ρ_Λ in our universe with its time evolution of the heterogeneity. For it, a relatively small correction factor has been derived, whereby $\rho_{\Lambda,c.,h.}$ is modified by that correction factor, (Carmesin, 2021d, S. 6.6, 7.5, 8.5, 8.6), Carmesin (2021c).

(5.4) According to (5.2) and (5.3), at each region in spacetime, the density ρ_Λ of the vacuum is locally present. Thus, the global information of the light horizon is locally present. Hence, the global information of the light horizon can in principle become physically effective at each region of spacetime.

(5.5) The SQ implies that the average of the curvature parameter k is zero, see e.g. (Carmesin, 2021d, THM 32(6)):

$$[k_j] = 0 \tag{2.11}$$

(5.6) The SQ implies that the local peculiar curvature of spacetime is derived and explained by the formation of vacuum, see e.g. Carmesin (2021d).

(5.7) The SQ implies that the gravitational interaction is derived and explained by the formation of vacuum, Carmesin (2021d).

(5.8) Altogether, the SQ does not assume the structure of space or time or spacetime. Instead, the SQ derives the formation, propagation and time evolution of vacuum, as well as the transformation of vacuum into elementary particles and into fundamental interactions.

The space and spacetime are mathematical concepts or tools that can be used for the investigation of invariants such as Gaussian curvature, or for navigation, architecture construction of engines, design of an antenna, for instance.

Thereby, the derived results of SQ are in precise accordance with observation, whereby no fit is executed, see e.g. Carmesin (2021d), Carmesin (2021a), Carmesin (2021f), for a particularly detailed comparison, see Carmesin (2021c).

2.2 Each mass forms vacuum

The space expands since the Big Bang, see e. g. Wirtz (1922), Hubble (1929), Perlmutter et al. (1998), Riess et al. (2000), Spergel et al. (2007), Smoot (2007), Riess et al. (2021), Planck-Collaboration (2020).

For it, each mass or dynamic mass M forms a part of the vacuum that is permanently forming since the Big Bang, see Carmesin (2021d). Analogously, each mass on Earth provides a part of the attractive gravitational force that forces the moon to its orbit around Earth.

In the next section (2.3), we show that the vacuum formed by each mass or dynamic mass M propagates as a wave according to a differential equation, DEQ.

In the following section (2.4), we show that the vacuum formed by each mass or dynamic mass M and that propagates as a wave according to the above mentioned DEQ is quantized, as a result of the complete dynamics of that vacuum. In particular, we derive the Schrödinger equation from the DEQ of the vacuum. Moreover, we derived the postulates of quantum physics from the complete dynamics of that vacuum, that is formed by each mass or dynamic mass M, see Carmesin (2022).

Altogether, we show that the vacuum formed by each mass or dynamic mass M causes the quantized behavior of that mass M. Thereby, we explain the quantization of each mass or dynamic mass M as a result of the vacuum that the mass M forms itself.

Note that the vacuum formed by each mass or dynamic mass M on Earth does additionally propagate to space and curve the surroundings of Earth. That curvature represents gravity and forces the moon to its orbit around Earth. So that formed vacuum additionally represents the graviton proposed by Blokhintsev and Galperin (1934), see Carmesin (2021d).

2.3 Rate gravity wave, RGW

In this section, we summarize properties of waves that form and propagate according to the SQ, see e.g. Carmesin (2021d), Carmesin (2022).

2.3.1 Elongations

In this section, we summarize the description of unidirectional elongations of space, see Fig. (2.5) and e.g. Carmesin (2021d), Carmesin (2022).

Example of the Schwarzschild metric: As an example, we consider the case of the Schwarzschild metric, discovered in the field of general relativity, GR.

In GR, the spacetime in the vicinity of a mass M experiences a curvature. It can be described by using polar coordinates $dx_1 = r$, $dx_2 = \theta$ and $dx_3 = \phi$ and with the time coordinate

$dx_0 = t$. The curvature can be described with help of an underlying *metric tensor* g_{ij}, so that the square of an infinitesimal line element ds is as follows:

$$ds^2 = \Sigma_{i=0}^{3}\Sigma_{j=0}^{3}\, g_{ij} \cdot dx_i \cdot dx_j \tag{2.12}$$

In the vicinity of a mass M, the metric tensor is as follows, whereby we use the sign convention outlined in equation (2.15):

$$g_{ij} = \begin{pmatrix} -(1-\frac{R_S}{r}) \cdot c^2 & 0 & 0 & 0 \\ 0 & \frac{1}{1-\frac{R_S}{r}} & 0 & 0 \\ 0 & 0 & r^2 & 0 \\ 0 & 0 & 0 & r^2 \cdot \sin^2(\theta) \end{pmatrix} \tag{2.13}$$

Hereby, the metric tensor describes the Schwarzschild metric, SM, and R_S is the Schwarzschild radius:

$$R_S = \frac{2GM}{c^2} \tag{2.14}$$

Note that there are two different sign conventions in the literature. Hereby, we use the sign convention described by the Cartesian metric tensor of flat space as follows:

$$\eta_{ij,Cartesian} = \begin{pmatrix} -1 & 0 & 0 & 0 \\ 0 & 1 & 0 & 0 \\ 0 & 0 & 1 & 0 \\ 0 & 0 & 0 & 1 \end{pmatrix} \tag{2.15}$$

Note that the opposite signs are used in Landau and Lifschitz (1971) or in Stephani (1980), for instance. For an overview of various signs used in the literature, see Hobson et al. (2006).

2.3.2 Change tensor

In this section we analyze possible unidirectional changes that are caused by the mass M. For it we introduce a change tensor $\hat{\varepsilon}_{ij}$, more generally. As above and as an example, we use the metric tensor of the SM.

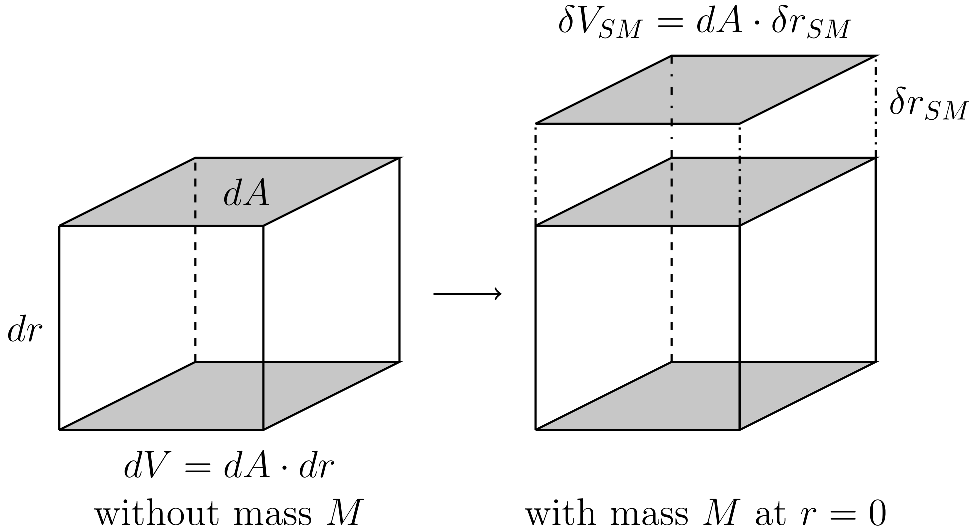

Figure 2.5: Unidirectional elongation in the radial direction: A cube with lower and upper surface dA is elongated by shifting the upper surface by an increment δr_{SM}.

The mass M changes the metric tensor g_{ij}, whereby there are only diagonal nonzero elements g_{ii}. In particular, we consider the radial direction in space only, so $d\theta$ and $d\phi$ are both zero. So Eq. (2.12) takes the following form:

$$ds^2 = g_{00} \cdot dt^2 + g_{rr} \cdot dr^2 \tag{2.16}$$

As the Schwarzschild metric is stationary, we may consider $dt = 0$. So we derive:

$$ds^2 = g_{rr} \cdot dr^2 \tag{2.17}$$

We insert $g_{rr} = \frac{1}{1-\frac{R_S}{r}}$, see Eq. (2.13). So the length dr is elongated to the length ds or dr' as a result of the mass M as follows:

$$ds = \frac{1}{\sqrt{1 - \frac{R_S}{r}}} \cdot dr = dr' \tag{2.18}$$

So the difference or *displacement* δr_{SM} is as shown below:

$$\delta r_{SM} = dr' - dr = \left(\frac{1}{\sqrt{1 - \frac{R_S}{r}}} - 1 \right) \cdot dr \tag{2.19}$$

That displacement δr_{SM} is illustrated in figure (2.5).

The derivative of such a displacement δr_{SM} with respect to the original length dr can be interpreted as an element of a *change tensor* $\hat{\varepsilon}_{rr}$, similarly to the strain tensor in elasticity theory, see (Landau and Lifschitz, 1975, equations 1.5, 1.8) or (Sommerfeld, 1978, equation 11):

$$\frac{\delta r_{SM}}{dr} = \hat{\varepsilon}_{rr} \tag{2.20}$$

Hereby, δr_{SM} and dr are regarded as differentials in the sense of the Leibniz calculus, see e.g. Bos (1974), Leibniz (1684) or Fig. (2.5).

For the case of other components, the change tensor takes the following form:

$$\frac{\delta r_i}{dr_j} = \hat{\varepsilon}_{ij} \tag{2.21}$$

Also the full change tensor is analogous to the strain tensor in elasticity theory, see (Landau and Lifschitz, 1975, equations 1.5, 1.8) or (Sommerfeld, 1978, equation 11).

2.3.3 Change of volume

Since the discovery of the dark energy, see e.g. Perlmutter et al. (1998), Riess et al. (2000), Smoot (2007), Spergel et al. (2007), Planck-Collaboration (2020), it has been clear that the vacuum has a density ρ_Λ. Accordingly, the volumes dV and δV_{SM} in figure (2.5) correspond to respective energies. So it is interesting to analyze the relative change of the volume:

The change can directly be applied to the volume in figure (2.5), $dV = dA \cdot dr$. The change of the volume δV_{SM} is the product of the area dA with the change δr_{SM}:

$$\frac{\delta V_{SM}}{dV} = \frac{dA \cdot \delta r_{SM}}{dA \cdot dr} = \frac{\delta r_{SM}}{dr} = \hat{\varepsilon}_{rr} = \frac{1}{\sqrt{1 - \frac{R_S}{r}}} - 1 \tag{2.22}$$

In general, the relative change of the volume is the sum of the changes for each Cartesian coordinate in a D dimensional space. So it is the sum of the diagonal elements of the change tensor:

$$\frac{\delta V}{dV} = \Sigma_{j=1}^{D} \hat{\varepsilon}_{jj} \tag{2.23}$$

This result corresponds to respective terms in elasticity theory, see (Landau and Lifschitz, 1975, equations 1.5, 1.6) or (Sommerfeld, 1978, equations 18 - 20). Here we call the relative change of the volume ε:

$$\frac{dV' - dV}{dV} = \frac{\delta V}{dV} = \varepsilon \tag{2.24}$$

We summarize our derivation as follows, see Carmesin (2022):

Proposition 1 Elongation in the SM

A mass or dynamical mass M causes an elongation $\delta r_{SM,elo}$ of a radial coordinate distance dr. Thereby, $\delta r_{SM,elo}$ is a function of the distance r as follows:

$$\delta r_{SM,elo} = dr' - dr = \left(\frac{1}{\sqrt{1 - \frac{R_S}{r}}} - 1 \right) \cdot dr \tag{2.25}$$

That elongation can be expressed by the radial element of the change tensor:

$$\hat{\varepsilon}_{rr} = \frac{\delta r_{SM,elo}}{dr} = \frac{1}{\sqrt{1 - \frac{R_S}{r}}} - 1 \tag{2.26}$$

As a consequence, the volume $dV = 4\pi r^2 \cdot dr$ of the shell with radius r and thickness dr is increased by the volume $\delta V_{SM,elo} = 4\pi r^2 \cdot \delta r_{SM,elo}$ as follows:

$$\hat{\varepsilon}_{rr} = \frac{\delta V_{SM,elo}}{dV} = \frac{1}{\sqrt{1 - \frac{R_S}{r}}} - 1 \tag{2.27}$$

2.3.4 Dynamics of formed vacuum

In this section, we summarize the deterministic dynamics or time evolution of the formed vacuum. For it, we summarize the corresponding differential equation, DEQ. This DEQ has been derived from the SQ in Carmesin (2021d) or Carmesin (2022), and it is summarized as follows:

Theorem 2 Invariant formation of vacuum

For the case of formation of vacuum without any additional density ρ_{add}, the rate gravity scalar, RGS, in the DEQ

$$\boxed{RGS = \dot{\varepsilon}^2 - G^{*2}/c^2 = 0} \tag{2.28}$$

is an invariant for the following reasons:

(1) In a frame that is at free fall, or that is not accelerated, the only possible accelerations are particular accelerations taking place inside the frame. A field $\vec{G}^*$ of a particular acceleration can be measured by a local observer.

(2) A possible absolute velocity cannot be measured. The DEQ $RGS = 0$ is invariant with respect to a Lorentz transformation, as the RGS is a relativistic square of a four vector, the RGV. Accordingly, the RGS is a Lorentz scalar:

$$RGV_i = \begin{pmatrix} \dot{\varepsilon} \\ G_1^*/c \\ G_2^*/c \\ G_3^*/c \end{pmatrix} = \begin{pmatrix} \partial_t \varepsilon \\ -\partial_{r_1}\phi/c \\ -\partial_{r_2}\phi/c \\ -\partial_{r_3}\phi/c \end{pmatrix} \quad \text{thus} \tag{2.29}$$

$$RGS = \Sigma_{i=0}^3 \Sigma_{k=0}^3 RGV_i \cdot \eta_{i,k} \cdot RGV_k \tag{2.30}$$

(3) Corresponding inhomogeneous DEQs are as follows:

$$\dot{\hat{\varepsilon}}_{jj}^2 - \left(\frac{G_j^*}{c}\right)^2 = 8\pi G\rho_{add} = (\partial_t \hat{\varepsilon}_{jj})^2 - \left(\frac{\partial_j \phi}{c}\right)^2 \tag{2.31}$$

$$\dot{\hat{\varepsilon}}^2 - \left(\frac{G^*}{c}\right)^2 = 24\pi G\rho_{add} = (\partial_t \hat{\varepsilon})^2 - \Sigma_{j=0}^3 \left(\frac{\partial_j \phi}{c}\right)^2 \tag{2.32}$$

As the rate $\dot{\hat{\varepsilon}}_j$ represents a tensor, in general, we represent it with a hat.

Note that the sign of the rate is physically determined as follows: If the average of the particular radial accelerations is positive, then additional vacuum must be formed so that the universe expands (Carmesin (2020e), Carmesin (2020b)).

2.3.5 Waves of formed vacuum

In this section, we analyze solutions of the DEQs in theorem (2), see e.g. Carmesin (2021d), Carmesin (2022). For simplicity, we abbreviate $\hat{\varepsilon}_{jj}$ by $\hat{\varepsilon}_j$:

$$RGS = 8\pi G \cdot \rho_{add} \text{ with } RGS = \dot{\hat{\varepsilon}}_j^2 - (\partial_j \phi)^2/c^2 \tag{2.33}$$

2.3.5.1 Solutions in the vacuum

Firstly, we analyze the above DEQ for the case of zero additional density ρ_{add}. So we analyze solutions in the vacuum. Accordingly, we set the RGS in Eq. (2.33) equal to zero:

$$RGS = \dot{\hat{\varepsilon}}_j^2 - \left(\partial_{x_j}\phi/c\right)^2 = 0 \tag{2.34}$$

Similarly, the amplitudes of the corresponding waves represent a tensor, in general, and so they are marked with a hat as well, see e.g. Eq. (2.35). The following waves are possible solutions of the above DEQ:

$$\hat{\varepsilon}_j = \hat{\varepsilon}_{j,\omega} \cdot \exp(-i \cdot \omega \cdot t + i \cdot k_j \cdot r_j) + \hat{\varepsilon}_{j,const.} \tag{2.35}$$

$$\hat{\phi}_j = \hat{\phi}_{j,\omega} \cdot \exp(-i \cdot \omega \cdot t + i \cdot k_j \cdot r_j) + \hat{\phi}_{j,const.} \tag{2.36}$$

Hereby, we apply the usual sign convention of quantum physics in the exponent, see e.g. (Kumar, 2018, Eq. 3.2.11), (Ballentine, 1998, Eq. 4.26). We insert these solutions into the DEQ (2.34):

$$\hat{\varepsilon}_{j,\omega}^2 \cdot \omega^2 = \frac{k_j^2}{c^2} \cdot \hat{\phi}_{j,\omega}^2 \tag{2.37}$$

Thus the velocity of propagation of a wave in direction of the coordinates r_j or k_j is as follows:

$$v_{prop} = \frac{\lambda}{T} = \frac{\omega}{k_j} \tag{2.38}$$

We apply this result to (Eq. 2.37):

$$\hat{\phi}_{j,\omega} = \hat{\varepsilon}_{j,\omega} \cdot c \cdot v_{prop} \tag{2.39}$$

So we can express the wave in terms of a single amplitude $\hat{\varepsilon}_{j,\omega}$. Thus the waves are as follows, see equations (2.35, 2.36).

$$\hat{\varepsilon}_j(t, r_j) = \hat{\varepsilon}_{j,\omega} \cdot e^{-i\cdot\omega\cdot t + i\cdot k_j \cdot r_j} + \hat{\varepsilon}_{j,const.} \tag{2.40}$$
$$\hat{\phi}_j(t, r_j) = \hat{\varepsilon}_{j,\omega} \cdot c \cdot v_{prop} \cdot e^{-i\cdot\omega\cdot t + i\cdot k_j \cdot r_j} + \hat{\phi}_{j,const.} \tag{2.41}$$
$$\hat{\phi}_j(t, r_j) = \hat{\varepsilon}_{j,\omega}(t, r_j) \cdot c \cdot v_{prop} + \hat{\phi}_{j,const.} \tag{2.42}$$

For the case of waves with zero average, we neglect the constant:

$$\hat{\varepsilon}_j(t, r_j) = \hat{\varepsilon}_{j,\omega} \cdot \exp(-i \cdot \omega \cdot t + i \cdot k_j \cdot r_j) \tag{2.43}$$
$$\hat{\phi}_j(t, r_j) = \hat{\varepsilon}_{j,\omega}(t, r_j) \cdot c \cdot v_{prop} \tag{2.44}$$

2.3.5.2 DEQ for stationary fields

The DEQ of the RGWs (2.34) describes the relation between a field G_j^* and a rate $\dot{\hat{\varepsilon}}_j$. Physically, there are two essential cases:

1. If there is no additional source, then the field and the rate cause each other, and an oscillatory or an exponential solution occur.

2. If the field is caused by an additional source such as a mass or dynamic mass M_q, then the field causes the rate according to the DEQ of the RGWs (2.34).

In the presence of a source, the field $G_j^*(R)$ at a distance R from M_q is determined according to Gaussian gravity as follows, see section (1.2.1):

$$G_j^*(R) = \frac{G \cdot M_q}{R^2} \quad \text{whereby} \quad j \hat{=} \text{radial} \tag{2.45}$$

In order to derive the corresponding rate of unidirectional formation of vacuum, we apply the DEQ of RGWs (2.34):

$$\dot{\hat{\varepsilon}}_j = G_j^*(R)/c = \frac{G \cdot M_q}{R^2 \cdot c} \tag{2.46}$$

We summarize our results as follows:

Theorem 3 Properties of RGWs

The RGWs (Eqs. 2.40, 2.41 and 2.42)

$$\hat{\varepsilon}_j(t, r_j) = \hat{\varepsilon}_{j,\omega} \cdot e^{-i\cdot\omega\cdot t + i\cdot k_j \cdot r_j} + \hat{\varepsilon}_{j,const.} \tag{2.47}$$

$$\hat{\phi}_j(t, r_j) = \hat{\varepsilon}_{j,\omega} \cdot c \cdot v_{prop} \cdot e^{-i\cdot\omega\cdot t + i\cdot k_j \cdot r_j} + \hat{\phi}_{j,const.} \tag{2.48}$$

$$\hat{\phi}_j(t, r_j) = \hat{\varepsilon}_{j,\omega}(t, r_j) \cdot c \cdot v_{prop} + \hat{\phi}_{j,const.} \tag{2.49}$$

have the following **properties***:*

(1) Some RGWs are **plane waves or** *discrete or continuous* **linear combinations** *of these. These linear combinations include waves with various symmetries, as the plane waves establish a* **complete orthonormal basis** *of a Fourier transform including Fourier integrals, see e.g. Sakurai and Napolitano (1994) or Teschl (2014), (Ballentine, 1998, p. 17-22).*

(2) In general, the amplitudes $\hat{\varepsilon}_{j,\omega}$ and $\hat{\phi}_{j,\omega}$ are tensors.

(3) RGWs **propagate** *at a velocity v_{prop} with $v_{prop} \leq c$. If an RGW describes the propagation of vacuum, then its velocity*

is $v_{prop} = c$, *as otherwise an object with* $m_0 > 0$ *could exhibit velocity* $v < c$ *relative to vacuum, in contrast to SR.*

(4) In general, RGWs represent solutions of the inhomogeneous DEQ in THM (2). Accordingly, the rates $\dot{\hat{\varepsilon}}$ *can also describe the* **formation of vacuum** *with a nonzero time average.*

(4.1) RGWs can describe the formation of vacuum in the vicinity of a mass M_q, *whereby there occurs a stationary additional volume as follows:*

$$\dot{\hat{\varepsilon}}_j = G_j^*(R)/c = \frac{G \cdot M_q}{R^2 \cdot c} \qquad \text{with} \;\; \rho_{f,In} = \frac{G^{*2}}{8\pi G c^2} \tag{2.50}$$

$$\dot{\hat{\varepsilon}}_j^2 = 8\pi G \rho_{f,In} \tag{2.51}$$

Hereby, $\rho_{f,In}$ *represents the positive or inertial density of the field* G^*, *for details see Carmesin (2022).*

(4.2) The RGWs describe the formation vacuum during the expansion of space and at a density ρ *as follows:*

$$\dot{\hat{\varepsilon}}_j^2 = 8\pi G\rho \;\text{ and }\; 3\dot{\hat{\varepsilon}}_j^2 = 24\pi G\rho = \dot{\varepsilon}^2 = \left(\frac{\delta V}{dV\delta t}\right)^2 \tag{2.52}$$

2.4 SQ explains QP and QG

Based on the SQ, the formation of vacuum, the resulting elongation and the corresponding RGW can be derived, see section (2.3). Based on the RGWs, the quantization in nature can be derived and explained, see Carmesin (2022).

In this section, we summarize the structure of the vacuum solutions in section (2.3). Based on these solutions, we derive the quantization in nature.

In order to derive the velocity v_{prop} of propagation or phase velocity v_{phase}, we insert Eq. (2.39) into equation (2.37):

$$\hat{\varepsilon}_{j,\omega} \cdot \omega = \frac{k_j}{c} \cdot \hat{\varepsilon}_{j,\omega} \cdot c \cdot v_{prop} \tag{2.53}$$

We solve for the velocity of propagation:

$$\omega/k_j = v_{prop} = v_{phase} \tag{2.54}$$

2.4.1 Quantization derived

In this section, we analyze RGWs that propagate at the velocity $v_{prop} = c$. So Eq. (2.54) implies the following relation:

$$\frac{\omega}{k_j} = c \tag{2.55}$$

Each wave that propagates at the velocity of light c, and that is emitted during a finite interval of time from a finite source, has the following properties:

(1) The wave forms a wave packet, as it essentially has a finite extension in space and time.

(2) The wave packet has an energy E and a momentum p, as it essentially has a finite extension in space and time.

(3) As the wave packet propagates at c, its energy E and its momentum p obey the following relation:

$$\frac{E}{p} = c \tag{2.56}$$

(4) As the wave packet propagates at c, its circular frequency ω and its wave number k obey the following relation:

$$\frac{\omega}{k} = c \tag{2.57}$$

(5) So the two above fractions are equal:

$$\frac{E}{p} = \frac{\omega}{k} = c \tag{2.58}$$

(6) As ω is nonzero, we can divide by ω and multiply by p. So the following fractions are equal:

$$\frac{E}{\omega} = \frac{p}{k} = \frac{p \cdot c}{\omega} \neq 0 \tag{2.59}$$

(7) In particular, the first two fractions do not depend on time, as E and p are conserved according to the laws of conservation of energy and momentum, and as ω and k of the RGW do not change as a function of time:

$$\frac{p}{k} = K(k) \text{ and } \frac{E}{\omega} = K(k) \text{ and } K(k) = constant(k) \quad (2.60)$$

Hereby, $constant(k) = K(k)$ is the constant of quantization. It could be a function of the wave number k, most generally.

(8) The energy E of the wave packet is constant and proportional to ω, so the energy of the wave packet is quantized. Similarly, the momentum p of the wave packet is constant and proportional to k, so the momentum of the wave packet is quantized. Thereby, that quantization are as follows:

$$E = K(k) \cdot \omega \text{ and } p = K(k) \cdot k \quad (2.61)$$

That constant has been measured. It is the Planck constant h divided by 2π. It is named reduced Planck constant (see 11.1):

$$K(k) = \hbar \quad (2.62)$$

However, we should first prove that $K(k)$ does not depend on k, see section (2.4.2).

2.4.2 Universality of Planck's constant derived

In this section, we show that $K(k)$ does not depend on k. For it, we analyze the standard deviations or uncertainties inherent to the wave functions.

These standard deviations are characterized by an uncertainty relation as follows:

$$\Delta x \cdot \Delta p \geq \frac{K(k)}{2} = \frac{\text{quantization factor}}{2} \quad \text{with} \quad (2.63)$$

$$\Delta p = \sqrt{\langle p^2 \rangle - \langle p \rangle^2} \quad (2.64)$$

Hereby, Δx is the standard deviation of x and Δp is the standard deviation of p.

However, there is a universal uncertainty relation, which holds for wave functions (in the corresponding Hilbert space, see Carmesin (2022), it is a mathematical fact, see e.g. Carmesin et al. (2020), (Sakurai and Napolitano, 1994, p. 56-57):

$$\Delta x \cdot \Delta k \geq \frac{1}{2} \text{ with } k\psi = -i\partial_x \psi(x,k) \qquad \text{and} \tag{2.65}$$

$$\Delta k = \sqrt{\langle k^2 \rangle - \langle k \rangle^2} \tag{2.66}$$

Hereby, Δx is the standard deviation of x and Δk is the standard deviation of k.

In particular, the product of the uncertainties Δx and Δk has a minimum, which does not depend on k (in a usual mathematical normalization, that minimum has the value 1/2). That mathematical result about the (Hilbert space of) wave functions does hold for the physical wave functions as well, as it is a mathematical fact. Thus $\frac{K(k)}{2}$ in Eq. (2.63) must be a constant. This shows that $K(k)$ does not depend on k, q. e. d.

2.4.3 Schrödinger equation derived

In this section, we show that the DEQ of the RGW (2.34) is the Schrödinger equation, SEQ. For it, we solve that equation for $\dot{\hat{\varepsilon}}_j$. Thereby, we choose different signs of the square roots (so we obtain positive energy):

$$\partial_t \hat{\varepsilon}_j(t, r_j) = -\partial_j \hat{\phi}(t, r_j)/c \tag{2.67}$$

In order to find the wave equation, we apply the solution in Eq. (2.44),

$$\hat{\phi}_j(t, r_j) = \hat{\varepsilon}_{j,\omega}(t, r_j) \cdot c^2, \tag{2.68}$$

so we derive:

$$\partial_t \hat{\varepsilon}_j(t, r_j) = -\partial_j \hat{\varepsilon}_j(t, r_j) \cdot c \tag{2.69}$$

For comparison, the Schödinger equation is as follows, see e.g. Carmesin (2022):

$$i\hbar\partial_t\psi(t,r_j) = -i\cdot\hbar\cdot c\cdot\partial_{r_j}\psi(t,r_j) \tag{2.70}$$

In fact, the above Eq. (2.69) is already mathematically equivalent to the Schrödinger equation. However, the square of the wave function should be proportional to the energy density $u_{f,In}$, as the energy density $u_{f,In}(\vec{R},t)$ is proportional to the probability of finding the object at $(\vec{R},t)$, see Carmesin (2022). Moreover, the wave function should have the physical dimension or unit $[\psi]=1$. For that purpose, we apply the time derivative to Eq. (2.69), and we multiply with a normalization factor of time t_n. That factor t_n is determined so that the wave function ψ has an amplitude corresponding to the respective physical situation under investigation. In particular, the sum or integral of all probabilities or probability densities is normalized to one:

$$\partial_t\dot{\hat{\varepsilon}}_j(t,r_j)\cdot t_n = -\partial_{r_j}\dot{\hat{\varepsilon}}_j(t,r_j)\cdot t_n\cdot c \tag{2.71}$$

In order to show that the DEQ of the RGW is equivalent to the Schödinger equation, we multiply Eq. (2.71) by $i\hbar$:

$$\boxed{i\hbar\partial_t\dot{\hat{\varepsilon}}_j(t,r_j)\cdot t_n = -i\hbar\partial_{r_j}\dot{\hat{\varepsilon}}_j(t,r_j)\cdot t_n\cdot c} \tag{2.72}$$

We conclude that the DEQ of the RGW (2.72) is equivalent to the Schödinger equation (2.70), whereby we identify the normalized unidirectional rate $\dot{\hat{\varepsilon}}_j(t,r_j)\cdot t_n$ with the normalized wave function $\psi(t,r_j)\cdot f_n$, see figure (2.5), whereby f_n denotes a normalization factor of a wave function ψ:

$$\boxed{\dot{\hat{\varepsilon}}_j(t,r_j)\cdot t_n = \psi(t,r_j)\cdot f_n} \tag{2.73}$$

In order to make the Schödinger equation (2.72) even more obvious, we apply the momentum operator $\hat{p}_j = -i\hbar\partial_{r_j}$, the operator of kinetic energy $\hat{E}_{kin} = \hat{p}_{r_j}\cdot c = -i\hbar\partial_{r_j}\cdot c$ and the operator of energy $\hat{E} = i\hbar\partial_t$, see e.g. Carmesin (2022):

$$\hat{E}\dot{\hat{\varepsilon}}_j(t,r_j)\cdot t_n = \hat{p}_j\dot{\hat{\varepsilon}}_j(t,r_j)\cdot t_n\cdot c = \hat{E}_{kin}\dot{\hat{\varepsilon}}_j(t,r_j)\cdot t_n \tag{2.74}$$

2.4.4 Objects with $v_{prop} < c$

An object with a velocity $v_{prop} < c$ has a rest mass m_0. According to SR, the energy momentum relation holds:

$$E^2 = p^2 c^2 + m_0^2 \cdot c^4 \tag{2.75}$$

In order to obtain the Schödinger equation, we apply the root:

$$E = \sqrt{p^2 c^2 + m_0^2 \cdot c^4} \tag{2.76}$$

In many applications, the non-relativistic approximation of the above root is applied. Usually, the linear order in $p/(m_0 c)$ is used:

$$E \hat{=} m_0 \cdot c^2 + \frac{p^2}{2m_0} \tag{2.77}$$

It is convenient to use the kinetic energy $E_{kin,non-relativistic} = E - m_0 \cdot c^2$:

$$E_{kin,non-relativistic} \hat{=} \frac{p^2}{2m_0} \tag{2.78}$$

In order to obtain the Schödinger equation, we apply the corresponding operators. In particular, we use Eq. (2.78), we insert the operator $\hat{p}$ for the momentum p, see e.g. Carmesin (2022), we insert the operator $\hat{E}$ for the energy $E_{kin,non-relativistic}$, see e.g. Carmesin (2022). Moreover, we multiply by the wave function:

$$\boxed{i\hbar \partial_t \psi(t, r_j) = -\frac{\hbar^2}{2m_0} \partial_{r_j}^2 \psi(t, r_j)} \tag{2.79}$$

This is the non-relativistic Schödinger equation, see for instance Carmesin (2022), whereby we identify the normalized unidirectional rate $\dot{\varepsilon}_j(t, r_j) \cdot t_n$ with the normalized wave function $\psi \cdot f_n$:

$$\dot{\varepsilon}_j(t, r_j) \cdot t_n = \psi(t, r_j) \cdot f_n \tag{2.80}$$

We summarize our results as follows:

Theorem 4 Emergence of quanta

(1) Each wave that propagates at the velocity of light $v_{prop} = c$*, and that is emitted at a finite interval of time and from a finite source, has the following properties:*

(1.1) The wave forms a wave packet with an energy E*, a momentum* p*, a circular frequency* ω *and a wave number* k*.*

(1.2) The wave packet is quantized as follows:

$$E = K \cdot \omega \quad \text{and} \tag{2.81}$$

$$p = K \cdot k \quad \text{with} \tag{2.82}$$

$$K = \text{universal constant of quantization} \tag{2.83}$$

Hereby, the universal constant of quantization K *does not depend on* E *or* ω*,* K *has been measured, and* K *is Planck's constant* h *divided by* 2π*, so* K *is the reduced Planck constant* $\hbar = \frac{h}{2\pi} = K$*, see table (11.1).*

(1.3) If that wave is a rate gravity wave, RGW, it obeys the Schödinger equation, SEQ. Hereby, the normalized wave function is equal to the normalized rate of the unidirectional relative change of the volume of vacuum, see figure (2.5):

$$\dot{\hat{\varepsilon}}_j(t, r_j) \cdot t_n = \psi(t, r_j) \cdot f_n \tag{2.84}$$

$$i\hbar\partial_t \dot{\hat{\varepsilon}}_j(t, r_j) \cdot t_n = -i\hbar\partial_{r_j} \dot{\hat{\varepsilon}}_j(t, r_j) \cdot t_n \cdot c \tag{2.85}$$

(2) Each RGW that propagates at the velocity of light $v_{prop} < c$*, and that is emitted at a finite interval of time and from a finite source, has the following properties:*

(2.1) The RGWs are quantized. From the above one dimensional SEQ, the three dimensional SEQ is constructed as usual, see e.g. Sakurai and Napolitano (1994), Ballentine (1998), Kumar (2018).

(2.2) The RGW obeys the Schödinger equation, SEQ. Hereby, the normalized wave function is equal to the normalized rate of

the unidirectional relative change of the volume, see figure (2.5). For $v/c << 1$, the SEQ is as follows:

$$\dot{\varepsilon}_j(t, r_j) \cdot t_n = \psi(t, r_j) \cdot f_n \tag{2.86}$$

$$i\hbar\partial_t\psi(t, r_j) = -\frac{\hbar^2}{2m_0} \cdot \partial^2_{r_j}\psi(t, r_j) \tag{2.87}$$

Hereby, m_0 is the rest mass of the described quantum object.

All results derived in this theorem are based on the spacetime-quadruple.

Moreover, Carmesin (2022) derived the postulates of quantum physics, QP, in order to show that SQ does indeed imply QP. Furthermore, Carmesin (2022) derived, explained and clarified many properties of quantum physics.

2.5 Mass forms via QG

In this section, we summarize how mass forms from vacuum. That summary is based on derivations and explanations obtained on the basis of the SQ. The findings have been confirmed by precise accordance between derived and observed values, whereby no fit has been used.

2.5.1 Gravity can fold vacuum

The attractive gravity tends to decrease the distance between masses or dynamical masses. As a consequence, the density increases. However, when the largest possible density, the Planck density ρ_P is reached, then the masses cannot be moved towards each other in space. as a consequence, gravity increases the dimension D of space, so that the distance decreases, though the density remains the same, see Fig. (2.7). That change of dimension takes place at dimensional phase transitions at respective critical densities $\tilde{\rho}_{D,c}$.

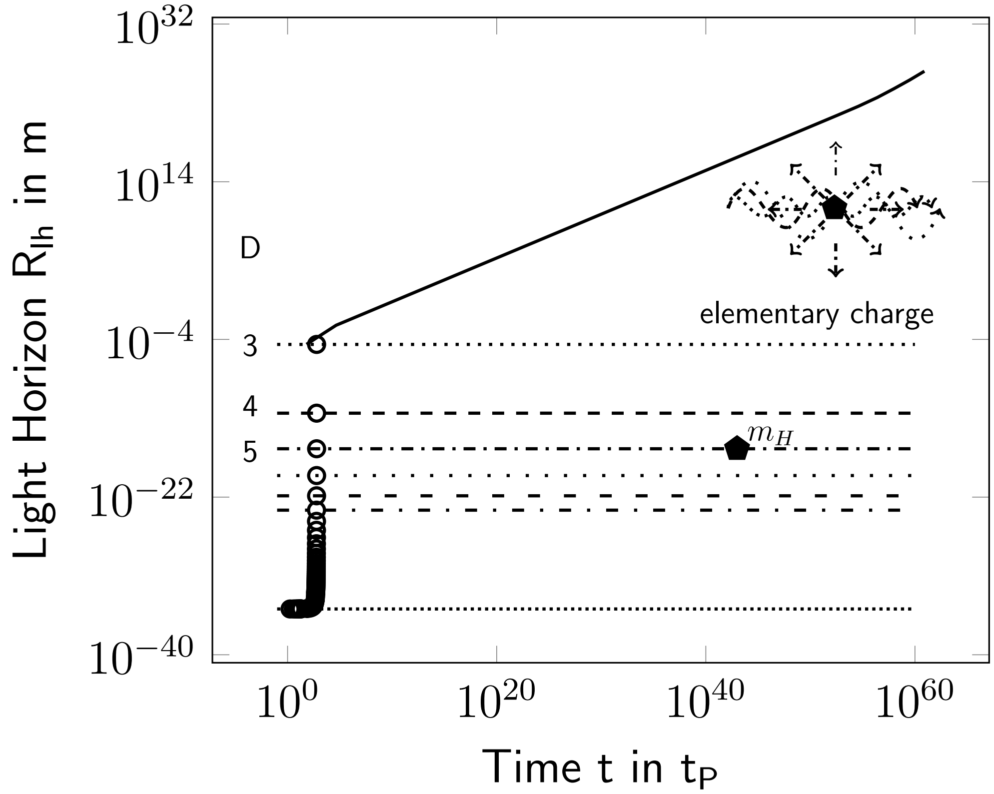

Figure 2.6: Time evolution of the vacuum enclosed in the present-day light horizon $R_{lh}(t)$: For $R_{lh}(t) \approx> 10^{-5}$ m, three-dimensional space became stable. At smaller $R_{lh}(t)$, dimensional phase transitions occurred at critical densities $\tilde{\rho}_{D,c}$.

The density ρ_Λ of vacuum contains information about $R_{lh}(t)$ and about vacuum at all dimensions $D \geq 3$. So five-dimensional vacuum can form at any time: thereby masses and charges of elementary particles form from vacuum via a local dimensional phase transition.

For instance, based on the SQ, the dynamics of the vacuum has been derived. With it, the formation of the mass of the Higgs boson, m_H, as well as the formation of the elementary electric charge has been derived, see e.g. Carmesin (2021d), Carmesin (2021a), Carmesin (2021f). Hereby, precise accordance with observation has been achieved, whereby no fit has been executed.

Thus, the mechanisms of the electric charge and electromagnetic interaction have been derived and explained.

Theoretical evidence for dimensional phase transitions: the dimensional phase transitions have been derived with five mutually independent methods:

Carmesin (2017b) analyzed these phase transitions using a van der Waals type model, see also for instance Carmesin (2018b), Carmesin (2019d), Carmesin (2020e).

Moreover, these dimensional phase transitions have been confirmed by the time evolution of dark energy, see e.g. Carmesin (2018c), or in Carmesin (2018b), Carmesin (2019d), Carmesin (2021d), Carmesin (2021a).

Furthermore, these phase transitions have been confirmed by a Bose gas model, see for instance Carmesin (2021d), Sawitzki and Carmesin (2021).

Additionally, these phase transitions have been confirmed by an analysis of the connectivity of locations in space, see Carmesin (2021d).

Moreover, these phase transitions have been confirmed by a droplet model, see Carmesin and Schöneberg (2022).

Empirical evidence for dimensional phase transitions: In fact, Lohse et al. (2018) as well as Zilberberg et al. (2018) discovered physics taking place at higher dimension $D > 3$ in experiments utilizing electrons and in other experiments using photons.

Guth (1981) discovered the horizon problem. That problem has been solved on the basis of the dimensional phase transitions, see e.g. Carmesin (2019d), Schöneberg and Carmesin (2021a), Carmesin and Schöneberg (2022).

Using dimensional phase transitions, the energy problem has been solved, Carmesin (2020e).

Utilizing dimensional phase transitions, the flatness problem has been solved, Carmesin (2019d), Carmesin (2021d).

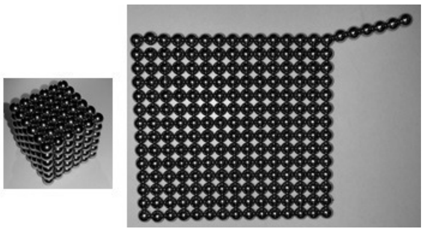

Figure 2.7: 216 magnetic balls model local objects or observable regions at high density and illustrate the relation between the distance and the dimension D: If the dimension increases from two (right) to three (left), then the largest distance decreases. More generally and conversely, a decrease of the dimension D implies an increase of the largest distance.

On the basis of dimensional phase transitions, the formation of mass and of charge have been derived and explained, Carmesin (2021a), Carmesin (2021f).

The dimensional phase transitions from $D = 4$ to $D = 3$ has probably been observed by Ratzinger and Schwaller (2021), see (Carmesin, 2021a, p. 169-170) or section (8.7.2.1).

2.5.2 Cosmic unfolding

In the early universe, the present-day light horizon R_{lh} took its smallest possible value, twice the Planck length L_P, see table (11.3), at the dimension $D_{horizon} = 301$ or $D_{hori} = 301$, see e.g. Carmesin (2017b), Carmesin (2019d), Carmesin (2021a). This dimension $D_{hori} = 301$ is named **dimensional horizon**.

Then vacuum formed and caused the well known expansion of space since the Big Bang. As a consequence, the density decreased. Whenever the density achieved a critical density, then the respective dimensional phase transition took place, whereby the distances increased, see Fig. (2.7).

Thus, a sequence of dimensional phase transitions took place, we name that sequence the **cosmic unfolding**. That sequence has been calculated in detail, see for instance Carmesin (2019d), Carmesin (2021a). The phase transitions of the cosmic unfold-

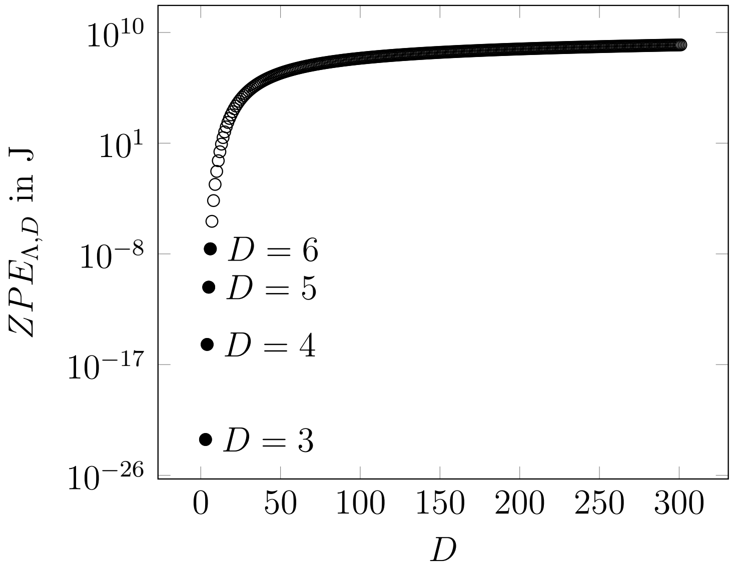

Figure 2.8: Zero-point energy $ZPE_{\Lambda,D}$ of the dark energy as a function of the dimension of the space D.

ing are marked by open circles in Fig. (2.6). The energies of the corresponding quanta of the vacuum are zero-point energies $ZPE_{\Lambda,D}$. These have been derived, see e.g. Carmesin (2018b), Carmesin (2021a), and these $ZPE_{\Lambda,D}$ are illustrated in Fig. (2.8).

2.5.3 Availability of quanta of cosmic unfiolding

In this section, we show that a present-day quantum of vacuum, $ZPE_{\Lambda,D=3}$, experiences in its nearest vicinity the full structure (or information) about all quanta of vacuum $ZPE_{\Lambda,D}$ of the cosmic unfolding. For additional details, see section (10.3). Thus, a present-day quantum of vacuum $ZPE_{\Lambda,D=3}$ can take each quantum of vacuum $ZPE_{\Lambda,D}$ of the cosmic unfolding as an excitation state. The derivation is as follows:

(1) The dimensional horizon is the solution of the following equation, see ((Carmesin, 2019d, Eq. 2.163)):

$$\tilde{\rho}_{r,D_{hori}} = 2^{\frac{4(D_{hori}-3)}{3}} \cdot \frac{1}{4 \cdot \tilde{R}_{lh}^4 \cdot \tilde{\rho}_{r,t_0}} \tag{2.88}$$

Hereby, all quantities with a tilde are noted in Planck units, see table (11.3), $\tilde{R}_{lh}$ represents the light horizon, $\tilde{\rho}_{r,D_{hori}}$ marks the density of radiation at the dimensional horizon, and $\tilde{\rho}_{r,t_0}$ is the present day density of radiation.

(2) The density $\tilde{\rho}_{r,D_{hori}}$ in (1) is equal to the critical density $\tilde{\rho}_{D_{hori},c}$ of D_{hori}. It is a consequence of the laws of nature, so that information is in principle present or effective at a present-day quantum of vacuum, $ZPE_{\Lambda,D=3}$.

(3) The present day density of radiation in (1) is present or effective in the vicinity of a present-day quantum of vacuum, $ZPE_{\Lambda,D=3}$.

(4) The information about the value of the light horizon $\tilde{R}_{lh}$ is inherent to the density of vacuum ρ_Λ, see THM (1, part (5.4)). The density of vacuum ρ_Λ is present or effective in the vicinity of a present-day quantum of vacuum, $ZPE_{\Lambda,D=3}$. So the information of the value of the light horizon $\tilde{R}_{lh}$ is present or effective in the vicinity of a present-day quantum of vacuum, $ZPE_{\Lambda,D=3}$.

(5) According to items (1), (2), (3) and (4), the information of the value of the dimensional horizon D_{hori} is present or effective in the vicinity of a present-day quantum of vacuum, $ZPE_{\Lambda,D=3}$.

(6) As a consequence of the dimensional phase transitions from $D = D_{hori} = 301$ towards a dimension $D \geq 3$, the universe and the light horizon increased by the dimensional enlargement factor as follows, see (Carmesin, 2021a, Eq. (7.2)):

$$Z_{D_{hori}\to D} = 2^{(D_{hori}-D)/D} \tag{2.89}$$

(7) According to items (5) and (6), the information of the values of the dimensional enlargement factors $Z_{D_{hori}\to D}$ is present or effective in the vicinity of a present-day quantum of vacuum, $ZPE_{\Lambda,D=3}$.

(8) The energy of a quantum of vacuum of the cosmic unfolding

is as follows, see (Carmesin, 2021a, Eq. (7.4)):

$$ZPE_{\Lambda,D} = E_{D_{hori}} \cdot \frac{D-1}{Z_{D_{hori} \to D} \cdot 300} \tag{2.90}$$

(9) According to items (7) and (8), the information of the energy of each quantum of vacuum of the cosmic unfolding is present or effective in the vicinity of a present-day quantum of vacuum, $ZPE_{\Lambda,D=3}$.

Thus we derived the desired result, and we summarize it as follows:

Proposition 2 Excitation states via cosmic unfolding

(1) The present-day quantum of vacuum, $ZPE_{\Lambda,D=3}$, experiences in its vicinity the full information of all quanta of vacuum of the cosmic unfolding, $ZPE_{\Lambda,D}$.

(2) So the quanta of vacuum of the cosmic unfolding, $ZPE_{\Lambda,D}$, **are possible excitation states**.

(3) The present-day quantum of vacuum, $ZPE_{\Lambda,D=3}$, experiences the light horizon R_{lh}, see THM (1). The size of a system that performs dimensional phase transitions determines the corresponding enlargement factors and zero-point energies, as illustrated in Fig. (2.7). So the quanta of vacuum of the cosmic unfolding, $ZPE_{\Lambda,D}$, **are the only possible excitation states of cosmic unfolding**.

(4) Additional excitation states are caused by **transitions** *to various symmetries described by tensors, see Carmesin (2021a).*

(4.1) The most simple excitation states are unidirectional and longitudinal quanta, see Carmesin (2021a).

(5) In addition, there occur excitation states according to **harmonic oscillations, described by ladder operators**, *see (Carmesin, 2021d, chapter 6), Carmesin (2021a).*

(6) If an object in three-dimensional vacuum is formed from the most simple excitation states (unidirectional and longitudinal quanta), then the object is constituted by three quanta (in order to fill $D = 3$-vacuum).

(7) Objects in (6) derive and explain the formation of masses:

(7.1) If the objects in (6) have the lowest energy, then the objects are excitation states of transitions in (4) and of harmonic oscillations, described by ladder operators in (5), and then these objects provide the sum of masses of the neutrinos, see Carmesin (2021a).

(7.2) If the objects in (6) are constituted by excitation states to dimension four, then the objects exhibit relatively low stability, see Carmesin (2021a).

(7.3) If the objects in (6) are constituted by excitation states to dimension five, then these objects provide the mass m_H of the Higgs boson, see Carmesin (2021a).

2.6 Charge forms via QG

In this section, we summarize the mechanism of the formation of the elementary electric charge:

(1) An object in PROP (2, number (3)) is constituted by a triple of longitudinal and unidirectional quanta.

(2) Each quantum of the triple in (1) causes forced oscillations at the other two quanta of the triple, see Carmesin (2021f).

(3) The forced oscillations in (2) can form the elementary electric charge, see Carmesin (2021f). That charge gives rise to electromagnetism, see Carmesin (2021f).

Chapter 3

Explanation of Traditional Theories

In this chapter, we explain useful traditional theories by application of my new and basic theory, see chapter (2).

3.1 Principle of Least Action, PLA, in QP

Based on the SQ, we derived the rate gravity waves as well as quantum physics, QP. In quantum physics, an object is described by a wave functions ψ, see e.g. Sakurai and Napolitano (1994), Ballentine (1998), Kumar (2018), Carmesin (2022). In this section, we analyze a particular semiclassical limit of QP.

We consider a freely propagating quantum object. So it is described by a plane wave. As usual, we name the wave vector $\vec{k}$, the circular frequency ω and the time t. So the wave function can be expressed with a normalization factor f_n as follows:

$$\psi(t, \vec{x}) = f_n \cdot \exp(i \cdot \vec{k} \cdot \vec{x} - i \cdot \omega \cdot t) \qquad \text{with} \tag{3.1}$$

$$\vec{k} = \vec{p}/\hbar \;\text{ and }\; \omega = E/\hbar \tag{3.2}$$

Hereby, $\vec{p}$ is the momentum and E is the energy of a corresponding quantum, Carmesin (2022). Moreover, $\hbar = \frac{h}{2\pi}$ is the reduced Planck constant, while h is Planck's constant, see table

(11.1). Thus we derive:

$$\psi(t,\vec{x}) = f_n \cdot \exp\left(i \cdot \frac{\vec{p}\cdot\vec{x} - E\cdot t}{\hbar}\right) \tag{3.3}$$

In the above Eq., the fraction is a real number, Planck's constant h represents an action S, and so the numerator represents an action S as well:

$$S(t,\vec{x}) = \vec{p}\cdot\vec{x} - E\cdot t \qquad \text{with} \tag{3.4}$$

$$\psi(t,\vec{x}) = f_n \cdot \exp(i \cdot S(t,\vec{x})/\hbar) \tag{3.5}$$

3.1.1 Semiclassical path $\vec{x}(t)$

If a quantum object propagates freely from a point A to a point B, and if the quantum object can be described by one semiclassical path $\vec{x}(t)$, and if these paths start at the point A and end at the point B, then the action $S(t,\vec{x}(t))$ and the wave function $\psi(t,\vec{x})$ can be calculated for each path as follows, as Eq. (3.4) can be applied:

$$S(t,\vec{x}(t)) = \vec{p}\cdot\vec{x} - E\cdot t \qquad \text{with} \tag{3.6}$$

$$\psi(t,\vec{x}(t)) = f_n \cdot \exp(i \cdot S(t,\vec{x}(t))/\hbar) \tag{3.7}$$

Moreover, we identify the ratio $S(t,\vec{x}(t))/\hbar$ by the phase ϕ:

$$\phi(t,\vec{x}(t)) = S(t,\vec{x}(t))/\hbar \qquad \text{with} \tag{3.8}$$

$$\psi(t,\vec{x}(t)) = f_n \cdot \exp(i \cdot \phi(t,\vec{x}(t))) \tag{3.9}$$

3.1.2 Fermat's Minimum Principle

In this section, we analyze how light propagates from a point A to a point B.

3.1.2.1 Reflection

Hero of Alexandria (ca. 10 AD - 70 AD) as well as Chambre (1662) realized that light takes that path from A to B, that requires the least time, whenever the light propagates through a homogeneous medium, whereby the light may also be reflected.

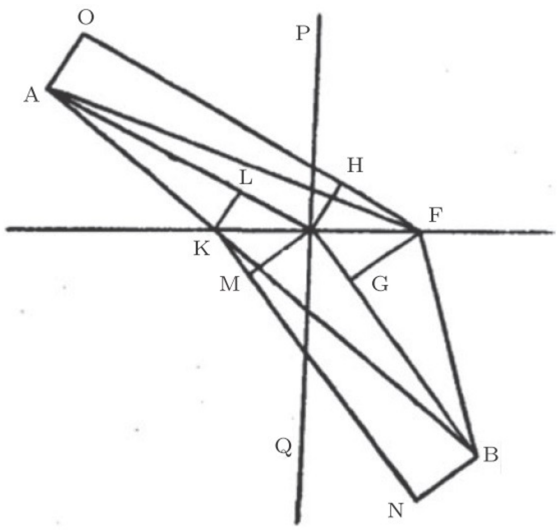

Figure 3.1: Huygens (1690) provided essentially the above illustration of the refraction of light. Moreover, he realized that the angle of refraction and Snell's law of refraction can be explained on the basis of two assumptions: The light takes the path from A to B that requires the least time, and there are appropriate velocities of propagation of light in the two media.

3.1.2.2 Refraction: Fermat's Minimum Principle

Fermat (1657) analyzed the case of refraction of light propagating from one medium I to another medium II, see Fig. (3.1). He noted that the angle of refraction can be explained on the basis of two assumptions:

(1) If light propagates from a point A to a point B, then it takes the path that requires the least time. This rule is called **Fermat's Minimum Principle**, see e. g. Born and Wolf (1980), Rojo and Bloch (2018), Erb (1992).

(2) There are appropriate velocities v_I and v_{II} of propagation of light in the two media.

3.1.2.3 Proof of Fermat's Minimum Principle

Fermat's Minimum Principle can be proven on the basis of wave theory, see (Born and Wolf, 1980, S. 3.3.2). Thereby, (Born and

Wolf, 1980, S. 3.3.2) derives the following:

If a wave with a wavelength λ propagates freely, and if the wave can take paths $\vec{x}(t)$, and if these paths start at the point A and end at the point B, and if the limit λ to zero is applied, then the light takes that path $x(t)$ that requires the least time.

3.1.3 Application of Fermat's Principle to QP

A quantum object is described by a wave function, see e. g. Kumar (2018), Carmesin (2022). If the object propagates freely, and if the object takes one path $x(t)$ in an appropriate semiclassical limit, then Fermat's Minimum Principle can be applied to the wave function.

Firstly and consequently, and in the limit λ to zero, the quantum object takes that path $x(t)$ that requires the least time.

Secondly, the path that requires the least time does also require the least phase ϕ, as the frequency of a freely propagating object is constant, see Eqs. (3.8, 3.9).

Thirdly, the path that requires the least action S, as the phase ϕ is equal to the action divided by $\hbar$, see Eqs. (3.6, 3.7, 3.8, 3.9).

We summarize:

(1) If a quantum object propagates freely, and if the object takes one path $x(t)$ in an appropriate semiclassical limit, and if the path starts at a point A and ends at a point B, then the object takes that path $x(t)$ that has the least action $S(t, x(t))$ among all conceivable paths from A to B, see Eqs. (3.6, 3.7).

(2) The above rule represents the **Principle of Least Action, PLA**[1].

[1]Such a principle is described in (Landau and Lifschitz, 1965, § 6) or Rojo and Bloch (2018).

3.1.4 Lagrangian

In this section, we represent the action in terms of an integral $\int ...dt$ of a **Langange function** L or a **Lagrangian** $\mathcal{L}$ as follows, see e.g. Landau and Lifschitz (1960), for a mechanical system

$$S(t, x(t)) = \int_{t_1}^{t_2} L(x(t), \dot{x}(t))dt \tag{3.10}$$

see e.g. (Landau and Lifschitz, 1971, § 27), for the case of the electric field $\vec{E}$ and the magnetic field $\vec{H}$:

$$S_f = \int_{t_1}^{t_2} \mathcal{L}_f dt \qquad \text{with} \tag{3.11}$$

$$\mathcal{L}_f = \frac{1}{8\pi} \cdot \int dV(\vec{E}^2 - \vec{H}^2) \tag{3.12}$$

A Lagrangian of a field is usually marked by a calligraphic $\mathcal{L}$. Altogether, the SQ implies RGWs and quantum physics, QP. Moreover, for the case of semiclassical paths in a system described by QP, the Principle of Least Action, PLA, including a corresponding description by a Lagrangian are further implications of the SQ.

Next we analyze objects that propagate under the influence of an interaction, instead of propagating freely. For it, we use the Lagrangian, and we apply the Principle of Gauge Invariance, PGI, see e.g. (Pich, 2007, S. 2), (Griffiths, 2008, S. 10.3).

3.2 Principle of Gauge Invariance, PGI

Using the basic theory, see chapter (2), we derived quantum physics. For it, we derived the semiclassical description of a freely propagating quantum object in terms of a Lagrangian $\mathcal{L}_0$, see section (3.1). However, a quantum object may interact, more generally. Accordingly, we show how the Lagrangian $\mathcal{L}_0$

can be supplemented by additional terms that represent the interaction of the object.

For it, we summarize the Principle of Gauge Invariance, PGI, and its application, see e. g. (Pich, 2007, S. 2), (Griffiths, 2008, S. 10.3). A typical Lagrangian of an object with a mass parameter m is as follows, see (Griffiths, 2008, Eq. 10.26):

$$\mathcal{L}_0 = i\hbar c \Psi^{cc}(x)\gamma^\mu \partial_\mu \Psi(x) - m \cdot c^2 \Psi^{cc}(x)\Psi(x) \tag{3.13}$$

Hereby, Ψ^{cc} is the conjugate complex of Ψ, γ^μ is a matrix in Dirac theory, ∂_μ represents a partial derivative in spacetime, whereby the sum convention is applied.

In the traditional theory of quantum physics, see e. g. Sakurai and Napolitano (1994), Ballentine (1998), Griffiths (2008), Kumar (2018), the phase has no physical meaning. So the wave function may be multiplied by a local or global phase factor as follows:

$$\Psi_\Theta = \Psi \cdot \exp(i \cdot \Theta(x)) \qquad \text{local factor} \tag{3.14}$$

$$\Psi_\Theta = \Psi \cdot \exp(i \cdot \Theta) \qquad \text{global factor} \tag{3.15}$$

Hereby, Θ and $\Theta(x)$ are some real numbers. Thus the derivative in Eq. (3.13) is as follows:

$$\partial_\mu \Psi_\Theta(x) = \partial_\mu(\Psi(x) \cdot \exp(i \cdot \Theta(x))) \tag{3.16}$$

$$= \exp(i \cdot \Theta(x)) \cdot (\partial_\mu + i\partial_\mu \Theta(x))\Psi(x) \tag{3.17}$$

However, the above derivative enters the Schrödinger equation, SEQ. The SEQ describes the dynamics of the vacuum, see Carmesin (2022). So the local phase $\Theta(x)$ enters the SEQ. Thus $\Theta(x)$ destroys the translation invariance of the SEQ and of the vacuum, which is not physical, as the vacuum itself is translation invariant. Hence, the local phase $\Theta(x)$ must be compensated in the SEQ. This requirement is named **Principle of Gauge Invariance, PGI**. For it, a correction term must be added. This is achieved by a **covariant derivative** as follows:

$$D_\mu \Psi(x) = [\partial_\mu + i \cdot q \cdot A_\mu(x)] \cdot \Psi(x) \qquad \text{with} \tag{3.18}$$

$$A_{\mu,\Theta}(x) = A_\mu(x) - \frac{1}{q}\partial_\mu \Theta(x) \tag{3.19}$$

Hereby, A_μ represents the vector potential and the electric potential, see e. g. Landau and Lifschitz (1971), Aharonov and Bohm (1959). In order to test the correction term, we apply Eq. (3.16) to Eq. (3.18):

$$D_\mu e^{i\Theta(x)}\Psi(x) = e^{i\Theta(x)}[\partial_\mu + i\partial_\mu \Theta(x) + iqA_{\mu,\Theta}(x)]\Psi(x) \quad \text{so} \tag{3.20}$$

$$D_\mu e^{i\Theta(x)}\Psi(x) = e^{i\Theta(x)}[\partial_\mu + iqA_\mu(x)] \cdot \Psi(x) \tag{3.21}$$

Hereby, we used Eq. (3.19). Next, we apply $e^{i\Theta(x)}\Psi(x) = \Psi_\Theta(x)$:

$$D_\mu \Psi_\Theta(x) = [\partial_\mu + iqA_\mu(x)] \cdot \Psi_\Theta(x) \tag{3.22}$$

The above transformed derivative is the same as the original derivative in Eq. (3.18). So our test confirms the correction term, and the Principle of Gauge Invariance, PGI is obeyed. More generally, the phase factor $\exp(i\Theta(x))$ can be replaced by a transformation of the group $SU(2)$ or $SU(3)$, see e. g. (Pich, 2007, S. 2), Griffiths (2008).

This example shows how the electromagnetic interaction can be derived from the PGI, if the charge q is known, see e. g. Feynman (1985), Carmesin (2021f).

Altogether, the SQ implies the PLA in an appropriate semi-classical limit, which in turn implies the PGI, in the framework of traditional quantum theory with phases without physical meaning. The precise relation to the theory of vacuum, including physical interpretation, is elaborated in the main chapters of the book.

3.3 SMEP

Using the basic theory, see chapter (2), we derived the mass of the Higgs boson, which is underlying for the mass of the electron, for instance, according to the Higgs mechanism. Moreover, we derived the sum of the masses of neutrinos.

In this section we apply the pair (electron, electronic neutrino), in order to present a short description of the standard model of elementary particles, see e.g. Tanabashi et al. (2018). The model is essentially constituted by three generations, see e.g. Kobel et al. (2017). These are basically understood by the beta decay.

3.3.1 β-decay

In the beta decay, a neutron, n, decays into a proton, p, an electron, e^- and an electronic antineutrino, $\bar{\nu}_e$:

$$n \to p + \bar{\nu}_e + e^- \tag{3.23}$$

On the level of quarks, the beta decay can be modeled by the decay of a down quark, d, into an up quark, u, an electron, e^- and an electronic antineutrino, $\bar{\nu}_e$:

$$d \to u + \bar{\nu}_e + e^- \tag{3.24}$$

3.3.2 Isospin - pairs

In the above reaction Eq. (3.24), we transfer the antineutrino from the products to the educts by changing it to a neutrino:

$$d + \nu_e \to u + e^- \tag{3.25}$$

This is interpreted by a transformation of a down quark into an up quark combined with a transformation of an electronic neutrino into an electron. Correspondingly, the down quark and the up quark are interpreted as two states such as two spin states. Accordingly, a new isospin has been introduced, and the down quark has isospin $I_z = -1/2$, while the up quark has isospin $I_z = 1/2$. So these two quarks form a pair:

$$\begin{pmatrix} u \\ d \end{pmatrix} \tag{3.26}$$

Similarly, and the electronic neutrino has the isospin $I_z = 1/2$, while the electron has the isospin $I_z = -1/2$, see Eq. (3.29). Thus, these two leptons constitute another isospin pair:

$$\begin{pmatrix} \nu_e \\ e^- \end{pmatrix} \tag{3.27}$$

As these two isospin pairs are combined in the beta decay, they are combined to the following quadruple:

$$\begin{pmatrix} \begin{pmatrix} u \\ d \end{pmatrix} \\ \begin{pmatrix} \nu_e \\ e^- \end{pmatrix} \end{pmatrix} \tag{3.28}$$

3.3.3 Isospin

The usual spin states are related to rotations, and these are represented by the special (with determinant one) orthogonal group in three dimensions, the $SO(3)$. Similarly, the isospin states are related to transformations, and these are again represented by a group, the special unitary group in two dimensions, $SU(2)$.

3.3.4 Generations

The quadruple in Eq. (3.28) is a first quadruple that had been developed in several steps: Pauli proposed the existence of the neutrino as a part of the beta decay in 1930. That neutrino has been directly observed since 1953. The quark model has been proposed around 1960.

Later, two similar quadruples have been discovered. Thereby the top quark was discovered in 1993 and completed these three quadruples. The numbers of these three quadruples are called generations, see Eq. (3.30). The particles of the second and third generation in Eq. (3.30) are the charm quark, c, strange quark, s, top quark, t, bottom quark, b, muon, μ, tauon, τ as well as corresponding neutrinos ν_μ and ν_τ.

$$\begin{pmatrix} gen.1 \\ \begin{pmatrix} u \\ d \end{pmatrix} \\ \begin{pmatrix} \nu_e \\ e^- \end{pmatrix} \end{pmatrix} \rightarrow \begin{pmatrix} I_z \\ \begin{pmatrix} \frac{1}{2} \\ -\frac{1}{2} \end{pmatrix} \\ \begin{pmatrix} \frac{1}{2} \\ -\frac{1}{2} \end{pmatrix} \end{pmatrix} \rightarrow \begin{pmatrix} q \\ \begin{pmatrix} \frac{2}{3} \\ -\frac{1}{3} \end{pmatrix} \\ \begin{pmatrix} 0 \\ -1 \end{pmatrix} \end{pmatrix} \tag{3.29}$$

$$\begin{pmatrix} gen.1 \\ \begin{pmatrix} u \\ d \end{pmatrix} \\ \begin{pmatrix} \nu_e \\ e^- \end{pmatrix} \end{pmatrix} \rightarrow \begin{pmatrix} gen.2 \\ \begin{pmatrix} c \\ s \end{pmatrix} \\ \begin{pmatrix} \nu_\mu \\ \mu \end{pmatrix} \end{pmatrix} \rightarrow \begin{pmatrix} gen.3 \\ \begin{pmatrix} t \\ b \end{pmatrix} \\ \begin{pmatrix} \nu_\tau \\ \tau \end{pmatrix} \end{pmatrix} \tag{3.30}$$

In addition to these particles, the standard model contains bosons that transmit interactions:

The weak interaction is transmitted by W bosons, W^+, W^- and W^0 (also called Z-boson, Z represents zero). The electromagnetic interaction is transmitted by virtual photons. The strong interaction is transmitted by gluons. Beyond the standard model is the hypothetical graviton, see Blokhintsev and Galperin (1934), Carmesin (2021d). The masses of most particles of the standard model are based on the Higgs boson, see e.g. (Peskin, 2015, p. 9-10) or Tanabashi et al. (2018).

3.3.5 Two additional symmetries

We remind that the isospin states form pairs and are related to transformations that represent a group, the special unitary group in two dimensions, the $SU(2)$. Similarly, the quarks u, d and s form a triplet and are related to transformations that represent a group, the special unitary group in three dimensions, the $SU(3)$. That group can explain several elementary particles that are formed from the quarks u, d and s.

An additional symmetry is related to the electromagnetic interaction. An effect of that interaction can be modeled by a change of a phase of a complex number. As numbers represent one dimension, the corresponding group is the special unitary group in one dimension, the $SU(1)$. Altogether, symmetries inherent to elementary particle physics are described by using the groups $SU(1)$, $SU(2)$ and $SU(3)$ including their combinations. Possible relations to higher dimensional groups are being investigated since many decades.

3.3.6 Mixing

The system of elementary particles (Eq. 3.30) has been developed according to reactions such as the beta decay and according to symmetries of $SU(1)$, $SU(2)$ and $SU(3)$. However, the neutrinos of the three generations ν_e, ν_μ and ν_τ can periodically transform into each other, that phenomenon is called neutrino oscillation, see e.g. Tanabashi et al. (2018). Correspondingly, these neutrinos ν_e, ν_μ and ν_τ are modeled as linear combinations of underlying neutrinos ν_1, ν_2 and ν_3. That linear combination is called neutrino mixing and it is described by a mixing matrix U, see e.g. (Tanabashi et al., 2018, S. 14).

Similarly, the masses of the six quarks of the three generations (see Eq. 3.30) are derived on the basis of a mixing matrix, called V_{CKM}, see e.g. (Tanabashi et al., 2018, S. 12).

3.4 SMEWI

In this section, we explain and summarize the Standard model of the weak interaction, SMEWI, see Pich (2007).

3.4.1 Explanation of two couplings

Using the basic theory, see chapter (2), we derived the elementary electric charge. That derivation shows already, that the elementary charge gives rise to a two-dimensional **vector space of charges**, see Fig. (6.2). Using that vector space of charges, we can directly understand the traditional description of the SMEWI, which uses two couplings, which correspond to two charges.

3.4.2 Explanation of the $SU(2)$-group of isospin

As we derived two components of the elementary electric charge, Carmesin (2021f), there is a two-dimensional vector space of charges, see Fig. (6.2).

Thereby, a quantum object has a charge according to its **own dynamics**, see Carmesin (2021f). That charge of the quantum object is represented in the two-dimensional vector space of charges. Since that charge of the quantum object is generated by the own dynamics alone, that charge is not influenced from outside, and the object generates freely the corresponding charge vector in the vector space of charges. This shows that there is no influence at all from outside, when the object generates its charge state. Accordingly, the **object experiences an isotropic or symmetric two-dimensional charge space**, in which the object can generate its charge freely according to its own dynamics, see Carmesin (2021f):

$$\text{charge space is isotropic} \tag{3.31}$$

This fact can be expressed as follows: If a state $\vec{v}$ in charge space is rotated in charge space by a rotation $\hat{D}$, then the state remains physically equivalent:

$$\hat{D} \cdot \vec{v} \ \text{ equivalent } \ \vec{v} \tag{3.32}$$

The equivalence means that an observable A, represented by an operator $\hat{A}$, provides the same results in both cases, whereby state $\vec{v}$ is represented by its wave function ψ:

$$\hat{A} \cdot \hat{D} \cdot \psi = \hat{A} \cdot \psi \tag{3.33}$$

The basic theory, see chapter (2), implies quantum physics, QP, including known facts about QP. Such a fact about QP is Wigner's theorem, see Wigner (1931), Wigner (1959). According to Wigner's theorem, the rotation $\hat{D}$ in charge space is a unitary or anti-unitary transformation multiplied by a phase factor, most generally. Here we exclude the anti-unitary transformation, as it is not plausible. As the charge space has the dimension two, the unitary transformation $\hat{D}$ is in the group $SU(2)$.

For that relation of the two-dimensional space of charges to a the group $SU(2)$ acting on a two-dimensional space, we note an analogy: There is a number N_c of different color charges, (Pich, 2007, S. 2.2 or Fig. 3), (Cottingham and Greenwood, 2007, S. 1 or Fig. 1.7). Observations show that N_c is equal to three, see e. g. (Pich, 2007, S. 2.2 or Fig. 3), (Cottingham and Greenwood, 2007, S. 1 or Fig. 1.7). Accordingly, the corresponding states in Hilbert space $\mathcal{H}$ are invariant with respect to the group $SU(3)$ of color charges, see e. g. Pich (2007), (Cottingham and Greenwood, 2007, S. 1 or Fig. 1.7), Zyla (2020).

3.4.3 Traditional description

Salam and Ward (1959), Glashow (1959) and Weinberg (1967) proposed a unification of the electromagnetic and of the weak interaction. This proposal turned out to be very successful in describing observations. Accordingly, this proposal essentially represents the present day standard model of the electroweak interaction, SMEWI. In this section, we summarize essential results of the standard model of the electroweak interaction, SMEWI, see e.g. Pich (2007).

3.4.4 Electromagnetic and weak interaction

In this section, we summarize the sources of interactions. For instance, the source of the gravitational interaction is a mass or dynamical mass. Similarly, the source of the electromagnetic interaction is the electric charge q_e. Accordingly, in the case of the weak interaction, there should be a corresponding source q_Z that has zero electric charge.

However, in general, a physical object has a mass or dynamical mass as a source of gravity and it may have both sources or charges q_e and q_Z. Thus the sources q_e and q_Z carried by an object form linear combination of q_e and q_Z, most generally. Accordingly, the sources q_e and q_Z carried by an object can naturally be represented in a two dimensional **vector space of charges** or **vector space of sources**.

3.4.4.1 Strength of source and of interaction

In this section, we summarize the relation between the strength of the source and the strength of the interaction.

For this purpose, we analyze the electromagnetic interaction: The strength of the source of an object is described by its electric charge q_e. Thereby, the electric charge is at best described as a product of the elementary charge e and a number n_e of elementary charges carried by that object[2].

The strength of the interaction is at best described by the fine structure constant α.

Moreover, the fine structure constant α is the square of the elementary charge in Planck units $\tilde{e}$:

$$\alpha = \tilde{e}^2 \tag{3.34}$$

So the elementary charge in Planck units $\tilde{e}$ describes the strength of the charge as well as the strength of the interac-

[2]For the case of quarks, n_e may be a fraction with the denominator three, whereas n_e is an integer for other elementary particles, see e. g. Zyla (2020), Carmesin (2021f).

tion. Thus the two strengths are unified in Planck units. Note that these two strengths are also unified in the Gaussian system of units, see Gauss (1833) or (Zyla, 2020, S. 7), (Landau and Lifschitz, 1971, § 27), whereas these strengths are not unified in the SI system. Of course, there is a unique method of transformation, see e.g. (Jackson, 1975, p. 818).

We use the Planck system in the following. So the sources q_e and q_Z of the interactions include the strengths of these interactions.

In the literature, these charges are also called couplings, see e.g. (Weinberg, 1996, 21.3.19), (Zyla, 2020, Eqs. 10.4b,c). Accordingly, we will also use the word couplings as a synonym for such charges.

3.4.4.2 Effect of an interaction

In many cases, an interaction causes an acceleration. Examples are attractive or repulsive interactions. However, in quantum physics, an interaction has an effect upon the Hamiltonian or the energy term of an object or of a system of objects, Ballentine (1998), Kumar (2018), Carmesin (2022). Thus there is an effect upon the corresponding wave function, most generally. For instance, the spin described by the wave function might change. More generally, the isospin of an object may change, as an effect of an interaction. In particular, there may be an effect upon the third component of the isospin. It is an observable described by the following operator:

$$\hat{t}_3 = \frac{1}{2}\sigma_3 = \frac{1}{2} \cdot \begin{pmatrix} 1 & 0 \\ 0 & -1 \end{pmatrix} \tag{3.35}$$

In the context of the electroweak interaction, the isospin is denoted by operators

$$\hat{t}_j = \frac{1}{2}\sigma_j \quad \text{with} \quad j \in \{1, 2, 3\} \tag{3.36}$$

Hereby, σ_j denote the Pauli matrices.

3.4.4.3 Charge g of the isospin interaction

The electroweak interaction has an effect upon the isospin. So the corresponding Langrangian contains a product of $\hat{t}_3$ and a respective charge. That charge is called g, see e.g. (Tanabashi et al., 2018, S. 10) or (Pich, 2007, S. 3.4) or (Weinberg, 1996, S. 21.3). So there are terms in the Lagrangian proportional to $\hat{t}_3 \cdot g$.

3.4.4.4 Charge g' of the hypercharge interaction

The electroweak interaction has an effect proportional to the electric charge q_e and proportional to a novel non-electric charge q_Z. Both charges are summarized by a common charge of an object j. It is the **hypercharge** $y_j \cdot g'$ of the object j. Hereby, y_j is the **hypercharge - number** of an object j, whereas g' is a **hypercharge - coupling**. Note that some authors name the hypercharge - number shortly 'hypercharge', see e.g. (Zyla, 2020, S. 11.2) or Pich (2007). The hypercharge - number y_j can take the same values that the charge number n_e can take. Accordingly, there are terms in the Lagrangian proportional to the hypercharge $y_j \cdot g'$.

3.4.5 Lagrangian

In this section, we summarize a Lagangian that describes the SMEWI, see e.g. Pich (2007).

3.4.5.1 Free Lagrangian

The free Lagrangian for three possible bosons $j = 1, 2, 3$ is as follows, see e.g. (Pich, 2007, Eq. 3.6), :

$$\mathcal{L}_{free} = i\Sigma_{boson\ j=1}^{3} \Psi_j^{cc} \gamma^\mu \partial_\mu \Psi_j \tag{3.37}$$

Note that the factor i comes from the momentum operator, e.g. $\hat{p}_x = -i\hbar\partial_x$, see e.g. Kumar (2018), Carmesin (2022).

3.4.5.2 Lagrangian in QED

According to the principle of minimal coupling, see e.g. Landau and Lifschitz (1971), the free Lagrangian $\mathcal{L}_{free}$ is supplemented by the Lagrangian of quantum electrodynamics, QED, $\mathcal{L}_{QED}$. Thereby, the Lagrangian $\mathcal{L}_{QED}$ is as follows, see e.g. (Pich, 2007, Eq. 3.27):

$$\mathcal{L}_{QED} = -e \cdot A_\mu \Sigma^3_{boson\ j=1} \Psi^{cc}_j Q_j \gamma^\mu \Psi_j \tag{3.38}$$

Hereby, the Q_j represent charge numbers of the bosons $j = 1, 2, 3$.

3.4.5.3 Structure of the electroweak interaction

Based on the empirical findings in the field of the weak interaction, the **electric interaction** can be generalized by a concept of **electroweak interaction**. Thereby, the **electric charge** can be generalized by a concept of **neutral - current**.

Hereby, the electroweak interactions consist of **neutral - current interactions** and the **charged - current interactions**. Thereby, the **neutral - current interactions** are mediated by photons or by electrically neutral Z bosons of the electroweak interaction, and the **charged - current interactions** are mediated by electrically charged W^+ bosons or W^- bosons of the electroweak interaction, see e.g. (Pich, 2007, S. 3).

Fields and currents in the Lagrangian: The Lagrangian $\mathcal{L}_{EW}$ representing the electroweak interaction, can be expressed as follows, see e.g. (Pich, 2007, Eq. 3.23) or (Tanabashi et al., 2018, S. 10):

$$\mathcal{L}_{EW} = A_\mu J^\mu_{em} + Z_\mu J^\mu_Z \qquad \text{with} \tag{3.39}$$

Hereby, A_μ represents the usual electromagnetic field (including the three dimensional vector potential and the scalar potential

Φ) in the framework of spacetime, while Z_μ represents an electrically neutral field inherent to the electroweak interaction. The corresponding currents are described in the following.

Electrically charged current: The field A_μ corresponds to the **electrically charged current** J^μ_{em} as follows, see for instance (Pich, 2007, Eq. 3.23):

$$J^\mu_{em} = -\gamma^\mu \Sigma^3_{boson\ j=1} \Psi^{cc}_j \left[g\frac{\sigma_3}{2} \sin\Theta_W + g' \cdot y_j \cdot \cos\Theta_W \right] \Psi_j \tag{3.40}$$

Hereby, g and g' are the **couplings of the electroweak interaction**, (Zyla, 2020, p. 204). Moreover, Θ_W is the angle describing the electroweak interaction. It is a mixing angle, see e.g. (Tanabashi et al., 2018, p. 875). It is also called **weak angle**, see e.g. (Tanabashi et al., 2018, p. 161), or **Weinberg angle** (Tanabashi et al., 2018, p. 607). Furthermore, y_j is the **hypercharge - number** of the boson j, see for instance (Pich, 2007, Eqs. 3.8, 3.9). Additionally, σ_3 is the third Cartesian component of the **isospin** of the object under consideration, see for instance (Pich, 2007, p. 12). Hereby, σ_3 is a Pauli matrix, see e.g. (Pich, 2007, p. 41).

Electrically neutral current: The field Z_μ corresponds to the **electrically neutral current** J^μ_Z as follows, see for instance (Pich, 2007, Eq. 3.23):

$$J^\mu_Z = \gamma^\mu \Sigma^3_{boson\ j=1} \Psi^{cc}_j \left[g\frac{\sigma_3}{2} \cos\Theta_W - g' \cdot y_j \cdot \sin\Theta_W \right] \Psi_j \tag{3.41}$$

3.5 Units used in the SMEWI

In this section, we summarize the units that are usually used in the SMEWI.

The elementary electric charge used in the SMEWI, $\tilde{e}_{SMEWI}$ is obtained from the elementary electric charge in Planck units,

$\tilde{e}$, by multiplication by $\sqrt{4\pi}$, see e.g. (Weinberg, 1996, p. 310):

$$\tilde{e}_{SMEWI} = \tilde{e} \cdot \sqrt{4\pi} \tag{3.42}$$

The explanation of the factor $\sqrt{4\pi}$ will be prepared in chapters (5, 6, 8) and presented in chapters (10). Additionally, for the case of the bosons of the weak interaction, the charge $\tilde{e}_{SMEWI}$ is multiplied by the correction factor $\sqrt{\frac{137}{129}}$, based on diagrammatic corrections of the QFT, see e.g. (Weinberg, 1996, p. 311):

$$\tilde{e}_{eff} = \tilde{e}_{SMEWI} \cdot \sqrt{\frac{137}{129}} = \tilde{e} \cdot \sqrt{4\pi} \cdot \sqrt{\frac{137}{129}} \tag{3.43}$$

Note that this correction factor corresponds to the largest perturbation in table (5.1), according to $\tilde{e} = \sqrt{\alpha} \approx \sqrt{1/137}$. Such a correction is sometimes named a correction due to a perturbation or **gliding coupling**, see e.g. (Weinberg, 1996, p. 311).

Next, we insert the theoretical value of the elementary electric charge in Planck units, $\tilde{e}_{theo}$, derived on the basis of the SQ, see (Carmesin, 2021f, THM 4):

$$\tilde{e}_{theo} = 0.085\,424\,547\,738 \quad \text{with} \tag{3.44}$$

$$\Delta_{rel.,theo,obs,e} = 5.4 \cdot 10^{-8} = 0.054\,\text{ppm} \tag{3.45}$$

Hereby, $\Delta_{rel.,theo,obs,e}$ represents the relative difference between the theoretical value and the observed value.

Altogether, the corrected elementary electric charge in the SMEWI is as follows:

$$\tilde{e}_{eff} = 0.312\,070\,738 \quad \text{with} \quad \Delta\tilde{e}_{rel.,corr} \approx 1\% \tag{3.46}$$

Hereby, we estimate the relative error by 1%, as we estimate the relative error of the correction factor $\sqrt{\frac{137}{129}}$ by 1%.

Chapter 4

Aim

In this chapter, we realize that many essential parameters of the SMEP and the SMEWI, such as charges and masses of elementary particles, are not explained or derived by the SMEP or by the SMEWI. Accordingly, we formulate a list of questions that are open in the SMEP and the SMEWI. The aim of the book is to use the SQ, in order to derive answers to the following questions:

4.1 Open questions in SMEP and SMEWI

A 'fundamental theory' should provide the values of the parameters of the standard model, such as charges and masses of elementary particles, from first principles, (Zyla, 2020, p. 507, line 37-41). Accordingly, we summarize the following questions that are not answered in SMEP and SMEWI:

1. How is the mass m_H of the **Higgs boson** explained and derived (Zyla, 2020, p. 507, line 37-41)?

2. How is the **elementary electric charge** $\tilde{e}$ explained and derived (Zyla, 2020, p. 507, line 37-41)?

3. How are the **couplings of the electroweak interaction**, g and g', explained and derived, (Zyla, 2020, p. 507, line 37-41)?

4. How is the **weak angle** Θ_W of the electroweak interaction explained and derived (Zyla, 2020, p. 507, line 37-41)?

5. How is the assumed mechanism of **electroweak symmetry breaking** explained and derived (Zyla, 2020, p. 204), (Weinberg, 1996, p. 308, lines 9-10)?

6. How is the **vacuum expectation value, VEV**, explained and derived (Zyla, 2020, p. 204)?

Additionally, we summarize the following questions about fundamental principles used in SMEP and SMEWI:

7. What fundamental physical entity is the **basis of the principle of least action, PLA, or stationary action, PSA** (Landau and Lifschitz, 1965, S. 18), Griffiths (2008), Schwartz (2014)?

8. What fundamental physical entity is the **basis of the principle of gauge invariance, PGI**, see e.g. (Landau and Lifschitz, 1965, S. 18), (Pich, 2007, S. 2), (Griffiths, 2008, S. 10.3), Schwartz (2014)?

9. Has general relativity, GR, been derived by the PLA or PSA, see e.g. Hilbert (1915), Landau and Lifschitz (1971), Hobson et al. (2006)?

10. Has general relativity, GR, been derived by the PGI, see e.g. Lasenby et al. (1998), Santos (2019)?

Chapter 5

Formation of hypercharge

In this chapter, we apply the SQ, in order to derive and explain the formation of the hypercharge.

5.1 Structure of electric charge $\tilde{e}$

In this section, we apply the fact that the field emitted by the electric charge $\tilde{e}$ is formed as a sum of squares of fields, see equation ((Carmesin, 2021f, Eq. 3.73)). We use two groups of squares: those that are added and those that are subtracted.

It turns out that these two groups are naturally represented in a plane or two dimensional vector space, see Fig. (5.1). What physical entities are in that space?

The charge $\tilde{e}$ is an observable, so it can be represented by a linear operator $\hat{\tilde{e}}$ that acts in the Hilbert space $\mathcal{H}$ of quantum physics. We realize that this linear operator $\hat{\tilde{e}}$ is represented in a plane, see Fig. (5.1), corresponding to the two-dimensional charge space. So the linear operator can naturally be decomposed into components in that plane. Two possibilities of linear decomposition of the operator $\hat{\tilde{e}}$ are elaborated in the following.

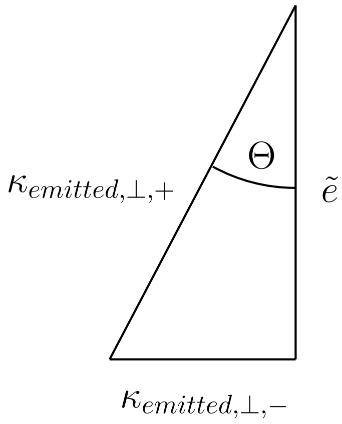

Figure 5.1: Vector space of sources makes transparent the structure of the elementary charge: The elementary charge $\tilde{e}$ is constituted by two components of emitted fields $\kappa_{emitted,\perp,+}$ and $\kappa_{emitted,\perp,-}$, that add according to the theorem of Pythagoras (Carmesin, 2021f, Eq. 3.73). Correspondingly, these two components and the resulting elementary charge form a right-angled triangle and add like vectors.

5.1.1 The component $\kappa_{emitted,\perp,+}$ of $\tilde{e}$

From equation ((Carmesin, 2021f, Eq. 3.73)), we derive the following relation:

$$\tilde{e}^2 = \kappa^2_{emitted,\perp,+} - \kappa^2_{emitted,\perp,-} \qquad \text{or} \tag{5.1}$$

Hereby, we introduced the following abbreviations:

$$\kappa^2_{emitted,\perp,+} = \frac{\hat{G}^{*2}_{\alpha,1\to2} + \hat{G}^{*2}_{\alpha,1\to3} + \hat{G}^{*2}_{\alpha,2\to1} + \hat{G}^{*2}_{\alpha,2\to3}}{G^{*2}_{m_c}} \quad \text{and} \tag{5.2}$$

$$\kappa^2_{emitted,\perp,-} = \frac{\hat{G}^{*2}_{\alpha,3\to1} + \hat{G}^{*2}_{\alpha,3\to2}}{G^{*2}_{m_c}} \tag{5.3}$$

Thereby, the $\hat{G}^*_{\alpha,j\to i}$ represent fields that are emitted by the following forced oscillations: The formation of mass has been modeled on the basis of the SQ, and in terms of a triple of rate gravity waves, RGW, whereby the result is in precise accordance with observation, and whereby no fit has been used, see section (2.5) and Carmesin (2021a). As a consequence, each of these three RGWs generates a forced oscillation at the two other RGWs, see e.g. Landau and Lifschitz (1976). These forced oscillations emit the above fields $\hat{G}^*_{\alpha,j\to i}$, see section (2.6) and Carmesin (2021f).

We solve equation (5.1) for $\kappa^2_{emitted,\perp,+}$:

$$\kappa^2_{emitted,\perp,+} = \tilde{e}^2 + \kappa^2_{emitted,\perp,-} \tag{5.4}$$

The above equation represents the theorem of Pythagoras.

Thereby $\kappa_{emitted,\perp,+}$ represents the hypotenuse, while $\tilde{e}$ and $\kappa_{emitted,\perp,-}$ are the two legs of the right-angled triangle, see Fig. (5.1). In that triangle, we denote the angle at the sides $\tilde{e}$ and $\kappa_{emitted,\perp,+}$ by Θ.

Algebraically, the angle is characterized as follows:

$$\tilde{e} = \kappa_{emitted,\perp,+} \cdot \cos\Theta_W \qquad \text{or} \tag{5.5}$$

$$\kappa_{emitted,\perp,+} = \tilde{e}/\cos\Theta_W \tag{5.6}$$

5.1.2 Calculation of the angle Θ

In this section, we calculate the angle Θ. For it, we apply Eq. (Carmesin, 2021f, Eq. 6.20):

$$\hat{G}^*_{\alpha,j\to i} = G^*_{m_c} \cdot \frac{1}{\kappa_{sim.}} \cdot \ln\left(1 + \frac{\kappa_{sim.}}{|\bar{n}_i^2 - \bar{n}_j^2|}\right) \text{ with} \tag{5.7}$$

$$\bar{n}_j = 2j + 1 \quad \text{and} \quad j \in \{1,2,3\}; \quad i \in \{1,2,3\}; \tag{5.8}$$

Hereby, $\kappa_{sim.}$ represents a correction factor obtained by an iteration essentially including Eq. (5.7), for details see Carmesin (2021f). Its value is as follows, see Eq. (Carmesin, 2021f, Eq. 6.35):

$$\kappa_{sim.} = 1 + \kappa^{(5)}_{emitted,\perp} = 1.085\,523\,610\,521 \qquad \text{with} \tag{5.9}$$

$$\kappa^{(5)}_{emitted,\perp} = 0.085\,523\,610\,521 \tag{5.10}$$

With it, we derive the following values $\hat{G}^*_{\alpha,j\to i}/G^*_{m_c}$, which have been derived in (Carmesin, 2021f, Eq. 3.39) and on the basis of QG, which is based on the SQ:

$$\frac{\hat{G}^*_{\alpha,j\to i}}{G^*_{m_c}} = \frac{1}{\kappa_{sim.}} \cdot \ln\left(1 + \frac{\kappa_{sim.}}{|\bar{n}_i^2 - \bar{n}_j^2|}\right) \quad \text{with} \tag{5.11}$$

$$\frac{\hat{G}^*_{\alpha,1\to 2}}{G^*_{m_c}} = 0.060\,474\,324\,951 \quad \text{and} \tag{5.12}$$

$$\frac{\hat{G}^*_{\alpha,1\to 3}}{G^*_{m_c}} = 0.024\,666\,875\,723 \quad \text{and} \tag{5.13}$$

$$\frac{\hat{G}^*_{\alpha,2\to 3}}{G^*_{m_c}} = 0.040\,752\,509\,621 \tag{5.14}$$

Using these results, we calculate the positive and negative components, see Eqs. (5.2, 5.3):

$$\kappa^2_{emitted,\perp,+} = 0.009\,583\,509\,754\,90 \quad \text{and} \tag{5.15}$$

$$\kappa^2_{emitted,\perp,-} = 0.002\,269\,221\,798\,39 \quad \text{and} \tag{5.16}$$

$$\kappa_{emitted,\perp,+} = 0.097\,985\,540\,211\,32 \quad \text{and} \tag{5.17}$$

$$\kappa_{emitted,\perp,-} = 0.047\,636\,349\,549\,37 \tag{5.18}$$

$$\sqrt{\kappa^2_{emitted,\perp,+} - \kappa^2_{emitted,\perp,-}} = 0.085\,523\,610\,520\,78 = \tilde{e} \tag{5.19}$$

According to the triangle in Fig. (5.1), we obtain the following angle:

$$\sin^2(\Theta_W) = \frac{\kappa^2_{emitted,\perp,-}}{\kappa^2_{emitted,\perp,-} + \tilde{e}^2} = 0.236\,784 \quad \text{or} \tag{5.20}$$

$$\Theta_W = 29.117\,653^{\text{o}} \tag{5.21}$$

5.1.3 Perturbation theory for α

In the SMEP, the couplings of the electromagnetic interaction, of the weak interaction and of the strong interaction are related to the same constant, the fine structure constant α, see e.g. Zyla (2020), Weinberg (1996), Griffiths (2008). Moreover, the square root of the fine structure constant, $\sqrt{\alpha}$, is equal to the elementary electric charge in Planck units $\tilde{e}$, see e.g. Feynman (1985), Carmesin (2021f):

$$\tilde{e} = \sqrt{\alpha} \tag{5.22}$$

Moreover, the above three interactions are based on charges with different signs or colors, consequently, these charges can screen each other. Thus an observer who measures the charge in its vicinity obtains a larger value than an observer measuring the same charge at a distant location. Usually, a measurement of a charge in its vicinity requires a quantum object with a small wavelength, corresponding to a high energy E.

Accordingly, the observed charge can be described by an effective charge $\tilde{e}_{eff}(E)$ and by an effective fine structure constant $\alpha_{eff}(E)$ as follows:

$$\tilde{e}_{eff}(E) = \sqrt{\alpha_{eff}(E)} = \tilde{e} \cdot q_{corr}(E) \quad \text{with} \tag{5.23}$$

$$q_{corr}(E) = \sqrt{\frac{\alpha_{eff}(E)}{\alpha}} \quad \text{and} \tag{5.24}$$

$$\tilde{e}_{SMEWI,eff}(E) = \tilde{e}_{SMEWI} \cdot q_{corr}(E) \tag{5.25}$$

Hereby, we introduced the correction factor $q_{corr}(E)$.

The above measured values $\alpha_{eff}(E)$ are theoretically described with help of a perturbation theory, see e.g. table (5.1). In the present study, we apply results of perturbation theory, see e.g. Jegerlehner (2001), Jegerlehner (2011), Jegerlehner (2019), (Zyla, 2020, S. 10.2), (Weinberg, 1996, p. 311), see table (5.1).

$\frac{E}{\text{GeV}}$	0.01	0.1	1	10	80
$\frac{1}{\alpha_{eff}(E)}$	136.8	136.24	134.95	132.28	129

Table 5.1: Inverse effective fine structure constant $\frac{1}{\alpha_{eff}(E)}$ as a function of the energy E in GeV, see e.g. Jegerlehner (2001), Jegerlehner (2011), Jegerlehner (2019), (Weinberg, 1996, p. 311).

Accordingly, we apply the correction factor to Eq. (5.20):

$$\sin^2 \Theta_W(E) = \frac{\kappa^2_{emitted,\perp,-}}{\kappa^2_{emitted,\perp,-} + \tilde{e}^2 q^2_{corr}(E)} = \frac{\kappa^2_{emitted,\perp,-}}{\kappa^2_{emitted,\perp,-} + \alpha_{eff}(E)} \tag{5.26}$$

Using the above Eq., we obtain the values $\sin^2 \Theta_W(E)$ shown in table (5.2).

$\frac{E}{\text{GeV}}$	0.01	0.1	1	10	80
$\sin^2 \Theta_W(E)$	0.23665	0.23628	0.23542	0.233627	0.2314

Table 5.2: Values for $\sin^2 \Theta_W(E)$ as a function of the energy E in GeV.

5.1.4 Amount of perturbations

If the energy varies in the interval $\frac{E}{\text{GeV}} \in [0.01, 80]$, then the relative difference of the effective fine structure constant $\alpha_{eff}(E)$ and the fine structure constant α varies in the following interval, see table (5.1):

$$\frac{|\alpha_{eff}(E) - \alpha|}{\alpha} \in [0, 6.2\%], \quad \text{if} \quad \frac{E}{\text{GeV}} \in [0.01, 80] \tag{5.27}$$

Similarly, the square relative difference of the $\sin^2\Theta_W(E)$ varies as follows, see table (5.2):

$$\frac{|\sin^2\Theta_W(E) - \sin^2\Theta_W(0.01\text{GeV})|}{\sin^2\Theta_W(0.01\text{GeV})} \in [0, 2.27\%], \tag{5.28}$$

$$\text{if} \quad \frac{E}{\text{GeV}} \in [0.01, 80] \tag{5.29}$$

Altogether, the perturbations are relatively small.

5.1.5 Application of perturbations

The perturbations are applied to couplings as follows, see Figs. (5.1, 6.1, 6.2):

$$g'(E) = \tilde{e}_{eff}(E)/\cos\Theta_W(E) \qquad \text{and} \tag{5.30}$$

$$g(E) = \tilde{e}_{eff}(E)/\sin\Theta_W(E) \qquad \text{and} \tag{5.31}$$

$$g_z(E) = \sqrt{g^2(E) + g'^2(E)} \tag{5.32}$$

5.1.6 Comparison of Θ with the weak angle Θ_W

In this section, we compare the angle Θ derived from our theory, see dotted line in Fig. (5.2), with the weak angle or Weinberg angle Θ_W based on observations, see data points Fig. (5.2). We emphasize that we derived the values of the angle Θ without application of any fit. Next, we investigate the angle Θ derived from our theory:

(1) The dotted lines in Fig. (5.2) show the angle Θ, as well as the angle Θ as a function of E, **derived from our theory**.

(2) Our derived values of the angle Θ are in **accordance with the observed values** of the weak angle Θ_W.

(3) So our theory **explains the weak angle** Θ_W.

(4) In particular, our theory is in precise accordance, that is in accordance within the errors of measurement, for the cases of the APV-experiment, CMS-experiment, ATLAS-experiment and Tevatron-experiment, see Fig. (5.2).

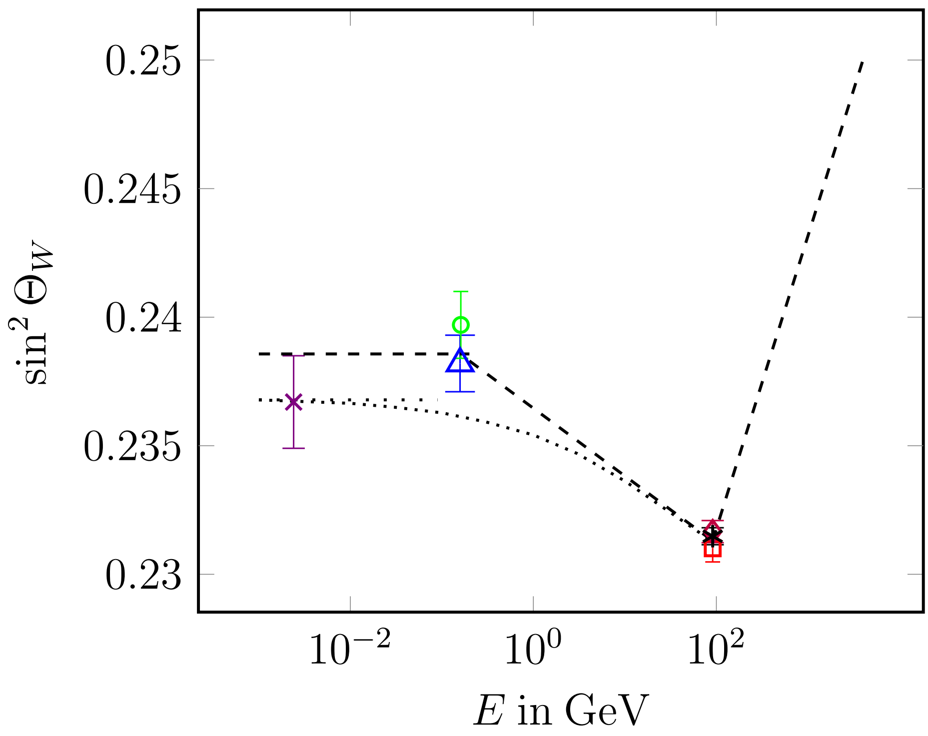

Figure 5.2: Square of the weak angle or weak mixing angle or Weinberg angle $\sin^2 \Theta_W$ (Weinberg, 1996, p. 307) or (Tanabashi et al., 2018, Fig. 10.2) as a function of the energy E of the probe.
Probes:
$\times$, APV (atomic parity violation) (Tanabashi et al., 2018, p. 166).
o, SLAC (Tanabashi et al., 2018, p. 166).
Δ, weak charge of a proton used (Tanabashi et al., 2018, p. 166).
$\square$, CMS (Erler and Schott, 2019, p. 34).
$\diamond$, ATLAS (Erler and Schott, 2019, p. 34).
$*$, Tevatron (Tanabashi et al., 2018, Eq. 10.43).
Theories:
loosely dotted: present derivation, see Eq. (5.20).
dotted: present derivation, including perturbations, see table (5.2).
$-\,-\,-\,-\,-$ SMEP, hereby, different schemes have been matched with help of fitted and scheme dependent matching terms (Tanabashi et al., 2018, p. 166).

Chapter 6

Formation of isospin

In this section, we use the SQ, in order to derive and explain the formation of the isospin.

6.1 Components q_e and q_Z of hypercharge

It is useful to introduce a coordinate system in Fig. (5.1). For it we use the two components of the hypercharge.

The vertical component of the hypercharge in Fig. (5.1) represents the electrical charge q_e, as it represents the elementary charge $\tilde{e}$ in particular.

The horizontal component of the hypercharge in Fig. (5.1) represents the non-electric component. Accordingly, we mark the horizontal axis by q_Z, in order to mark a zero electric component of the hypercharge.

Altogether, we arrive at the coordinate system in Fig. (6.1).

6.2 Linear independence of hypercharge and isospin

In this section, we analyze the relation between hypercharge and isospin I, see e.g. section (3.3.2). In the context of the electroweak interaction, the isospin is denoted by t_j, see (Tanabashi et al., 2018, p. 173), Zyla (2020), (Weinberg, 1996, S.

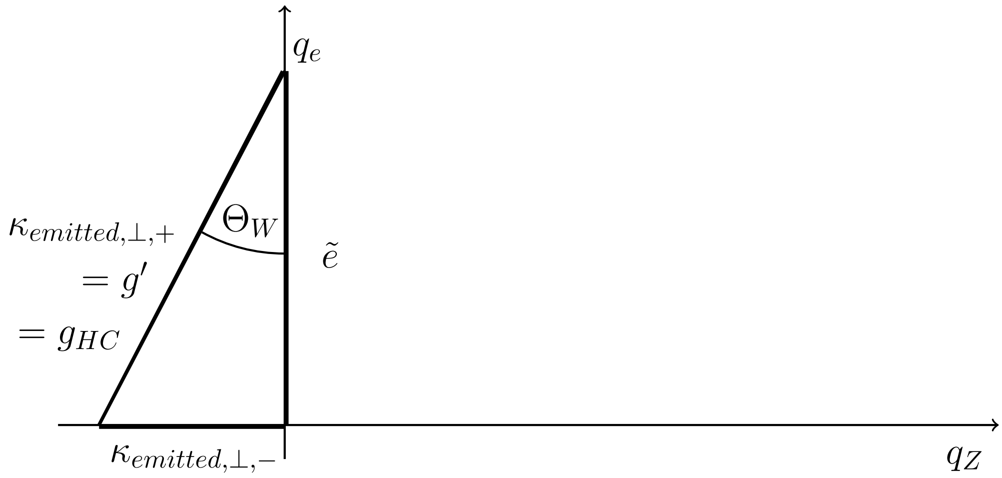

Figure 6.1: The vector space of sources makes transparent the components of hypercharge: The coupling $g_{HC} = \kappa_{emitted,\perp,+}$ of the hypercharge has two orthogonal components: the elementary charge $\tilde{e}$ and the non-electric component $\kappa_{emitted,\perp,-}$, see Fig. (5.1). The corresponding coordinate axes represent the electric component q_e and the non-electric component q_Z. Hereby, perturbations are treated in S. (3.5, 5.1.3, 5.1.4, 5.1.5).

21.3). The third component t_3 of the isospin represents an observable physical quantity, see Eq. (3.29). So it is represented by an operator $\hat{\vec{t}}$ in quantum physics, see Carmesin (2022), Kumar (2018), Ballentine (1998), Sakurai and Napolitano (1994). In particular, the third component t_3 of the isospin $\hat{\vec{t}}$ is represented by an operator $\hat{t}_3$. The operator of the isospin $\hat{\vec{t}}$ is equal to the vector of the Pauli spin matrices multiplied by one half, so that the eigenvalues in Eq. (3.29) are reproduced:

$$\sigma_3 = \begin{pmatrix} 1 & 0 \\ 0 & -1 \end{pmatrix} = 2 \cdot \hat{t}_3, \tag{6.1}$$

$$\sigma_1 = \begin{pmatrix} 0 & 1 \\ 1 & 0 \end{pmatrix} = 2 \cdot \hat{t}_1 \text{ and } \sigma_2 = \begin{pmatrix} 0 & -i \\ i & 0 \end{pmatrix} = 2 \cdot \hat{t}_2 \tag{6.2}$$

The normalization has been introduced as a convention.

As a matter of empirical fact, isospin and hypercharge are quantities by their own, see e.g. Tanabashi et al. (2018). In

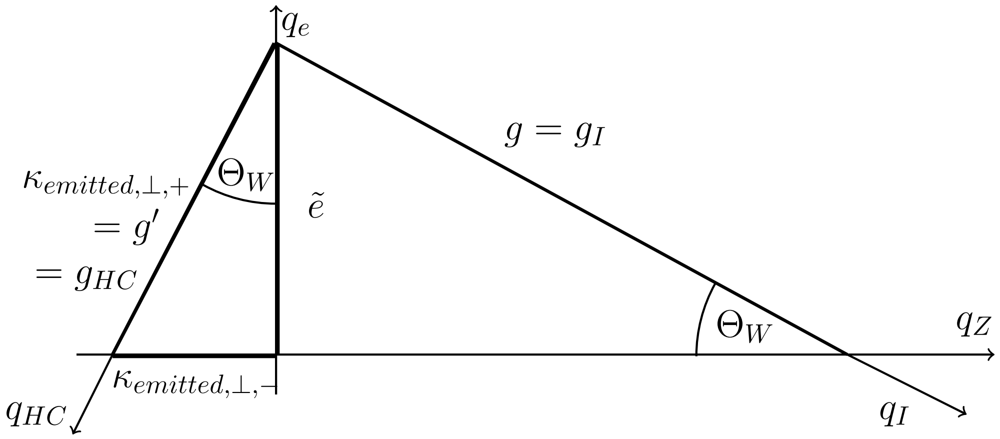

Figure 6.2: Vector space of sources with coordinates q_{HC} and q_I corresponding to the couplings g_{HC} of the hypercharge and g_I of the isospin. Hereby, perturbations are treated in S. (3.5, 5.1.3, 5.1.4, 5.1.5).

particular, they are linear independent. Accordingly, the coupling $g' = g_{HC}$ of the hypercharge, HC, should be orthogonal to a possible coupling g or g_I of isospin I.

6.3 Coordinates corresponding to g_{HC} and g_I

The coupling g_{HC} of the hypercharge and g_I of the isospin are orthogonal to each other. So the coordinate axes including g_{HC} and g_I in Fig. (6.2) constitute an orthogonal coordinate system. We denote the axes by q_{HC} and q_I, as the constants g_{HC} and g_I represent corresponding charges.

The charge g_I of the isospin includes an electric charge $\tilde{e}$, see Fig. (6.2). As the elementary charge $\tilde{e}$ is universal, see Carmesin (2021f), the charge g_I must have the electric component $\tilde{e}$. So the charge g_I ranges from the top of the triangle in Fig. (6.2) towards the axis q_Z. Altogether, we obtain the charges g_{HC} of the hypercharge and g_I of the isospin as well as the corresponding coordinates as shown in Fig. (6.2).

Theorem 5 Derivation of charge space

(1) Derivation of two-dimensional charge space: *Based on the SQ, Carmesin (2021f) derived the electric elementary charge, $\tilde{e}$. As an additional result, that charge has two components, $\kappa_{emitted,\perp,+}$ and $\kappa_{emitted,\perp,-}$. Thus, a two dimensional charge space is derived, see Fig. (6.2).*

(2) Derivation of three couplings: *The derived charge $\tilde{e}$ and its two components $\kappa_{emitted,\perp,+}$ and $\kappa_{emitted,\perp,-}$ in (1) represent couplings.*

(3) Derivation and explanation of the weak angle: *The couplings in (2) form a triangle in charge space, see Fig. (6.2).*

(3.1) Derivation of the enclosed angle Θ: *Thereby, the angle Θ enclosed by $\tilde{e}$ and $\kappa_{emitted,\perp,+}$ has been* **derived**. *Thereby, that enclosed angle Θ is algebraically described as follows:*

$$\sin^2(\Theta) = \frac{\kappa^2_{emitted,\perp,-}}{\kappa^2_{emitted,\perp,-} + \tilde{e}^2} = 0.236\,784 \tag{6.3}$$

(3.2) Derivation of the enclosed angles $\Theta(E)$: *Moreover, the angle enclosed by $\tilde{e}$ and $\kappa_{emitted,\perp,+}$ has been* **derived** *as a function of the energy E, by using results of perturbation theory. Utilizing these results, a correction factor $q_{corr}(E)$ has been derived, see tables (5.1, 5.2). That enclosed angle $\Theta(E)$ is algebraically described as follows:*

$$\sin^2(\Theta(E)) = \frac{\kappa^2_{emitted,\perp,-}}{\kappa^2_{emitted,\perp,-} + \tilde{e}^2 q^2_{corr}(E)} \tag{6.4}$$

(3.3) Comparison of derived and observed angles:

Furthermore, the derived enclosed angle $\Theta(E)$ has been compared with the weak angle $\Theta_W(E)$, Fig. (5.2). Thereby, derived and observed angles are in accordance. In addition, derived and observed angles are in precise accordance within errors of observation for the APV-experiment, CMS-experiment, ATLAS-experiment and Tevatron-experiment, see Fig. (5.2).

(3.4) Explanation of the weak angle: *As a result of (3.1), (3.2) and (3.3), our theory explains the weak angle on the basis of the SQ, whereby, no fit has been applied.*

(4) Derivation of the electroweak couplings g and g': *The electroweak couplings g and g′ have been derived. Hereby, perturbations are treated in S. (3.5, 5.1.3, 5.1.4, 5.1.5):*

(4.1) Microscopic derivation of g': *The electroweak coupling g' has been derived on the basis of the microscopic model of the elementary charge in Carmesin (2021f). That model is based on the SQ, applies no fit, provides $\kappa_{emitted,\perp,+}$, and its results are in precise accordance with observation:*

$$g' = \kappa_{emitted,\perp,+} \tag{6.5}$$

(4.2) Quantum physical derivation of g: *Based on the SQ, quantum physics (QP) has been derived in Carmesin (2022). Thereby, it has been shown that QP includes a far distant limit so that the* **external behavior of a quantum object is described***, while the detailed internal behavior of the quantum object need not to be specified. Using QP and (4.1), the coupling g has been derived:*

$$g = \tilde{e}/\sin\Theta_W \quad \text{without perturbations} \tag{6.6}$$

$$g(E) = \tilde{e}_{eff}(E)/\sin\Theta_W(E) \quad \text{with perturbations at } E \tag{6.7}$$

The results of (4.1) and (4.2) are illustrated by the triangle in charge space, see Fig. (6.2). Eq. (6.7) includes perturbations such as screening, see tables (5.1,5.1), Fig. (5.2), S. (3.5, 5.1.5) or e.g. Zyla (2020).

(4.3) Comparison with observation: *The electroweak couplings g and g' are usually compared with experiments by application of the weak angle Θ_W, the elementary electric charge $\tilde{e}$ and the Eqs. (6.5, 6.6), see e.g. Zyla (2020).*

(4.4) Explanation of the couplings g and g': *Based on (4.1), (4.2) and (4.3), the coupling g' has been explained on a* *microscopic basis, while the coupling g has been explained on a quantum physical basis. Both couplings g and g' have been explained on the basis of the SQ.*

(5) Charges derived by QG:

Based on SQ, the electric charge, a non-electric charge, hypercharge and an isospin charge have been derived. Hereby, perturbations are treated in S. (3.5, 5.1.3, 5.1.4, 5.1.5).

(5.1) Hypercharge derived by QG:
The component $\kappa_{emitted,\perp,+}$ of the elementary charge has been **derived microscopically***, see (4.1) or Carmesin (2021f).*

Combined with (3.4), it has been shown that $\kappa_{emitted,\perp,+}$ is equal to the coupling g'. In Planck units, the elementary electric charge $\tilde{e}$ is equal to the square root of the coupling (fine structure constant), $\sqrt{\alpha}$. Correspondingly, the derived coupling, g' can be interpreted as a hypercharge $\tilde{y}$, if desired.

(5.2) Isospin charge derived by QG: *The coupling $g = \frac{\tilde{e}_{eff}(E)}{\sin\Theta_W(E)}$ has been derived, based on the external quantum physical behavior, see (4.2). Similarly as in (5.1), the derived coupling, g can be interpreted as isospin charge, if desired.*

(5.3) Isospin orthogonal to hypercharge: *In charge space, the coupling g' of hypercharge is orthogonal to the coupling g of isospin, see Fig. (6.2). This result is based on the empirically observed independence of the hypercharge and the isospin.*

(5.4) Electric charge orthogonal to non-electric charge: *In charge space, the coupling $\tilde{e}$ of electric charge is orthogonal to the coupling $\sqrt{g^2 + g'^2}$ of the non-electric charge, see Fig. (6.2). This finding is based on the microscopically derived elementary charge, see Carmesin (2021f).*

Chapter 7

Derivation of the Lagrangian

In this section, we show how the Lagrangian can be derived and explained from the spacetime-quadruple, SQ.

Of course, it is possible to find various methods for an introduction of a Lagrangian or of equations in Quantum Field Theory, see e. g. (Weinberg, 1996, S. 1-16), Schwartz (2014), Bialynicki-Birula and Bialynicki-Birula (1975), Swanson (2017), Fewster and Rejzner (2019).

However, such introductions usually start with assumed principles or postulates. In contrast, we start with the transparent basic concepts of gravity and relativity, which we elaborated and presented in the form of the spacetime-quadruple, SQ, see chapters (1, 2) or Carmesin (2022), Carmesin (2021d).

7.1 PLA and Free Lagrangian

In this section, we show how the free Lagrangian is derived from the spacetime-quadruple. This is achieved by the following sequence of steps:

(1) The SQ implies QP and QG, see Carmesin (2022).

(2) So an object forms vacuum according to a rate $\dot{\hat{\varepsilon}} \cdot t_n$, and the rate is equal to the wave function $\dot{\hat{\varepsilon}} \cdot t_n = \psi \cdot f_n$, (Carmesin, 2022, THM 6).

(3) **If** a wave function describes a free object,

and if a semiclassical limit allows that a path from a point A to a point B can be applied,

then that path from A to B occurs in nature, that obeys the principle of least time, see (Born and Wolf, 1980, S. 3.3.2).

(4) **If** a wave function describes a free object,

and if a semiclassical limit allows that a path from a point A to a point B can be applied,

then that path from A to B that requires the least time, is equal to the path from A to B that has the least time action.

(5) The above steps (3) and (4) imply the following:

If a wave function describes a free object,

and if a semiclassical limit allows that a path from a point A to a point B can be applied,

then that path from A to B occurs in nature that has the least action.

(6) The consequence of the SQ in step (5) is usually called the *principle of least action, PLA*.

(7) The *principle of least action, PLA*, can be applied, in order to introduce a Langrangian, $\mathcal{L}$, and in order to derive the Euler-Lagrange equations for $\mathcal{L}$, see e. g. Landau and Lifschitz (1971), (Schwartz, 2014, S. 3.2).

(8) It is possible and typical in QFT, to represent the starting point of the underlying path, that is considered explicitly or implicitly, by an assumed vacuum state Ω_{in}, see e. g. (Schwartz, 2014, S. 14), (Bialynicki-Birula and Bialynicki-Birula, 1975, § 19), (Weinberg, 1996, S. 16.1 or p. 63), Fewster and Rejzner (2019).

Similarly, it is possible and typical in QFT, to represent the ending point of that path by an assumed vacuum state Ω_{out}.

Altogether, this derivation proves the following theorem:

Theorem 6 Free Lagrangian based on SQ

Based on the spacetime-quadruple, the following can be derived:

(1) **If** *an object propagates freely from a point A to a point B,*

and if *the wave function of the object can be described in a semiclassical limit that allows a path from A to B,*

then *that path from A to B occurs in nature that has the least action. So the PLA holds for such an object.*

(2) **If** *an object propagates freely from a point A to a point B,*

and if *the wave function of the object can be described in a semiclassical limit that allows a path from A to B,*

then *the object can be described by a free Lagrangian $\mathcal{L}_0$.*

Thereby, *the Euler-Lagrange equation holds.*

(3) In numbers (1) and (2), the start A and the end B of the underlying path can be represented by assumed vacuum states Ω_{in} and Ω_{out}.

7.2 Principle of Gauge Invariance, PGI

In this section, we apply the SQ in order to show that the PGI can be applied to a free Lagrangian $\mathcal{L}_0$. Note that the free Lagrangian $\mathcal{L}_0$ has also been derived on the basis of the SQ, see THM (6).

This is achieved by the following sequence of steps:

(1) The SQ implies QP and QG, see Carmesin (2022).

(2) The theorem (6) implies:

If an object propagates freely from a point A to a point B,

and if the wave function of the object can be described in a semiclassical limit that allows a path from A to B,

then the object can be described by a free Lagrangian $\mathcal{L}_0$.

Thereby, the Euler-Lagrange equation holds.

(3) Each object forms vacuum according to a rate $\dot{\hat{\varepsilon}} \cdot t_n$, and the rate is equal to the wave function $\dot{\hat{\varepsilon}} \cdot t_n = \psi \cdot f_n$, (Carmesin, 2022, THM 6).

(4) **If** the wave function of the object in step (3) remains coherent (no decoherence occurs), see e. g. (Ballentine, 1998, S. 19, 20), **then** the wave function has a global phase Θ.

(5) The global phase in (4) can be disturbed at locations $\vec{x}$ or x_μ by a local interaction, that is proportional to a **charge** or hypercharge or isospin-charge/isospin-coupling q. An example for it has been provided by Aharonov and Bohm (1959). Hereby, Pearle (2017) elaborated in detail, how the phase of the wave function is modified by the vector potential A_μ, and how that phase explains the shift of the maxima of diffraction. **Thereby**, there occurs a **local phase** $\Theta(\vec{x})$ or $\Theta(x_\mu)$, different from the global phase Θ.

(6) The local phase $\Theta(x_\mu)$ in (5) of a wave function in (4)

$$\psi_\Theta = \exp(i \cdot \Theta(x_\mu)) \cdot \psi \tag{7.1}$$

causes an additional summand Δ in the derivative

$$\partial_\mu \psi(x_\mu) \tag{7.2}$$

as follows:

$$\partial_\mu \psi_\Theta(x_\mu) = \exp(i\Theta(x_\mu))[\partial_\mu + i\partial_\mu \Theta(x_\mu)]\psi(x_\mu) \qquad \text{or} \tag{7.3}$$

$$\partial_\mu \psi_\Theta(x_\mu) = \exp(i\Theta(x_\mu))\partial_\mu \psi(x_\mu) + \Delta \qquad \text{with} \tag{7.4}$$

$$\Delta = i\psi_\Theta(x_\mu) \cdot \partial_\mu \Theta(x_\mu) \tag{7.5}$$

(7) The additional summand Δ in the derivative in (6) causes an additional summand in the Schrödinger equation SEQ, see Carmesin (2022). However, the SEQ describes the propagation of vacuum, see Carmesin (2022). Hereby, the vacuum exhibits **translation invariance in space and possibly time**, in time at least at small and intermediate scales, see Carmesin

(2021d), Carmesin (2021c). Thus the additional summand Δ in the SEQ must be compensated. That demand for the compensation of the additional summand Δ represents the **Principle of Gauge Invariance, PGI**, see (Pich, 2007, S. 2), (Schwartz, 2014, 14.5).

(8) The compensation of the additional summand Δ in (7) is achieved with the covariant derivative, see chapter (3). For instance, for the case of the electric charge q_e, the covariant derivative is as follows:

$$D_\mu \psi(x_\mu) = [\partial_\mu + i \cdot q \cdot A_\mu(x_\mu)]\psi(x_\mu) \qquad \text{with} \tag{7.6}$$

$$A_{\mu,\Theta}(x_\mu) = A_\mu(x_\mu) - \frac{1}{q_e}\partial_\mu \Theta(x_\mu) \tag{7.7}$$

Hence, $D_\mu \psi_\Theta(x_\mu)$ is as follows, see Eq. (7.3):

$$D_\mu \psi_\Theta(x_\mu) = e^{i\Theta(x_\mu)}[\partial_\mu + i\partial_\mu \Theta(x_\mu) + iq_e A_{\mu,\Theta}(x_\mu)]\psi(x_\mu) \qquad \text{so} \tag{7.8}$$

$$D_\mu \psi_\Theta(x_\mu) = e^{i\Theta(x_\mu)}[\partial_\mu + i \cdot q_e \cdot A_\mu(x_\mu)]\psi(x_\mu) \qquad \text{thus} \tag{7.9}$$

$$D_\mu \psi_\Theta(x_\mu) = [\partial_\mu + i \cdot q_e \cdot A_\mu(x_\mu)]\psi_\Theta(x_\mu) \tag{7.10}$$

Thence, the form of the covariant derivative in Eqs. (7.6) and (7.10) is the same. Consequently, the covariant derivative compensates Δ, as demanded by the PGI.

(9) The PGI provides the functional form of the interaction. See for instance Eq. (7.6).

(10) Similarly as for the case of the SEQ, the local phase $\Theta(x)$ in (5) causes a summand $\mathcal{L}_{\Theta(x)}$ in the Lagrangian that occurs in addition to the free Lagrangian $\mathcal{L}_0$, since $\mathcal{L}_0$ contains derivatives ∂_μ.

(11) The additional term $\mathcal{L}_{\Theta(x)}$ in the Lagrangian can be compensated by the interaction term $\mathcal{L}_{int}$ in the Lagrangian.

Thereby, $\mathcal{L}_{int}$ can be derived via the covariant derivative as outlined for the case of the SEQ. In this manner the interaction term $\mathcal{L}_{int}$ in the Lagrangian can be derived.

(12) Altogether, the form of the interaction is derived from the SQ as follows: The SQ provides the SEQ describing vacuum.
An interaction via a charge q causes a local phase $\Theta(x_\mu)$.
$\Theta(x_\mu)$ contributes to the SEQ.
Thus $\Theta(x_\mu)$ destroys translation invariance of the SEQ.
But the SEQ describes vacuum, according to the SQ.
Thence the term $\Theta(x_\mu)$ in the SEQ must be compensated.
The demand for that compensation is the PGI.

Theories that are obtained by this method are called **gauge theories**, whereby the method has been proposed by Weyl (1919), Fock (1926), Weyl (1929), Yang and Mills (1954).

Thereby, the interaction may be represented by using a group $SU(n)$, see section (3.4.2). A group that is used as representation of an interaction is named **gauge group**, see e. g. Schwartz (2014).

Altogether, the above derivation in steps (1) until (12) proves the following theorem:

Theorem 7 Principle of Gauge Invariance, PGI

Based on the spacetime-quadruple, the following can be derived:

(1) If an object propagates freely from a point A to a point B, and if the wave function of the object can be described in a semiclassical limit that allows a path from A to B, then the object can be described by a free Lagrangian $\mathcal{L}_0$. Thereby, the Euler-Lagrange equation holds.

(2) In (1), the start A and the end B of the underlying path can be represented by assumed vacuum states Ω_{in} and Ω_{out}.

(3) Each object forms vacuum according to a rate $\dot{\hat{\varepsilon}} \cdot t_n$, and the

rate is equal to the wave function $\dot{\hat{\varepsilon}} \cdot t_n = \psi \cdot f_n$, (Carmesin, 2022, THM 6).

(4) If the wave function ψ in (3) remains coherent, see e. g. (Ballentine, 1998, S. 19, 20), then ψ has a global phase Θ.

(5) The global phase in (4) can be disturbed locally by a local interaction proportional to a charge or hypercharge or isospin-charge/isospin-coupling q, so that a local phase $\Theta(x)$ occurs.

(6) The local phase $\Theta(x)$ in (5) enters the Schrödinger equation SEQ. As the SEQ describes the dynamics of the vacuum, it must be translation invariant. Thus the term $\Theta(x)$ in the SEQ must be compensated. The demand for that compensation is the PGI.

(7) That compensation can be achieved by constructing an appropriate covariant derivative. Thereby, the interaction term corresponding to the charge q can be derived. In this manner, the SQ provides the functional form of the interaction corresponding to the charge q. Hereby, q can represent the electric charge, as well as charges of the electroweak interaction or the strong interaction, provided the above conditions apply.

(8) In particular, that compensation provides the interaction term $\mathcal{L}_{int}$ in the Lagrangian.

7.3 SMEWI based on Gauge Group $SU(2)$

In this section, we derive the description of the electroweak interaction by the gauge group $SU(2)$, see sections (3.4.2, 7.2).

This is achieved by the following sequence of steps:

(1) We apply the conditions of THM (7).

(2) The SQ provides QG, and QG provides the derivation of the elementary electric charge e, Carmesin (2021f).

(3) In QG, the elementary electric charge e is generated by forced oscillations, Carmesin (2021f), and these can be grouped

to a two-dimensional charge space, see chapters (5, 6) and Fig. (6.2).

(4) The two-dimensional charge space in (3) causes a corresponding representation of the transformations of states in that two-dimensional charge space. Wigner (1931) showed that these transformations are represented by unitary operators in the group $SU(2)$, see also Wigner (1959) or chapter (3).

Altogether, this derivation proves the following theorem:

Theorem 8 $SU(2)$ **- symmetry of the SMEWI**

(1) The spacetime-quadruple, SQ, implies the PGI, see THM (7.

(2) The SQ implies quantum gravity, QG, which in turn implies the generation of the elementary charge via forced oscillations, Carmesin (2021f).

(3) The generation of the elementary charge via forced oscillations in (2) implies the two-dimensional charge space, see Fig. (6.2).

(4) The pair of the PGI in (1) and the two-dimensional charge space in (3) implies the $SU(2)$ *- symmetry of the SMEWI.*

7.4 Isospin doublets based on SQ

In this section, we derive the isospin doublets in Eqs. (3.29, 3.30) based on the gauge group $SU(2)$, see sections (3.4.2, 7.2). Thereby, the gauge group $SU(2)$ is based on the SQ, see section (7.3).

This is achieved by the following sequence of steps:

(1) We apply the conditions of THM (7).

(2) The SQ provides QG.

(3) In QG, the elementary electric charge e is generated by

forced oscillations, Carmesin (2021f), and these can be grouped to a two-dimensional charge space, see chapters (5, 6) and Fig. (6.2).

(4) The two-dimensional charge space in (3) causes a corresponding representation by the gauge group $SU(2)$, see (8).

(5) As a result of the PGI, the isospin gauge group $SU(2)$ can be represented as follows:

(5a) The elementary charge $\tilde{e}$ corresponds to the electromagnetic potential A_μ, while the non-electric charge q_Z corresponds to a field or potential Z_μ.

(5b) The fields or potentials A_μ and $Z_\mu$can be transformed as follows, see (Pich, 2007, Eq. 52):

$$\begin{pmatrix} W_\mu^3 \\ B_\mu \end{pmatrix} = \begin{pmatrix} \cos \Theta_W & \sin \Theta_W \\ -\sin \Theta_W & \cos \Theta_W \end{pmatrix} \cdot \begin{pmatrix} Z_\mu \\ A_\mu \end{pmatrix} \tag{7.11}$$

(5c) The fields or potentials W_μ^j with $j = 1, 2, 3$, form an operator $\hat{W}_\mu$ as a linear combination of Pauli matrices $\hat{\sigma}_j$ as follows, see (Pich, 2007, Eq. 40):

$$\hat{W}_\mu = \Sigma_{j=1}^{j=3} \frac{\hat{\sigma}_j}{2} \cdot W_\mu^j \tag{7.12}$$

(5d) Thus, elementary particles can be organized as doublets of eigenstates of the operator $\frac{\hat{\sigma}_j}{2}$. Thereby, the two particles of a doublet have an isospin differing by 1. This corresponds to the empirical finding in Eqs. (3.29, 3.30).

(5e) Moreover, the charge operator is as follows, see (Weinberg, 1996, Eq2. 21.3.22-21.3.24):

$$\hat{Q} = \frac{1}{2} \begin{pmatrix} 1 & 0 \\ 0 & -1 \end{pmatrix} - \frac{1}{2} \begin{pmatrix} 1 & 0 \\ 0 & 1 \end{pmatrix} = \begin{pmatrix} 0 & 0 \\ 0 & -1 \end{pmatrix} \tag{7.13}$$

Thus, for the case of the neutrino, we derive the eigenvalue zero:

$$\hat{Q} \begin{pmatrix} 1 \\ 0 \end{pmatrix} = \begin{pmatrix} 0 & 0 \\ 0 & -1 \end{pmatrix} \cdot \begin{pmatrix} 1 \\ 0 \end{pmatrix} = 0 \cdot \begin{pmatrix} 1 \\ 0 \end{pmatrix} \tag{7.14}$$

Similarly, for the case of the electron, we derive the eigenvalue -1:

$$\hat{Q}\begin{pmatrix} 0 \\ 1 \end{pmatrix} = \begin{pmatrix} 0 & 0 \\ 0 & -1 \end{pmatrix} \cdot \begin{pmatrix} 0 \\ 1 \end{pmatrix} = -1 \cdot \begin{pmatrix} 0 \\ 1 \end{pmatrix} \tag{7.15}$$

Both eigenvalues of the electric charge correspond to the observed charges.

Analogously, the eigenvalues of isospin and electric charge can be derived for the other five isospin doublets in Eqs. (3.29, 3.30).

Altogether, the SQ provides the correct eigenvalues of electric charge and isospin for the isospin doublets. Thus, this derivation proves the following theorem:

Theorem 9 Isospin doublets

(1) The spacetime-quadruple, SQ, implies the PGI, see THM (7).

(2) The SQ implies the gauge group $SU(2)$ of the isospin, see THM (8).

(3) The pair of the PGI in (1) and gauge group $SU(2)$ of the isospin in (2) implies the organization of the elementary particles in Eqs. (3.29, 3.30) in terms of the six isospin doublets in Eqs. (3.29, 3.30). Thereby, the eigenvalues of isospin and electric charge correspond to the observed values.

Chapter 8

Derivation of the masses

In this section, we derive and explain the masses of the bosons of the electroweak interaction, W^-, Z and W^+.

8.1 Lagrangian of electroweak interaction

In this section, we derive the Lagrangian of the electroweak interaction. For it, we apply Planck units.

8.1.1 Free Lagrangian $\mathcal{L}_0$

In this section, we present the free Lagrangian.

A relativistic object without spin and with a possible mass or dynamic mass m has the following free Lagrangian, see (Landau and Lifschitz, 1982, p. 32-36 or § 10 or Eq. 10.9):

$$\mathcal{L}_0 = \partial_\mu \psi^{cc} \cdot \partial^\mu \psi - m^2 \psi^{cc} \cdot \psi \tag{8.1}$$

8.1.2 On symmetries in the weak interaction

In this section, we summarize observations about very special symmetries occurring in the weak interaction.

A particle with a quantum number s of the spin and with a quantum number m_s of the z-direction of the spin has the following helicity:

$$\lambda = m_s / s \tag{8.2}$$

Thereby, the z-direction is usually chosen to be the direction of propagation, see e.g. (Griffiths, 2008, S. 4.4). For instance, a neutrino has $s = 1/2$ and $m_s = 1/2$ or $m_s = -1/2$. So, in principle, a neutrino can have the helicity $\lambda = \pm 1$. However, Goldhaber et al. (1957) discovered that neutrinos have the helicity $\lambda = -1$, also called left-handed, while antineutrinos have the helicity $\lambda = 1$, or right-handed.

More generally, Lee and Yang (1956) realized on the basis of experimental indications, that the weak interaction of a particle might depend on its helicity. This would not only apply to neutrinos, as the electroweak interaction applies to all particles with charge, hypercharge or isospin, see section (3.3.2) and chapters (5, 6). Indeed, Wu et al. (1957) observed in an experiment with a β decay, that the weak interaction applies to left-handed particles only (helicity $\lambda = 1$). This has been confirmed by many other experiments, see e.g. (Tanabashi et al., 2018, S. 13). This fact can be expressed with help of vectors and axial vectors, see e.g. Zyla (2020), or it can be expressed in terms of the hypercharge as follows, (Weinberg, 1996, p. 305, 306): We introduce a left-handed hypercharge operator:

$$\hat{Y}_L = g' \cdot \frac{1+\gamma^5}{4} \cdot \begin{pmatrix} \mathbb{I} & 0 \\ 0 & \mathbb{I} \end{pmatrix} \tag{8.3}$$

Hereby, we used a gamma matrix, see glossary. Next, we introduce the usual right-handed hypercharge operator:

$$\hat{Y}_R = g' \cdot \frac{1-\gamma^5}{2} \tag{8.4}$$

The above matrix is zero, in the present representation, indicating that right-handed particles do not experience the corresponding weak interaction. The hypercharge operator is the sum:

$$\hat{Y} = \hat{Y}_L + \hat{Y}_R \tag{8.5}$$

Moreover, Christenson et al. (1964) discovered, that also the product of parity and charge, CP, is not a conserved observable in all applications, see also (Tanabashi et al., 2018, S. 13).

A possible derivation of such symmetries on the basis of SQ is presented in S. (8.9).

8.1.3 Lagrangian $\mathcal{L}$ via PGI

In this section, we show how the PGI is applied to the free Lagrangian.

For it, we use the covariant derivative D_μ, see (Zyla, 2020, Eq. 11.4) or (Weinberg, 1996, Eq. 21.3.25):

$$D_\mu = \partial_\mu + ig\Sigma_{\alpha=1}^{\alpha=3}\frac{\sigma^\alpha}{2}W_\mu^\alpha + ig'\frac{1}{2}\hat{Y} \cdot B_\mu \tag{8.6}$$

Thereby, $\hat{Y}$ represents the operator of the hypercharge-number, while σ^α are Pauli matrices. We apply D_μ to the free Lagrangian $\mathcal{L}_0$. Additionally, we use the fact that the momentum is proportional to the derivative times the complex unit i. (Note that the fields W_μ^α in (Zyla, 2020, S. 11) correspond to the 'electromagnetic fields' or better vector potentials A_μ^α in (Weinberg, 1996, S. 21)).

So the Lagrangian is as follows, see (Weinberg, 1996, Eq. 21.3.25):

$$\mathcal{L} = -|(D_\mu\psi)|^2 - m^2\psi^{cc} \cdot \psi \qquad \text{or} \tag{8.7}$$

$$\mathcal{L} = -|(D_\mu\psi)|^2 - V(\psi) \tag{8.8}$$

Hereby, the covariant derivatives include the fields W_μ^α and B_μ, while the mass term $m^2\psi^{cc} \cdot \psi$, can be obtained from the energy momentum relation $E^2 = p^2c^2 + m_0^2c^4$, see e.g. (Landau and Lifschitz, 1982, p. 32-36 or § 10 or Eq. 10.9). However, the potential $V(\psi)$ of the SMEWI usually includes a term with a fourth power, which is not derived with help of the PGI in terms of a covariant derivative. Instead, such a term is postulated in addition to Eq. (8.7), see e.g. (Weinberg, 1996, S. 21.3).

8.2 Incompleteness of the PGI

Accordingly, the Lagrangian in Eq. (8.7) that is based on the PGI and on relativity is incomplete: That Lagrangian in Eq. (8.7) describes the electroweak interaction in terms of the fields W_μ^α and B_μ. However, these fields are mediated (or transported or propagated) by W bosons and Z boson of interaction, but the observed masses of these bosons are not described by the Lagrangian in Eq. (8.7). In this manner, the PGI is incomplete.

8.3 Solution by phase transition, PT

Higgs (1964), Englert and Brout (1964) and Guralnik et al. (1964) proposed a mechanism, in order to overcome that incompleteness. For it they introduced a new item into the SMEP: a **phase transition, PT** that provides mass. That proposal is named **Higgs mechanism**.

However, that mechanism cannot be derived from the PGI. Accordingly, (Weinberg, 1996, Eqs. 21.3.20 until 21.3.28) realized that assumptions about that Higgs mechanism are required.

We summarize these assumptions in section (8.4). However, it turns out that a Higgs vacuum with a vacuum expectation value VEV is proposed in the Higgs mechanism. Thereby, that Higgs vacuum is very different from the present day vacuum, see section (8.5).

We solve this problem in section (8.7). For it, we derive the required phase transition including its properties based on the SQ. Accordingly, based on the SQ, we provide a derivation of the PT that provides the VEV. Thereby, we provide an explanation of the formation of the VEV, whereby that formation has usually been modeled by the proposed Higgs mechanism with its assumptions, see (Weinberg, 1996, S. 21).

8.4 PT by Higgs mechanism

Higgs (1964) proposed a phase transition. With it, a mass m should be generated. For it, a **Higgs field** Φ has been proposed, see e. g. Higgs (1964), (Zyla, 2020, S. 11.2), (Weinberg, 1996, S. 21).

8.4.1 SMEP scalar potential

Landau (1937) proposed and developed a theory of phase transitions. Thereby, a potential $V(\Phi)$ as a function of a field Φ or order parameter is used. Hereby, the potential is constituted by a square and a fourth order term of Φ, with two parameters m and λ as follows:

$$V(\Phi) = m^2 \cdot \Phi^2 + \lambda \Phi^4 = V_{SMEP} \tag{8.9}$$

The above potential (Eq. 8.9) is used in the case of the Higgs mechanism, see e. g. (Zyla, 2020, Eq. 11.1). We name that potential **SMEP scalar potential**, V_{SMEP}. Note that a Φ^2-Φ^4 - potential has also been suggested by Jormakka (2020).

(Note that the potential is named SM scalar potential in (Zyla, 2020, Eq. 11.1 and S. 11.2). However, there is also a standard model of cosmology, SMC, see e. g. Planck-Collaboration (2020), Weinberg (1972). And the SMC will become essential for the explanation of the SMEWI, see below. So we name the potential V_{SMEP}.)

8.4.2 SMEP Higgs Lagrangian

(Weinberg, 1996, Eqs. 21.3.20 until 21.3.28 and S. 21) pointed out, that the Higgs mechanism requires assumptions. One of these assumptions provides a method by which the Higgs field Φ and the SMEP scalar potential $V_{SMEP}(\Phi)$ are introduced in the Lagrangian of the electroweak interaction in Eq. (8.7). That procedure consists of two steps:

Firstly, that procedure requires that the wave function in Eq. (8.8) is replaced by the Higgs field:

$$\text{replace} \quad \psi \quad \text{by} \quad \Phi \tag{8.10}$$

Of course, in traditional QP, a wave function should not be replaced by a potential. In the SMEWI, this replacement is part of an assumption about the Higgs mechanism, see e.g. (Weinberg, 1996, S. 21.3). In the SQ, we can explain and derive that replacement, see Carmesin (2022), and see below.

Secondly, that procedure requires that the potential in Eq. (8.8) is replaced by the SMEP scalar potential $V_{SMEWI}(\Phi)$ in Eq. (8.9):

$$\text{replace} \quad V \quad \text{by} \quad V_{SMEWI} \tag{8.11}$$

8.4.2.1 Symmetric phase

In the symmetric phase, the field, that is the order parameter of the phase transition, PT, is zero, see e.g. Landau (1937), Weinberg (1996), Carmesin (2021a):

$$\langle \Phi \rangle = 0 \qquad \text{symmetric phase} \tag{8.12}$$

8.4.2.2 Phase with broken symmetry

In the phase with broken symmetry, the field, that is the order parameter of the phase transition, PT, is non-zero, see e.g. Landau (1937). Its value is derived as usual in a Φ^2-Φ^4 model in PTs. Hereby, the order parameter is complex. Accordingly, it can be represented in two-dimensional real space, Weinberg (1996), Carmesin (2021a):

$$\langle \Phi \rangle = \frac{1}{\sqrt{2}} \cdot \begin{pmatrix} 0 \\ v_{opt} \end{pmatrix} \qquad \text{broken symmetry, with} \tag{8.13}$$

$$v_{opt} = \sqrt{\frac{|m|^2}{\lambda}} \qquad \text{shortly} \;\; v_{opt} = v \tag{8.14}$$

In the Φ^2-Φ^4 model, the value v_{opt} of the broken symmetry represents the ground state. In reality, the ground state represents the vacuum. In the SMEWI and in the SMEP, that value v_{opt} has been named **vacuum expectation value, VEV**, see e. g. (Pich, 2007, S. 4.2), (Zyla, 2020, 11.2). As a result of measurements, the VEV is as follows, see e. g. (Zyla, 2020, S. 11.2.1, table 1.1):

$$v = (\sqrt{2} \cdot G_F)^{-1/2} = 246.1965\,\mathrm{GeV} \pm 0.6\,\mathrm{ppm} \tag{8.15}$$

Hereby, G_F is the Fermi coupling, Fermi (1933), Zyla (2020).

8.5 Higgs vacuum VEV $\neq$ actual vacuum

In this section, we show that the VEV of the SMEP does not correspond to the observed density of the vacuum in the universe. Based on observations, see e. g. Riess et al. (2021), Planck-Collaboration (2020), the density of the vacuum is as follows:

$$\rho_\Lambda = \rho_{cr.} \cdot \Omega_\lambda \tag{8.16}$$

Thereby, $\rho_{cr.}$ is the critical density and Ω_λ is the density parameter of the vacuum. Hereby, the critical density can be derived from the Hubble constant H_0 as follows, see e. g. Hobson et al. (2006), Carmesin (2019d):

$$\rho_{cr.} = \frac{3H_0^2}{8\pi G} \quad \text{with} \tag{8.17}$$

$$H_0 \in [67.36; 73.43]\,\frac{\mathrm{km}}{\mathrm{s} \cdot \mathrm{Mpc}} \quad \text{thus} \tag{8.18}$$

$$\rho_\Lambda \in [5.8 \cdot 10^{-27}; 6.9 \cdot 10^{-27}]\,\frac{\mathrm{kg}}{\mathrm{m}^3} \tag{8.19}$$

Hereby, the observational values of H_0 are taken from Riess et al. (2021) and Planck-Collaboration (2020), while the observation of Ω_Λ is taken from Planck-Collaboration (2020)[1].

[1]For an explanation of the variation of H_0, see Carmesin (2021d), Carmesin (2021a), Carmesin (2021c).

Moreover, based on the SQ, which implies QG, see Carmesin (2022), the above density has correctly been modeled by quanta of the vacuum with an energy E_Λ, for details see e. g. Carmesin (2018c), Carmesin (2018b), Carmesin (2019d) or additionally (Carmesin, 2021a, Eq. 6.6), Carmesin (2021b), or with comparison to observation Carmesin (2021c). Thereby, the derived value of E_Λ is as follows:

$$E_\Lambda = 5.4 \cdot 10^{-5}\,\mathrm{eV} \tag{8.20}$$

Accordingly, the VEV is 15 orders of magnitude larger than the energy of the quanta of the vacuum:

$$\frac{VEV}{E_\Lambda} = \frac{v}{E_\Lambda} = 5.6 \cdot 10^{15} \tag{8.21}$$

Thus, the VEV does not represent the present-day vacuum.

8.6 Unspecific PT of the Higgs mechanism

In this section, we point out that the PT in the Higgs mechanism is very unspecific.

The Higgs mechanism does hardly describe the mechanism of the symmetry breaking, as the applied theory of phase transitions by Landau (1937) does only provide a framework of a variable Φ and powers thereof, Φ^2 and Φ^4. However, that variable Φ can be applied to each physical system. Thus Φ does not provide any specific information about the system under investigation.

8.7 Solution via PT based on SQ

In this section, and based on the SQ, we model the value VEV in a microscopic manner.

Based on the SQ, the mass m_H or energy E_H of the **Higgs boson** has been derived, (Carmesin, 2021a, THM 9):

$$\text{Higgs boson}: \;\; E_H = 125.5\,\mathrm{GeV} \tag{8.22}$$

In principle, two objects can form a pair[2]. Accordingly, we propose that pairs of Higgs bosons correspond to the VEV. Thereby, the pair of Higgs bosons exhibits an energy of interaction. We model it with the strong interaction.

Thereby, the energy of the interaction depends on the energy scale Q of the coupling, as observed by inelastic scattering, see (Zyla, 2020, Fig. 9.3). The energy scale corresponding to the scattering is expected to be the zero-point energy, ZPE. Based on the SQ, and in the case of the Higgs boson, the ZPE has been derived, for details see (Carmesin, 2021a, Eq. 9.7):

$$ZPE_H = 9.22\,\mathrm{GeV} \tag{8.23}$$

Based on observation, the corresponding strong coupling is as follows, see (Zyla, 2020, Fig. 9.3):

$$\alpha_s(ZPE_H) = 0.18 \tag{8.24}$$

The length scale of the distance of the Higgs bosons in the pair is obtained by the length scale of these bosons:

$$dr = \frac{h \cdot c}{E_H} = 9.9 \cdot 10^{-10}\,\mathrm{m} \tag{8.25}$$

The corresponding energy is estimated as follows: The basic energy of electric interaction, $dE = -\frac{e^2}{4\pi\epsilon_0 \cdot dr}$, is proportional to the coupling constant α. In the case of the strong interaction, α is replaced by α_s, equivalently, dE is increased by the factor $\frac{\alpha_s}{\alpha}$, with $\alpha \approx \frac{1}{137}$:

$$dE = -\frac{e^2}{4\pi\epsilon_0 \cdot dr} \cdot \frac{\alpha_s}{\alpha} \tag{8.26}$$

By inserting the above values, we obtain:

$$dE = -2.4\,\mathrm{GeV} \tag{8.27}$$

[2]For instance, many atoms in the atmosphere form pairs or dimers.

So the energy of the pair of Higgs bosons is as follows:

$$E_{pair} = 2E_H + dE = 247.6\,\mathrm{GeV} = VEV_{theo} \tag{8.28}$$

The above estimate shows that the VEV corresponds approximately to the energy of a pair of Higgs bosons.

Thereby, the relative difference amounts to

$$\frac{E_{pair} - VEV}{VEV} = \frac{247.6 - 246.1965}{246.1965} = 0.57\%, \tag{8.29}$$

whereas the ratio of the VEV and the energy of a quantum of present-day vacuum amounts to more than 10^{15}. Accordingly, we postulate that these pairs of Higgs bosons should be observed in the future, at a significance larger than 5 σ, of course.

8.7.1 Observation of Higgs boson pairs

Pairs of Higgs bosons have been observed at a significance of 4 σ, see e.g. ATLAS (2021), (Zyla, 2020, S. 11.3.4 or p. 216).

8.7.2 Symmetry breaking of vacuum based on the SQ

In this section, we analyze the symmetry breaking of vacuum on the basis of the SQ.

8.7.2.1 Wave function

In the SQ, the excitation states of the vacuum are physically effective at each location, see section (2.5).

In particular, the formation of the VEV, is based on the Higgs mechanism, see e.g. Zyla (2020), which is based on the formation of the Higgs boson, see Carmesin (2021a). Hereby, the formation of the Higgs boson, is based on the formation of five dimensional vacuum, see Carmesin (2021a). Thereby, the vacuum corresponds to a wave function, see Carmesin (2022).

Altogether, the formation of the VEV is described by the wave function in five-dimensional space, ψ_{5D}.

Accordingly, the process of formation of the bosons of the electroweak interaction, as well as the electroweak interaction, is described by a linear composition of three-dimensional and five-dimensional wave functions:

$$\psi_{EWI} = a \cdot \psi_{3D} + b \cdot \psi_{5D} \tag{8.30}$$

Hereby, the energy of a quantum of vacuum in three - dimensional space is $E_{\Lambda,D=3} = 5.4 \cdot 10^{-5}\,\mathrm{eV}$, see (Carmesin, 2021a, THM 5). For comparison, the energy of a quantum of vacuum in four-dimensional space is $E_{\Lambda,D=4} = 4.077\,\mathrm{MeV}$, see (Carmesin, 2021a, p. 169-170). Moreover, that energy has been emitted at the last dimensional phase transition during the cosmic unfolding (era of 'cosmic inflation') from $D = 4$ to $D = 3$, and it has probably been observed in gravitational waves emitted in the early universe, see Ratzinger and Schwaller (2021). Furthermore, the energy of a quantum of vacuum in five-dimensional space (essential for the formation of the Higgs boson and for the formation of the elementary charge) is $E_{\Lambda,D=5} = 9.22\,\mathrm{GeV}$, see (Carmesin, 2021a, S. 9.1.3).

As the normalization of the wave function is one in any case, and since $E_{\Lambda,D=3} << E_{\Lambda,D=5}$, the three-dimensional vacuum can be neglected in a very good approximation:

$$\psi_{EWI} \approx \psi_{5D} \tag{8.31}$$

8.7.3 Lagrangian derived by SQ

In this section, we show how the symmetry breaking based on the SQ, see section (8.7.2), is applied to the Lagrangian in Eq. (8.7), without any additional assumption:

$$\mathcal{L} = -|D_\mu \psi|^2 - m^2 \psi^{cc} \psi \tag{8.32}$$

8.7.3.1 Potential in $\mathcal{L}$

The potential V has been added in the Higgs mechanism, in order to describe the symmetry breaking in the SMEP.

However, in the SQ, the symmetry breaking of the vacuum is described by the wave function in Eqs. (8.30, 8.31) and section (2.5).

As a consequence, and in the present case of the phase transition that enables the formation of masses, the ψ^4 term inherent to the potential V is not needed any more.

Accordingly, the Lagrangian has the following form:

$$\mathcal{L} = -|D_\mu \psi_{EWI}|^2 - m^2 \cdot |\psi_{EWI}|^2 \tag{8.33}$$

8.8 Derivation of the masses m_W and m_Z

In this section, we investigate the formation of the masses M_Z and M_W. That have been observed, see e.g. Zyla (2020). For it, we apply the Lagrangian in Eqs. (8.33, 8.6):

$$\mathcal{L} = -|D_\mu \psi_{EWI}|^2 - m^2 \cdot |\psi_{EWI}|^2 \qquad \text{with} \tag{8.34}$$

$$D_\mu = \partial_\mu + ig\Sigma_{\alpha=1}^{\alpha=3}\frac{\sigma^\alpha}{2}W_\mu^\alpha + ig'\frac{1}{2}\hat{Y} \cdot B_\mu \tag{8.35}$$

Note that the hypercharge-number Y can be observed, and corresponds to an operator in QP, see e.g. Kumar (2018), Carmesin (2022). Next, we insert Eq. (8.35) into Eq. (8.33):

$$\mathcal{L} = \frac{1}{4}|(2\partial_\mu + i\frac{g}{2}\Sigma_\alpha^3\sigma^\alpha W_\mu^\alpha + i\frac{g'}{2}\hat{Y}B_\mu)\langle\psi_{EWI}\rangle|^2 - m^2|\psi_{EWI}|^2 \tag{8.36}$$

More explicitly, we express $\langle\psi_{EWI}\rangle$ by a two-dimensional vector in charge space:

$$|\langle\psi_{EWI}\rangle|^2 = \left|\begin{pmatrix} \langle\psi_{EWI,1}\rangle \\ \langle\psi_{EWI,2}\rangle \end{pmatrix}\right|^2 \tag{8.37}$$

Hereby, we apply the symmetry of the state $\langle\psi_{EWI}\rangle$ with broken symmetry in charge space. Moreover we use the definition of the VEV, see e.g. (Weinberg, 1996, 21.3.27), Carmesin (2021a):

$$|\langle\psi_{EWI}\rangle|^2 = |\langle\psi_{EWI,1}\rangle|^2 + |\langle\psi_{EWI,2}\rangle|^2 = 2|\langle\psi_{EWI,1}\rangle|^2 = 2v^2 \tag{8.38}$$

So the vector in Eq. (8.37) can be rotated so that the upper component is zero. So we derive:

$$\langle \psi_{EWI} \rangle = \begin{pmatrix} 0 \\ \sqrt{2}\langle \psi_{EWI,1} \rangle \end{pmatrix} = \begin{pmatrix} 0 \\ \sqrt{2}v \end{pmatrix} \tag{8.39}$$

Next, we insert Eq. (8.39) into Eq. (8.36):

$$\mathcal{L} = \frac{1}{4} \left| (2\partial_\mu + ig\Sigma_\alpha^3 \sigma^\alpha W_\mu^\alpha + ig'\hat{Y} B_\mu) \begin{pmatrix} 0 \\ v \end{pmatrix} \right|^2 - m^2 |\psi_{EWI}|^2 \tag{8.40}$$

In order to derive the formation of the masses M_Z and M_W, we do not need to analyze the partial derivative. Accordingly, we neglect these derivatives. The corresponding Lagrangian is named mass term, see (Weinberg, 1996, Eq. 21.3.29):

$$\mathcal{L}_m = \frac{1}{4} \left| (ig\Sigma_\alpha^3 \sigma^\alpha W_\mu^\alpha + ig'\hat{Y} B_\mu) \begin{pmatrix} 0 \\ v \end{pmatrix} \right|^2 - m^2 |\psi_{EWI}|^2 \tag{8.41}$$

Next, we use the matrix representation of the hypercharge number, see e.g. (Weinberg, 1996, 21.3.23):

$$\hat{Y} = - \begin{pmatrix} 1 & 0 \\ 0 & 1 \end{pmatrix} \tag{8.42}$$

Additionally, we apply the Pauli matrices:

$$\mathcal{L}_m = \frac{-1}{4} \left| (gW_\mu^1 - iW_\mu^2) \begin{pmatrix} v \\ 0 \end{pmatrix} - (gW_\mu^3 + g'B_\mu) \begin{pmatrix} 0 \\ v \end{pmatrix} \right|^2 \tag{8.43}$$

$$- m^2 |\psi_{EWI}|^2 \tag{8.44}$$

Next, we evaluate the square. Hereby, the product $(gW_\mu^1 - iW_\mu^2)^{cc} \cdot (gW_\mu^1 - iW_\mu^2)$ provides the following mixed terms: $gW_\mu^1 \cdot (-)iW_\mu^2$ and $-(i)^{cc} W_\mu^2 \cdot gW_\mu^1$. The sum of these two terms is

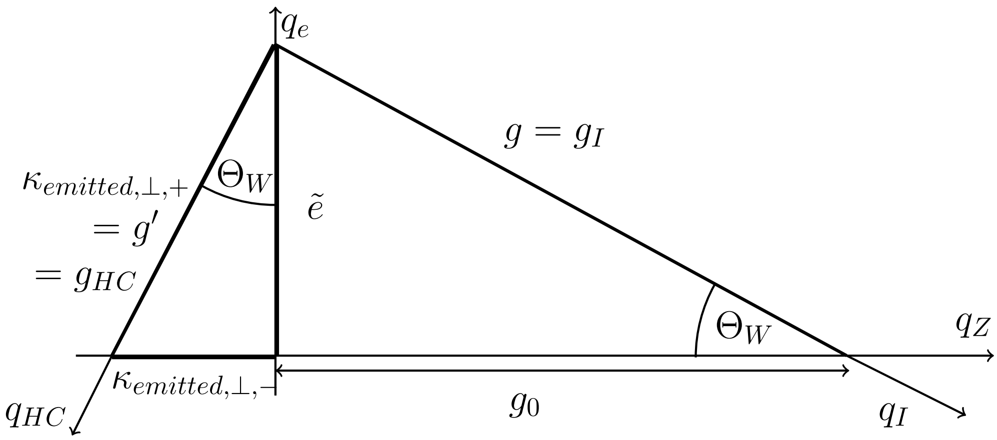

Figure 8.1: Vector space of sources with coordinates q_{HC} and q_I corresponding to the couplings g_{HC} of the hypercharge and g_I of the isospin. Hereby, perturbations are treated in S. (3.5, 5.1.3, 5.1.4, 5.1.5). g_0 is the non-electric component of g.

zero, as a result of the conjugate complex, $(i)^{cc} = -1$. So we obtain:

$$\mathcal{L}_m = \frac{v^2}{4}\left(g^2|W^1_\mu|^2 + g^2|W^2_\mu|^2 + |gW^3_\mu + g'B_\mu|^2\right) - m^2|\psi_{EWI}|^2 \tag{8.45}$$

Similarly as for the couplings g and g', there are the two short sides of the right-angled triangle in Fig. (8.1). The fields W^3_μ and B_μ in the above Eq. (8.45) are the corresponding short sides of a right-angled triangle with the same angle Θ_W. Thereby, the hypotenuse is the field Z_μ. Hereby, the projection of W^3_μ onto Z_μ is $\cos(\Theta_W) \cdot W^3_\mu$ see Fig. (8.1). Similarly, the projection of B_μ onto Z_μ is $\sin(\Theta_W) \cdot B_\mu$. These two projections constitute Z_μ, see Fig. (8.1). So the following holds:

$$Z_\mu = \cos(\Theta_W) \cdot W^3_\mu + \sin(\Theta_W) \cdot B_\mu \tag{8.46}$$

Using the right-angled triangle in Fig. (8.1), we name the hypotenuse g_z, and we derive the following relations:

$$g = g_z \cdot \cos(\Theta_W) \;\text{ and }\; g' = g_z \cdot \sin(\Theta_W) \tag{8.47}$$

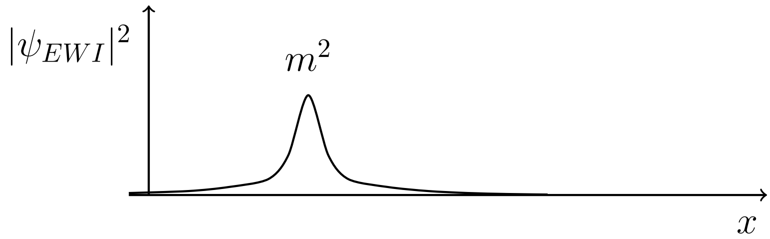

Figure 8.2: Mass m located at a peak of the wave function.

Next, we apply Eqs. (8.47) to Eq. (8.45):

$$\mathcal{L}_m = \frac{v^2}{4}\left(g^2|W_\mu^1|^2 + g^2|W_\mu^2|^2 + g_z^2|W_\mu^3 \cos\Theta_W + B_\mu \sin\Theta_W|^2\right) \tag{8.48}$$

$$- m^2|\psi_{EWI}|^2 \tag{8.49}$$

Here, we apply Eq. (8.46) to Eqs. (8.48, 8.49):

$$\mathcal{L}_m = \frac{v^2}{4}\left(g^2|W_\mu^1|^2 + g^2|W_\mu^2|^2 + g_z^2|Z_\mu Z^\mu|\right) - m^2|\psi_{EWI}|^2 \tag{8.50}$$

Additionally, according to the right-angled triangle in Fig. (8.1) and the theorem of Pythagoras, the following relation holds:

$$g_z^2 = g^2 + g'^2 \tag{8.51}$$

Usually, g_z is expressed according to Eq. (8.51). Thus to Eq. (8.50) takes the following form:

$$\mathcal{L}_m = \frac{v^2}{4}\left(g^2|W_\mu^1|^2 + g^2|W_\mu^2|^2 + (g^2 + g'^2)|Z_\mu Z^\mu|\right) - m^2|\psi_{EWI}|^2 \tag{8.52}$$

In Eq. (8.52), the absolute square $|\psi_{EWI}|^2$ represents the location of the square of the mass m^2, see Fig. (8.2). Similarly, the absolute square $|Z_\mu Z^\mu|$ represents the location of the square of the mass M_Z^2, see Fig. (8.3). So we derive the mass of the Z-boson:

$$M_Z^2 = \frac{v^2(g^2 + g'^2)}{4} \quad \text{or} \quad M_Z = \frac{v\sqrt{g^2 + g'^2}}{2} = \frac{v|g_z|}{2} \tag{8.53}$$

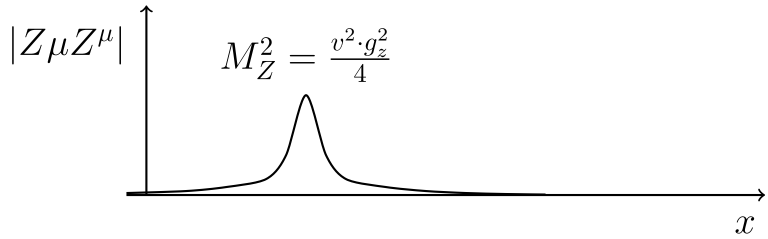

Figure 8.3: Mass M_Z located at a peak of the absolute square of the field $|Z\mu Z^\mu|$.

Analogously, the square $(W_\mu^1)^2$ represents the location of the square of the mass M_W^2, see Fig. (8.3). So we derive the mass of the W-boson:

$$(M_W^1)^2 = \frac{v^2 g^2}{4} \quad \text{or} \quad M_W^1 = \frac{v|g|}{2} = M_W^2 \tag{8.54}$$

Transformation of fields W_μ^1 and W_μ^2: The charge of the W-bosons can be observed. The corresponding fields W_μ^- and W_μ^+ are derived by the following transformation, see for instance (Weinberg, 1996, Eqs. 21.3.12, 21.3.13):

$$W_\mu^+ =(W_\mu^1 + iW_\mu^2)/\sqrt{2} \text{ and } W_\mu^- = (W_\mu^1 - iW_\mu^2)/\sqrt{2} \tag{8.55}$$

We multiply these equations with each other. Additionally, we multiply the product by two:

$$2W_\mu^+ \cdot W_\mu^- =(W_\mu^1)^2 + (W_\mu^2)^2 \tag{8.56}$$

Accordingly, Eq. (8.52) is represented as follows:

$$\mathcal{L}_m =\frac{v^2}{4}\left(2g^2|W_\mu^+ \cdot W_\mu^-| + (g^2 + g'^2)|Z_\mu Z^\mu|\right) - m^2|\psi_{EWI}|^2 \tag{8.57}$$

As the transformation does not change the sum $M_W^1 + M_W^2$ of the masses, the mass M_W of the W-bosons is as follows, see Eq. (8.54):

$$M_{W_\mu^+} = M_{W_\mu^-} = \frac{v|g|}{2} =: M_W \tag{8.58}$$

Calculation of the masses: In order to derive and calculate the masses M_W as well as M_Z, in Eq. (8.53), we apply the values of the weak angle and of the elementary charge corresponding to the energy M_W, see Fig. (5.2). Accordingly, we apply the coupling $\tilde{e}_{SMEWI,eff}(E = 80\,\text{GeV})$, the weak angle at $E = 80\,\text{GeV}$ in table (5.2), as well as the VEV_{theo} and relations corresponding to the triangle in Fig. (8.1):

$$M_Z = \frac{v\tilde{e}_{SMEWI,eff}}{2\sin(\Theta_W(E))\cos(\Theta_W(E))} \quad \text{with} \tag{8.59}$$

$$\sin^2(\Theta_W(E)) = 0.2314 \quad \text{at} \quad E = 80\,\text{GeV} \tag{8.60}$$

$$\tilde{e}_{SMEWI,eff} = \tilde{e} \cdot \sqrt{4\pi} \cdot \sqrt{\frac{137}{129}} = 0.312\,432 \quad \text{and} \tag{8.61}$$

$$VEV_{theo} = 247.6\,\text{GeV} \pm 0.57\,\% \tag{8.62}$$

So we obtain the following theoretical value of the mass:

$$M_{Z,theo} = 91.717\,\text{GeV} \tag{8.63}$$

The observed value and relative difference are as follows, (Zyla, 2020, p. 31):

$$M_{Z,obs} = 91.188\,\text{GeV} \pm 149\,\text{ppm} \quad \text{and} \tag{8.64}$$

$$\Delta_{rel.,M_Z,theo.,obs.} = 0.0058 = 0.58\% \tag{8.65}$$

Similarly, we calculate the mass M_W in Eq. (8.54), by using the coupling $\tilde{e}_{SMEWI,eff}$ and angle at $E = 80\,\text{GeV}$, as well as the VEV in Eq. (8.15) and the triangle in Fig. (8.1):

$$M_W = \frac{vg}{2} = \frac{v\tilde{e}_{SMEWI,eff}(E)}{2\sin(\Theta_W(E))} \tag{8.66}$$

So we obtain the following theoretical value of the mass:

$$M_{W,theo} = 80.409\,\text{GeV} \tag{8.67}$$

The observed value relative difference are as follows, (Zyla, 2020, p. 31):

$$M_{W,obs} = 80.379\,\text{GeV} \pm 149\,\text{ppm} \quad \text{and} \tag{8.68}$$

$$\Delta_{rel.,M_W,theo.,obs.} = \pm 372\,\text{ppm} \tag{8.69}$$

Altogether, the SQ provides the correct phase transition in the SMEP. Thereby, the SQ provides a basis for the Higgs mechanism. Moreover, the SQ provides the correct masses of the bosons of the weak interaction. This shows the next THM:

Theorem 10 Phase transition and masses

(1) The PGI is incomplete in SMEP, as the PGI does not provide the masses of elementary particles in the SMEP.

(2) The incompleteness of the PGI in the SMEP is traditionally resolved by phase transitions, PT.

(3) In traditional SMEP, these phase transitions are modeled by the proposed Higgs mechanism.

(3.1) In the Higgs mechanism, the phase with broken symmetry provides the Higgs field, including the vacuum expectation value, VEV. That VEV is orders of magnitudes larger than the energy of the quanta of the present-day vacuum.

(3.2) In the Higgs mechanism, the physical content of the order parameter of the PT, Φ, the VEV, is not modeled. Instead, the order parameter of the PT is schematically modeled by a usual Φ^2-Φ^4 *model of a PT.*

(4) In the SQ, the PT is derived, in contrast to the proposed Higgs mechanism.

(4.1) In the SQ, the mass of the Higgs boson m_H has been derived, without using any fit parameter, see Carmesin (2021a).

(4.2) In the SQ, the mass $m_{pair} = E_{pair}/c^2$ of a bound pair of Higgs bosons has been **derived***, see section (8.7):*

$$E_{pair} = 247.6\,\mathrm{GeV} \tag{8.70}$$

(4.3) The **comparison** *of the energy E_{pair} of a bound pair of Higgs bosons in (4.2) with the observed VEV,*

$$VEV_{obs} = 246.1965\,\mathrm{GeV} \tag{8.71}$$

shows a clear accordance of both energies, whereby the relative difference amounts to 0.57%*, see section (8.7).*

(4.4) According to items (4.1), (4.2) and (4.3), the phase transition that causes the formation of the VEV has been **explained** *on the basis of the SQ in a microscopic and detailed manner. Thereby, no fit has been executed.*

(5) In the SQ, the formation of the masses M_W and M_Z has been derived and explained, in precise accordance with observation:

(5.1) In the SQ, the wave function ψ_{EWI} describes the formation of three-dimensional and of five-dimensional vacuum, whereby the formation of five-dimensional vacuum describes the formation of m_H and of $E_{pair} = m_{pair}c^2$.

(5.2) In the SQ, the Lagrangian $\mathcal{L}_m$ describes the formation of the masses M_W and M_Z.
In particular, the derived masses of the bosons of the electroweak interaction are as follows:

$$M_{Z,theo} = 91.717\,\mathrm{GeV} \quad \text{and} \quad M_{W,theo} = 81.409\,\mathrm{GeV} \tag{8.72}$$

(5.3) The **comparison** *of derived masses $M_{Z,theo}$ and $M_{W,theo}$ with the corresponding observed masses provides an accordance with a deviation below* 0.6%*:*

$$M_{Z,obs} = 91.188\,\mathrm{GeV} \pm 149\,\mathrm{ppm} \quad \text{and} \tag{8.73}$$

$$\Delta_{rel.,M_Z,theo.,obs.} = 0.0058 = 0.58\% \quad \text{and} \tag{8.74}$$

$$M_{W,obs} = 80.379\,\mathrm{GeV} \pm 149\,\mathrm{ppm} \quad \text{and} \tag{8.75}$$

$$\Delta_{rel.,M_W,theo.,obs.} = \pm\, 372\,\mathrm{ppm} \tag{8.76}$$

The difference might essentially be due to the difference between the theoretical and observed value of the VEV.

(5.4) According to items (5.1), (5.2), and (5.3), the formation of the masses M_W and M_Z has been **explained** *on the basis of the SQ.*

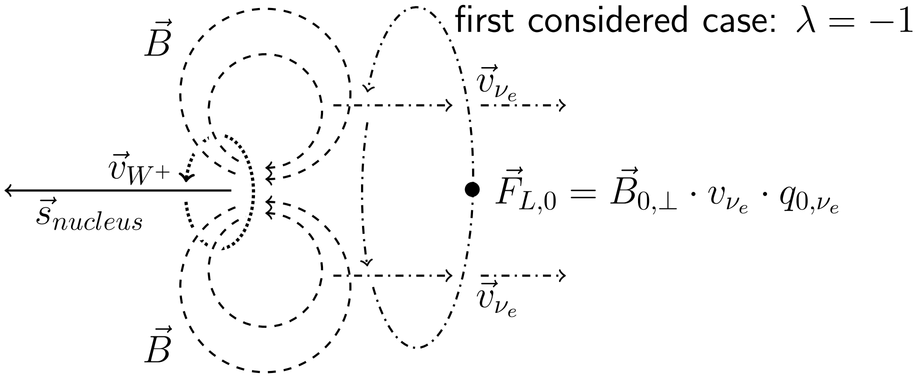

Figure 8.4: Semiclassical model of parity violation.

8.9 Explanation of parity violation

Goldhaber et al. (1957) showed in β^+ decay in a nucleus, that the helicity λ (sign of product of velocity $\vec{v}_{\nu_e}$ and spin $\vec{s}_{\nu_e}$) of a neutrino ν_e is negative, Fig. (8.4). A semiclassical SQ-model explains it: During β^+ decay, a W^+ forms (Griffiths, 2008, S. 2.4.3). Then it decays, whereby it forms the positron e^+ and neutrino ν_e (dashdotted), with a non-electric charge q_{0,ν_e} (Fig. 8.1). As W^+ and ν_e have spins parallel to $\vec{s}_{nucleus}$, W^+ and ν_e rotate (dotted, dashdotted) and W^+ causes a $\vec{B}$-field (dashed). As the coupling g has a non-electric component g_0, W^+ causes a non-electric $\vec{B}_0$-field too, according to PGI. $\vec{B}_{0,\perp}$ is $\perp$ to $\vec{v}_{\nu_e}$. So, a non-electric Lorentz force acts upon ν_e: $\vec{F}_{L,0} = \vec{B}_{0,\perp} \cdot v_{\nu_e} \cdot q_{0,\nu_e}$. That $\vec{F}_{L,0}$ favors ν_e with $\lambda = 1$ or -1, so that only the favored ν_e forms. As the **neutrino with** $\lambda = -1$ **does form**, that sign of $\vec{F}_{L,0}$ enables neutrino formation. However, if sign($\vec{v}_{\nu_e}$) is changed, then sign($\vec{F}_{L,0}$) is changed, so ν_e-formation is disabled. Thus, no ν_e forms with $\lambda = 1$. For the case of charge conjugation, $\mathcal{C}$, the signs of all components of charges change, see Carmesin (2021f), whereby $q_{0,W^+} = q_{0,W^-}$. So, ν_e in Fig. (8.4) changes to $\bar{\nu}_e$ with $q_{0,\bar{\nu}_e} = -q_{0,\nu_e}$. Thus, sign($\vec{F}_{L,0}$) changes. Hence, no $\bar{\nu}_e$ forms with $\lambda = -1$, but $\bar{\nu}_e$ **form with** $\lambda = 1$. So, parity violation is explained for all cases of λ and $\mathcal{C}$.

Chapter 9

Derivation of GR

In this chapter, we analyze general relativity, GR, including possible derivations of the Einstein field equation, EFE, see Eq. (9.36). Moreover, we use the SQ, in order to derive the EFE.

9.1 Smooth transformations

In this section, we investigate the smooth transformations of spacetime that are considered in GR.

(Straumann, 2013, S. 3.3.1) pointed out the type of smooth transformations of spacetime considered in GR:

$$\{x^j\} \rightarrow \{\bar{x}^j\} \qquad \text{is a} \tag{9.1}$$

$$\text{smooth coordinate transformation} \tag{9.2}$$

As the theory is **assumed to be covariant**, see e.g. (Hobson et al., 2006, p. 528), a covariant expression for the volume in spacetime is used, see e.e. (Straumann, 2013, S. 3.3.1):

$$dV^4 = \sqrt{-g} \cdot d^4x \quad \text{with} \quad g = det(g_{ij}) \tag{9.3}$$

Proposition 3 Smooth transformations of GR

(1) The theory of general relativity, GR, is restricted to the physics of smooth transformations of spacetime.

(2) The theory of GR does not describe the physics of possible discontinuous phase transitions, PT, of spacetime.

(3) Most theories of GR treat three-dimensional space.

So these theories of GR do not describe any transformations to higher dimensional space, though physics in higher dimensional space has been observed directly, see e.g. Lohse et al. (2018), Zilberberg et al. (2018), and indirectly, see Carmesin (2017b), or e.g. Carmesin (2018b), Carmesin (2019d), or also Carmesin (2021a), Carmesin (2021f).

9.2 Derivations based on the PLA or PSA

In this section, we investigate derivations of the EFE that are based on the principle of least action, PLA. Thereby, that principle is generalized to a principle of stationary action, PSA, see e.g. (Weinberg, 1972, chapter 12 or p. 357-664). Thereby, the action is stationary, if it is at a local minimum or at a local maximum, with respect to infinitesimal variations of the variables under investigation.

9.2.1 Paths

In this section, we investigate the **proposed paths** that are used in order to apply the PLA or PSA.

Usually, a path starts at a time coordinate $x_{0,start}$, extend in space without limitation, and ends at a time coordinate $x_{0,end}$, see e.g. (Landau and Lifschitz, 1971, § 93). Alternatively, the path may be generalized to compact regions of coordinates, these have been named **patches**, see e.g. (Straumann, 2013, S. 3.3.1).

Both, a path and a compact region of coordinates are non - quantized, and both can be interpreted as a semiclassical geometric object that is obtained from rate gravity waves, RGW, in the limit of zero wavelength, $\lim_{\lambda \to 0}$. Carmesin (2022) has shown already for the case of the Schwarzschild solution, that it can be interpreted and derived as a semiclassical geometric object in spacetime, whereby the semiclassical limit corresponds to the limit $\lim_{\lambda \to 0}$ of rate gravity waves, RGWs.

Proposition 4 GR as a semiclassical limit of RGWs

(1) The paths or patches used in GR can be interpreted as semiclassical geometric objects that occur in the limit of zero wavelength, $\lim_{\lambda \to 0}$*, of the rate gravity waves, RGW, of the SQ.*

(2) In particular, for the case of the Schwarzschild solution, Carmesin (2022) has shown that the Schwarzschild solution represents the limit $\lim_{\lambda \to 0}$ *of the RGWs.*

9.2.2 Action

In order to apply the PLA or the PSA, Hilbert (1915) proposed the **Einstein-Hilbert** action, S_{EH}, whereby he used results provided by Einstein (1911), Einstein (1915b) and Einstein (1915a), see Corry et al. (1997). So he postulated that action by a founded guess.

By an application of the PSA to the S_{EH}, the **Einstein field equation, EFE**, see Einstein (1915a), can be derived.

In fact, that action is still guessed in a founded manner, see e.g. (Landau and Lifschitz, 1971, § 93-95), (Weinberg, 1972, chapter 12), Stephani (1980), Carmeli (1982), (Hobson et al., 2006, chapter 19), (Straumann, 2013, chapter 3).

9.2.3 Gauge invariance

In GR, the *Einstein-Hilbert* action S_{EH} is usually obtained by a founded guess or postulate, see section (9.2.2). In contrast, in the SMEP, the action is usually obtained on the basis of the Principle of Gauge Invariance, PGI. In this section, we investigate, whether the action S_{EH} has also been obtained by the PGI. This would be nice advantage, since the EFE could be derived from the same postulate, that is used in the SMEP.

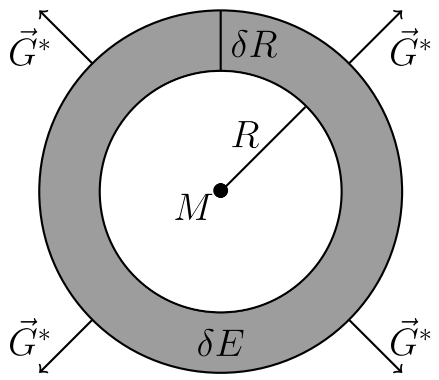

Figure 9.1: A shell with a mass M at its center, with a radius R, and with a thickness δR has an energy density u_f of the field $\vec{G}^*$ generated by M. Accordingly, the shell has an energy δE.

In fact, various studies of such an application have been elaborated. For instance, Lasenby et al. (1998) proposed a gauge theory of gravity, however, the action S_{EH} is still postulated, see (Lasenby et al., 1998, Eq. 4.14). Similarly, (Santos, 2019, Eq. 32) worked on the gauge theory of gravity, and he postulated the action S_{EH}, too.

Accordingly, in a systematic analysis of gauge invariant elements inherent to GR, Giesel et al. (2009) described gauge invariance in low orders of perturbation theory.

Altogether, the action S_{EH} has not been derived on the basis of gauge invariance. So the known attempts to derive the EFE from the SMEP failed.

9.3 EFE derived from the SQ

In this section, we derive the EFE from the SQ in a very transparent manner. For it, we use the Gaussian curvature, as it is very intuitive and invariant, see Gauss (1827).

(1) Energy density: Based on the PFF and GG, we use the energy density u_f of a gravitational field $\vec{G}^*$, see (Carmesin, 2021d, Eq. 2.7)

$$u_f = \frac{|\vec{G}^*|^2}{8\pi G} \tag{9.4}$$

(2) Energy in a shell: Using (1), we derive the energy δE in a shell around a mass or dynamical mass M, whereby the shell has a radius R and a thickness δR:

$$\delta E = u_f \cdot 4\pi R^2 \cdot \delta R \qquad \text{or} \tag{9.5}$$

$$\delta E = \frac{|\vec{G}^*|^2}{8\pi G} \cdot 4\pi R^2 \cdot \delta R \tag{9.6}$$

Hereby, we apply the area A:

$$\delta E = u_f \cdot A \cdot \delta R \qquad \text{or} \tag{9.7}$$

$$\delta E = \frac{|\vec{G}^*|^2}{8\pi G} \cdot A \cdot \delta R \qquad \text{with} \tag{9.8}$$

$$A = 4\pi \cdot R^2 \tag{9.9}$$

(3) Field: Based on the SQ, we apply the concepts of GG and PFF, in order to express the field as a function of the mass M:

$$|\vec{G}^*| = \frac{G \cdot M}{R^2} \tag{9.10}$$

(4) Chosen radius: Based on SQ, we apply the Schwarzschild radius R_S, see for instance Carmesin (2012), Carmesin (2016), Carmesin (2021d), Carmesin et al. (2022). For it, we vary the radius of the shell, according to GG inherent to the SQ. So the field in (3) is as follows:

$$|\vec{G}^*| = \frac{G \cdot M}{R_S^2} \qquad \text{with} \tag{9.11}$$

$$R_S = \frac{2G \cdot M}{c^2} \qquad \text{thus} \tag{9.12}$$

$$|\vec{G}^*| = \frac{c^2}{2}\frac{R_S}{R_S^2} = \frac{c^2}{2}\frac{1}{R_S} \tag{9.13}$$

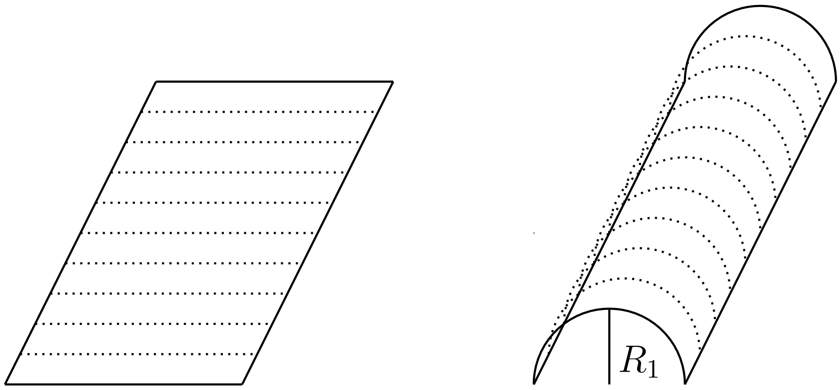

Figure 9.2: Embedding of a sheet of paper in three-dimensional space: In the left embedding, the two radii of curvature are infinite, $R_1 = \infty$ and $R_2 = \infty$. In the right embedding, $R_1 = 1$ and $R_2 = \infty$. In both forms of embedding, the Gaussian curvature $K = \frac{1}{R_1} \cdot \frac{1}{R_2}$ is zero. These two forms of embedding present an example for the invariance of Gaussian curvature K with respect to embedding, Gauss (1827).

(5) Gaussian curvature K: Next, we apply Eq. (9.12) to Eq. (9.8):

$$\delta E = \frac{1}{8\pi G} \cdot \frac{c^4}{4} \cdot \frac{1}{R_S^2} \cdot A \cdot \delta R \tag{9.14}$$

Hereby, we identify the radius R_S of curvature, as well as the Gaussian curvature K:

$$K = \frac{1}{R_1} \cdot \frac{1}{R_2} = \frac{1}{R_S^2} \quad \text{and} \tag{9.15}$$

$$\delta E = \frac{1}{8\pi G} \cdot \frac{c^4}{4} \cdot K \cdot A \cdot \delta R \tag{9.16}$$

This intermediate result is very essential:

(5.1) Gauss (1827) showed in his Theorema Egregium that the Gaussian curvature K is an inner property of the manifold corresponding to the shell. That means, the properties of the manifold can be completely obtained by measurements within the manifold. In particular, these inner properties are not modified, if the manifold is embedded in various manners in a higher dimensional space, see Figs. (9.2, 9.3). Thus K is an invariant with respect to all possible forms of embedding of the manifold in a higher dimensional space.

(5.2) The Gaussian curvature K can be transformed to the concept of curvature tensors used in Riemannian manifolds and utilized in the EFE.

(5.3) The energy δE of the field G^* in the shell corresponds to the invariant Gaussian curvature K.

(5.4) Since the thickness δr of the shell can be infinitesimal, the energy density u_f of the field G^* corresponds to the invariant Gaussian curvature K.

(5.5) Thus gravity can be described by the field G^* or by the invariant Gaussian curvature, whereby the invariant Gaussian curvature can be transformed to the curvature tensor used in Riemannian manifolds, see e.g. Lee (1997).

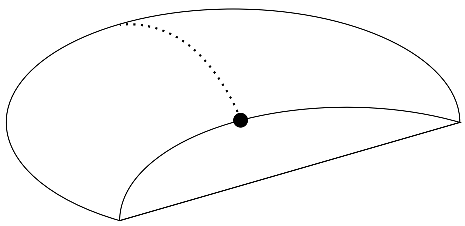

Figure 9.3: Invariant Gaussian curvature: At the marked point, the two radii of curvature are $R_1 = 2$ and $R_2 = 1$. So the Gaussian curvature is $K = \frac{1}{R_1} \cdot \frac{1}{R_2}$ or $K = \frac{1}{2} \cdot \frac{1}{1} = \frac{1}{2}$. This Gaussian curvature K does not depend on the embedding of the manifold, Gauss (1827).

(6) Sectional curvature: Gaussian curvature K describes the curvature of a two-dimensional manifold. Next, we generalize Gaussian curvature to higher-dimensional manifolds. For it, we consider a two-dimensional submanifold, see e.g. (Lee, 1997, p. 143-149). Correspondingly, there are two locally orthogonal directions in the submanifold, and these can be described by the partial derivatives (∂_1, ∂_2). If the corresponding radii of curvature R_1 and R_2 are equal to a radius of curvature R, then the sectional curvature can be introduced as follows:

$$K(II) = \frac{1}{R_1} \cdot \frac{1}{R_2} = \frac{1}{R^2} \qquad \text{and} \tag{9.17}$$

Hereby, $K(II)$ marks a Gaussian curvature at a point of a two-dimensional manifold, with a radius R_1 of curvature in the direction corresponding to a partial derivative ∂_1, and with a radius R_2 of curvature in the direction corresponding to a partial derivative ∂_2, see e.g. Lee (1997).

(7) Curvature scalar: The Gaussian curvature K in (5), as well as the sectional curvature in (6), can be expressed by the curvature scalar S as follows, see e.g. (Lee, 1997, Eq. 8.6 and p. 148):

$$K = \frac{1}{R_1} \cdot \frac{1}{R_2} = \frac{1}{R^2} = \frac{S}{2} \qquad \text{and} \tag{9.18}$$

$$K(II) = \frac{1}{R_1} \cdot \frac{1}{R_2} = \frac{1}{R^2} = \frac{S}{2} \tag{9.19}$$

(8) Application of the curvature scalar: Next, we apply the curvature scalar S in (7) to the energy δE in the shell, see Eq. (9.16). We emphasize that our theory includes higher dimensional space, according to (7):

$$\delta E = \frac{1}{8\pi G} \cdot \frac{c^4}{4} \cdot \frac{S}{2} \cdot A \cdot \delta R \tag{9.20}$$

(9) Including spacetime: While our description in Figs. (9.2, 9.3) is intuitive and geometric, the description in (8) provides a more algebraic description. Using SR inherent to the SQ, we can introduce spacetime in a covariant manner with help of the sign convention, see Eq. (2.15):

$$\eta_{ij,Cartesian} = \begin{pmatrix} -1 & 0 & 0 & 0 \\ 0 & 1 & 0 & 0 \\ 0 & 0 & 1 & 0 \\ 0 & 0 & 0 & 1 \end{pmatrix} \tag{9.21}$$

We emphasize that our theory includes higher dimensional space and spacetime, according to Eq. (9.21).

(10) Ricci tensor: The curvature scalar S in (8) can be expressed by the Ricci tensor R_{ij} or $\hat{Rc}$ as follows, see (Lee, 1997, p. 124):

$$S = g^{ij} R_{ij} = tr_g \hat{Rc} \tag{9.22}$$

Hereby, $\hat{g}$ and g^{ij} represent the metric tensor. As the trace represents a sum of $D = 4$ diagonal elements of the tensor, there occurs a factor four as follows, see (Lee, 1997, p. 125):

$$S\hat{g} = D \cdot \hat{Rc} = 4 \cdot \hat{Rc} \tag{9.23}$$

In order to apply that Eq. (9.23) to Eq. (9.20) we multiply by the metric tensor $\hat{g}$ first:

$$\delta E \cdot \hat{g} = \frac{1}{8\pi G} \cdot \frac{c^4}{4} \cdot \frac{S\hat{g}}{2} \cdot A \cdot \delta R \qquad \text{thus} \tag{9.24}$$

$$\delta E \cdot \hat{g} = \frac{c^4}{16\pi G} \cdot \hat{Rc} \cdot A \cdot \delta R \tag{9.25}$$

(11) Energy density: In order to obtain a similar representation of both sides of the above Eq. (9.25), we express the energy δE in terms of $u_f \cdot A \cdot \delta R$, see Eq. (9.7):

$$u_f \cdot \hat{g} \cdot A \cdot \delta R = \frac{c^4}{16\pi G} \cdot \hat{Rc} \cdot A \cdot \delta R \tag{9.26}$$

While u_f represents the energy of the field only, there may be additional energy densities, according to additional physical objects. In the framework of GR, such additional objects are modeled and must be modeled with an energy momentum tensor $\hat{T}$

or T_{ab}. If such a model of additional objects is included, then $u_f \cdot \hat{g}$ is replaced by $\hat{T}$:

$$\hat{T} \cdot A \cdot \delta R = \frac{c^4}{16\pi G} \cdot \hat{Rc} \cdot A \cdot \delta R \tag{9.27}$$

(12) Representation with coordinates: While the tensors in the above Eq. (9.27) are expressed in the form of tensors marked by a hat, tensors are often expressed with indices indicating the coordinates. In this paragraph, we explicate the indices inherent to Eq. (9.27).

Thereby, $\hat{T}$ is replaced by T_{ab}. Moreover, the surface A is replaced by an infinitesimal surface dA^b, so that we can introduce a corresponding integral representing the surface of the shell in Fig. (9.1). Accordingly, we replace δR by a vector k^a. Correspondingly, we replace $\hat{Rc}$ by R_{ab}. So Eq. (9.27)is represented as follows:

$$\int T_{ab} \cdot k^a \cdot dA^b = \int \frac{c^4}{16\pi G} \cdot R_{ab} \cdot k^a \cdot dA^b \tag{9.28}$$

According to GG, it is not necessary that the radius is R_S, or that the integral is applied to a sphere. Moreover, the infinitesimal elements $k^a \cdot dA^b$ can be chosen in an arbitrary manner. So the remaining terms must be equal:

$$T_{ab} = \frac{c^4}{16\pi G} R_{ab} \tag{9.29}$$

(13) Usual form: There are various forms of the EFE, see e.g. (Landau and Lifschitz, 1971, Eq. 95.8). In order to derive the traditional form of the EFE, we transform the Ricci tensor R_{ab} as follows:

$$R_{ab} = 2R_{ab} - R_{ab} \tag{9.30}$$

The curvature scalar is defined as follows:

$$R = g^{\beta b} R_{\beta b}, \tag{9.31}$$

We multiply by g_{ab}

$$g_{ab}R = g_{ab}g^{\beta b}R_{\beta b}, \tag{9.32}$$

and we use $\delta_a^\beta = g_{ab}g^{\beta b}$:

$$g_{ab}R = \delta_a^\beta R_{\beta b} = R_{ab} \tag{9.33}$$

We apply Eq. (9.33) to Eq. (9.30):

$$R_{ab} = 2R_{ab} - g_{ab}R \tag{9.34}$$

We use Eq. (9.34) in Eq. (9.29): So we derive:

$$T_{ab} = \frac{c^4}{16\pi G}(2R_{ab} - g_{ab}R) \tag{9.35}$$

(14) Einstein field equation EFE: We simplify the above Eq.:

$$T_{ab} = \frac{c^4}{8\pi G}(R_{ab} - g_{ab}R/2) \tag{9.36}$$

This is the **Einstein field equation, EFE**, without any cosmological constant Λ, see Einstein (1915a). In fact, that constant Λ has been proposed as a parameter that can be added to one half of the Ricci scalar, see e.g. Einstein (1917):

$$T_{ab} = \frac{c^4}{8\pi G}(R_{ab} - g_{ab} \cdot (R/2 + \Lambda)) \qquad \text{or} \tag{9.37}$$

Later, Perlmutter et al. (1998) and Riess et al. (2000), as well as Spergel et al. (2007), Smoot (2007), and many others noted in Carmesin (2021c), observed the dark energy, corresponding to Λ. Moreover, Carmesin (2018c), Carmesin (2018b), Carmesin (2019d), Carmesin (2021d), Carmesin (2021a) derived the dark energy from the SQ or from its implication QG. Hereby, these derived values of Λ are in precise accordance with observation, whereby no fit parameter has been applied.

Theorem 11 EFE derived from SQ and smoothness

(1) The Einstein field equation, EFE, has been derived from the spacetime-quadruple, SQ:

(2) For it, the smoothness of the transformations of spacetime has been used:

$$\text{SQ} \,\&\, \text{smoothness} \rightarrow \text{EFE} \qquad \text{with} \qquad (9.38)$$

$$T_{ab} = \frac{c^4}{8\pi G}(R_{ab} - g_{ab} \cdot R/2) \qquad (\text{EFE}) \qquad (9.39)$$

Corollary 1 EFE derived from SQ and smoothness

(1) The above derivation of the EFE does not use the **formation of vacuum, FV**. *Accordingly, the density of the vacuum ρ_Λ has not been derived on the basis of the EFE. Moreover, ρ_Λ can hardly be derived on the basis of the EFE. In contrast, ρ_Λ has been derived on the basis of the SQ, see e. g. (Carmesin, 2022, chapter 4 or THM 11) and with more details (Carmesin, 2021d, sections 6.6, 7.5, 8.5 and 8.6) and together with all derivable parameters of the SMC Carmesin (2021a) and in comparison with many observations including measurements at Laniakea Carmesin (2021c).*

(2) Accordingly to the fact that the above derivation of the EFE does not use FV, **quantum physics, QP***, has not been derived on the basis of the EFE. Moreover, QP can hardly be derived on the basis of the EFE. In contrast, QP has been derived on the basis of the SQ, see Carmesin (2022). Hereby the propagation of the vacuum in terms of rate gravity waves is essential.*

(3) For the above derivation of the EFE, the described transformations of spacetime are restricted to smooth transformations. Accordingly, phase transitions, PT, of spacetime have not been derived on the basis of the EFE. Moreover, such PT can hardly be derived on the basis of the EFE. In contrast, such PT have

been derived on the basis of the SQ, see e.g. Carmesin (2017b), Carmesin (2018b), Carmesin (2019d), Carmesin (2021d).

Hereby, five different derivations of such PTs have been elaborated. Thereby, the newest derivation is presented in Carmesin and Schöneberg (2022).

(4) The above items (1), (2) and (3) indicate three cases of incompleteness of the EFE and of GR, see sections (9.4, 9.5, 9.6). These cases of incompleteness of GR point out essential limitations of GR. Thereby, GR has been and still is a very successful theory in its domain of validity.

9.4 First incompleteness of GR

In this section, we compare GR and the SQ with respect to the derivation of the density of the vacuum ρ_Λ.

As a matter of fact, ρ_Λ has not been derived on the basis of GR or in the basis of the EFE. Moreover, the present-day GR does neither provide semiclassical objects corresponding to the vacuum, nor does GR provide quantum objects corresponding to the vacuum, see e.g. Einstein (1915a), Landau and Lifschitz (1971), Weinberg (1972), Hobson et al. (2006), Straumann (2013).

As a derivation of the density of the vacuum ρ_Λ is missing in GR, the EFE and GR are incomplete with respect to the density of the vacuum ρ_Λ.

In contrast, the SQ provides semiclassical as well as quantum physical derivations of the density of the vacuum ρ_Λ, see e.g. corollary (1 number (1)) or (Carmesin, 2021d, sections 6.6, 7.5, 8.5 and 8.6). Thus SQ is more general than GR.

9.5 Second incompleteness of GR

In this section, we compare GR and the SQ with respect to the derivation of quantum physics, QP.

As a matter of fact, QP has not been derived on the basis of GR or in the basis of the EFE. Moreover, the present-day GR does not provide quantum objects, see e.g. Einstein (1915a), Einstein et al. (1935), Landau and Lifschitz (1971), Weinberg (1972), Hobson et al. (2006), Straumann (2013).

As a derivation of QP is missing in GR, the EFE and GR are incomplete with respect to the derivation of QP.

In contrast, the SQ provides a derivation of QP, see e.g. corollary (1 number (2)) or Carmesin (2022). Thus SQ is more general than GR.

9.6 Third incompleteness of GR

In this section, we elaborate a third incompleteness of GR. The present-day light horizon R_{lh} has been analyzed as a function of time, see Fig. (9.4). For it, the values of $R_{lh}(t)$ at earlier times have been derived in the framework of GR, see e.g. Carmesin (2019d), Carmesin (2020e), Carmesin (2021d), Carmesin (2021a), Heeren et al. (2020).

According to the laws of physics, the density cannot be larger than the Planck density $\rho_P = 5.155 \cdot 10^{96}\,\frac{\mathrm{kg}}{\mathrm{m}^3}$, and lengths as small as the Planck length $L_P = 1.616 \cdot 10^{-35}\,\mathrm{m}$ can be observed, see e.g. Carmesin (2017b), Carmesin (2019d), Carmesin (2021a). Moreover, corresponding to the laws of physics, the length can be as small as the Planck length, see e.g. Carmesin (2017b), Carmesin (2019d), Carmesin (2021a).

Next, we compare the time evolution of the density $\rho(t)$ and of the value of $R_{lh}(t)$ of the light horizon in the universe. In the framework of GR, the Planck density $\rho_P = 5.155 \cdot 10^{96}\,\frac{\mathrm{kg}}{\mathrm{m}^3}$ is already achieved, when $R_{lh}(t)$ is approximately equal to 0.003 mm, see Fig. (9.4). As a consequence, GR is not complete, as GR does not describe the full physically possible time evolution of $R_{lh}(t)$, ranging from the Planck length $L_P = 1.616 \cdot 10^{-35}\,\mathrm{m}$ to the present day light horizon $R_{lh} \approx 4.1 \cdot 10^{26}\,\mathrm{m}$.

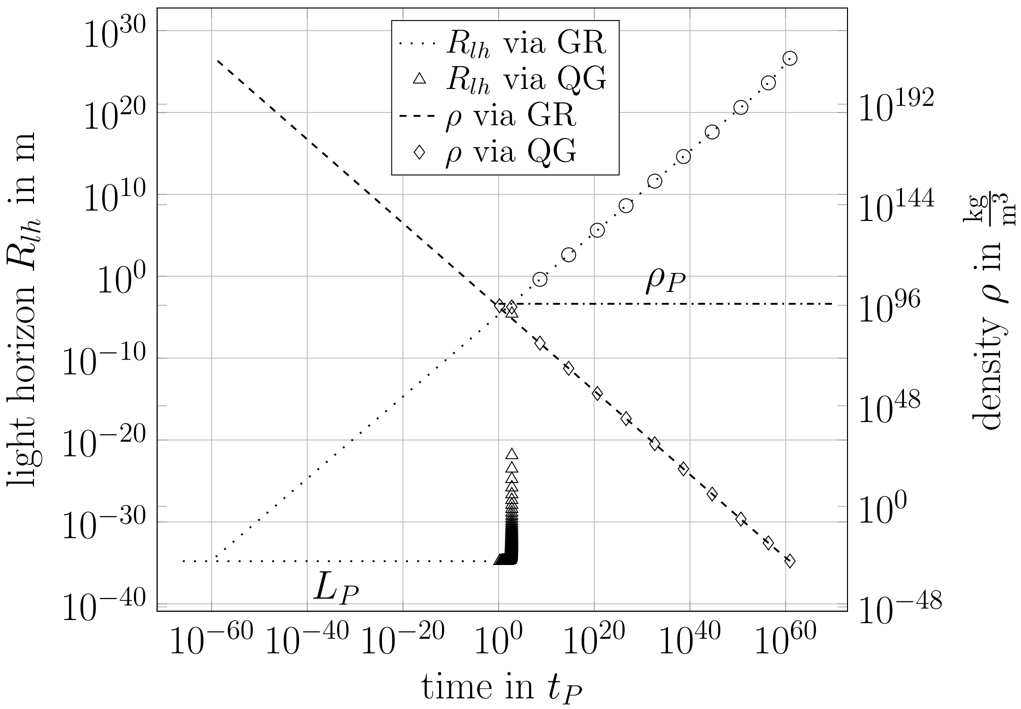

Figure 9.4: Density limit of expansion of space: The time evolution of R_{lh} according to the GR ($\circ$) ranges from the present-day value $4.14 \cdot 10^{26}$ m backwards to 0.003 mm, as at this point the density ($\diamond$) achieves the Planck density $\rho_P = 5.155 \cdot 10^{96} \frac{\text{kg}}{\text{m}^3}$ (dashdotted), and no higher density is physically possible.
However, the physically possible lengths can be as short as the Planck length L_P (loosely dotted). Hence the time evolution of the GR is **incomplete**.
In contrast, we derive the **complete time evolution** of $R_{lh}(t)$, ranging from the current value $4.14 \cdot 10^{26}$ m backwards to L_P. For it we apply GR ($\circ$) combined with dimensional phase transitions ($\triangle$) derived by quantum gravity. Thereby, the phase transitions cause the **extremely rapid distance enlargement in the early universe**

Proposition 5 Incompleteness of GR

(1) The theory of general relativity, GR, describes the time evolution of the light horizon $R_{lh}(t)$ *ranging from* $R_{lh} \approx 0.003\,\mathrm{mm}$ *towards the present day light horizon* $R_{lh} \approx 4.1 \cdot 10^{26}\,\mathrm{m}$.

(2) However, the physically observable lengths range from the Planck length $L_P = 1.616 \cdot 10^{-35}\,\mathrm{m}$ *towards the present day light horizon* $R_{lh} \approx 4.1 \cdot 10^{26}\,\mathrm{m}$.

(3) So GR is incomplete.

9.7 Solution of 3^{rd} incompleteness of GR

Carmesin (2017b) discovered dimensional phase transitions that solve the incompleteness of GR. Thereby, the phase transitions have been modeled in a van der Waals type model in Carmesin (2017b), or in Carmesin (2018b), Carmesin (2019d), Carmesin (2020e).
Moreover, these dimensional phase transitions have been confirmed by the time evolution of dark energy, see e.g. Carmesin (2018c), or in Carmesin (2018b), Carmesin (2019d), Carmesin (2021d), Carmesin (2021a).

Furthermore, these phase transitions have been confirmed by Bose gas model, see e.g. Carmesin (2021d), Sawitzki and Carmesin (2021).

Additionally, these phase transitions have been confirmed by an analysis of the connectivity of locations in space, see Carmesin (2021d).

Moreover, these phase transitions have been confirmed by a droplet model, see Carmesin and Schöneberg (2022).

Thereby, the results are based on the SQ, and no fit has been applied. The phase transitions are marked by the triangles in Fig. (9.4).

Theorem 12 Third incompleteness of GR solved by SQ

(1) The third incompleteness of GR, see PROP (5), is solved by the SQ.

(2) Thereby, the rapid increase of distances in the early universe has been explained. Thus the so-called era of 'cosmic inflation' has been explained by dimensional phase transitions of the vacuum or of dark energy, derived in the SQ.

(3) These dimensional phase transitions have been derived by five very different and independent models in SQ. Thereby, the results are based on the SQ, no fit has been applied, and precise accordance with observation has been achieved, see e.g. Carmesin (2021d), Carmesin (2021a).

(4) In particular, the formation of the sum of the neutrino masses, the formation of the mass of the Higgs boson, as well as the elementary charge have been derived in the framework of these phase transitions. Thereby, the results are based on the SQ, no fit has been applied, and precise accordance with observation has been achieved, see e.g. Carmesin (2021a), Carmesin (2021f).

(5a) GR is included in the SQ, as GR has been derived from the SQ, see THM (11).

(5b) SQ is more general than GR, as the SQ solves the three cases of incompleteness of GR, see sections (9.4, 9.5, 9.6) or PROP (5).

Chapter 10

Discussion

10.1 Results

In this section, we summarize results derived from the SQ.

(1) The observed expansion of the universe since the Big Bang is based on the **formation of vacuum**. The present-day vacuum at Earth is constituted by vacuum that has formed since the Big Bang and at all places within the light horizon R_{lh}. Thus, R_{lh} is inherent to the structure of the present-day vacuum and of its density[1], ρ_Λ.

(1.1) In the SQ, the formation of vacuum provides the structure of the present-day space, time and spacetime. Thus, the present-day space, time and spacetime are **not assumed, but derived**, see THM (1).

(1.2) In the SQ, quantum physics, QP, and quantum gravity, QG, have been derived and explained, see Carmesin (2022). Thus, QP and QG are **not assumed, but derived**.

(1.2) The four principles of the SQ have **two foundations: observation and thought experiment**, see section (2.1).

[1] That density has been derived on the basis of the SQ, and it is in precise accordance with observation, see THM (1) or e.g. Carmesin (2018c), Carmesin (2018b), Carmesin (2019d), Carmesin (2019b), Carmesin (2021d), Carmesin (2021a), Carmesin (2021b), Carmesin (2021c), Carmesin (2022).

(2.1) In the early universe, the vacuum exhibited a series of **dimensional phase transitions**.

(2.2) Thereby, the quanta of vacuum took corresponding zero-point energies, $ZPE_{\Lambda,D}$, see Figs. (2.6, 2.8). These $ZPE_{\Lambda,D}$ are present at all times and locations, as a consequence of the structure of vacuum in (1), see THM (1) and PROP (2). Thus, these energies $ZPE_{\Lambda,D}$ represent a **large scale excitation spectrum** of vacuum[2].

(3) In addition to the large scale excitation spectrum of vacuum in (2), there are intermediate scale excitation states corresponding to symmetries of tensors. In particular, a longitudinal unidirectional quantum of vacuum represents a **most simple excitation**, $ZPE_{longitudinal,D}$. Moreover, harmonic oscillations provide small scale excitation states, see Carmesin (2021a).

(4) A **triple** of the most simple excitation $ZPE_{longitudinal,D}$ in (3) can bind. Thereby, the triple of $ZPE_{longitudinal,D}$ can form a most simple $3D$-object in three-dimensional vacuum, see Carmesin (2021a).

(5) If a triple of $ZPE_{longitudinal,D=5}$ in (4) has the **lowest possible energy**, then the triple has the energy $E_H = m_H \cdot c^2$ of the Higgs boson, see Carmesin (2021a).

(6) Each of the three longitudinal quanta (see (3)) of the triple in (4) causes **forced oscillations** of the other two quanta. These forced oscillations emit transverse fields $G^*_{i\to j}$. These forced oscillations and fields $G^*_{i\to j}$ cause an interaction according to a charge $\tilde{e}_{theo}$. Thereby, $\tilde{e}_{theo}$ is equal to the observed elementary electric charge $\tilde{e}_{obs}$. Thereby, the difference between theory and observation amounts to $5.4 \cdot 10^{-8}$, whereby no fit is used, see Carmesin (2021f).

(7) Moreover, these forced oscillations and fields $G^*_{i\to j}$ provide

[2]See e.g. Carmesin (2018c), Carmesin (2018b), Carmesin (2019d), Carmesin (2019b), Carmesin (2021d), Carmesin (2021a).

two components, $\kappa_{emitted,\perp,-}$ and $\kappa_{emitted,\perp,+}$, see Fig. (5.1) and Carmesin (2021f).

(8) The charge $\tilde{e}$ in (6) and its two components $\kappa_{emitted,\perp,-}$ and $\kappa_{emitted,\perp,+}$ establish a triangle, whereby $\tilde{e}$ and $\kappa_{emitted,\perp,+}$ enclose an angle Θ. Comparison with observation shows that this angle Θ is equal to the **weak angle** Θ_W of the weak interaction, see Figs. (5.1, 5.2) and THM (5). Thus, the weak angle is explained via SQ.

(9) The triangle in (8) spans a two-dimensional **charge space**, see Fig. (6.1) and THM (5).

(10) In $2D$ charge space, there occur the two couplings $g' = \kappa_{emitted,\perp,+} = \tilde{e}/\cos\Theta_W$ and $g = \tilde{e}/\sin\Theta_W$. Moreover, in $2D$ charge space, there occurs the isospin, see Fig. (6.2) and THM (5). Comparison with the SMEWI shows that g' represents the **hypercharge**, while g represents the **isospin charge**. Hereby, perturbations are treated in S. (3.5, 5.1.3, 5.1.4, 5.1.5).

(11.1) In $2D$ charge space, the couplings g' and g can be transformed to couplings $\tilde{e}$ and $g_z = \sqrt{g^2 + g'^2}$. Hereby, $\tilde{e}$ is the **elementary electric charge**, while g_z represents the **non-electric charge**. see Fig. (6.2) and THM (5).

(11.2) The hypercharge g' and isospin charge g in (10) or the transformed pair of the elementary electric charge $\tilde{e}$ and the non-electric charge g_z in (11.1) are the **electroweak charges**.

(12) The isospin in (10) corresponds to the **gauge group** $SU(2)$ **of isospin**, as a consequence of the SQ, see THM (8).

(13) On the basis of the SQ, and in a semiclassical limit that provides paths, the **principle of least action, PLA**, has been derived, see THM (6).

(13.1) The PLA can be generalized to the **principle of stationary action, PSA**.

(13.2) On the basis of the SQ, and on the basis of the derivation of QP in (1.2), and in a semiclassical limit, which provides paths, the **principle of gauge invariance, PGI**, has been derived, see THM (7).

(14) Triples with mass m_H in (5) can form **pairs**. Comparison with the observed vacuum expectation value VEV shows, that a pair has the energy of VEV, $E_{pair} = VEV_{obs}$, see THM (10).

(15) The formation of E_{pair} corresponding to the VEV_{obs} in (13) is **explained by the large scale excitation spectrum in (2.2) and by phase transitions in (2.1)**.

(16) Thus, the phase transition modeled by the Higgs mechanism in the SMEWI and SMEP, has been **explained by the phase transitions in (2.1)**.

(16.1) Thereby, the phase transitions in (2.1) provide energies, electroweak charges as well as a founded and predictive unification of cosmology and elementary particle physics.

(17) On the basis of the SQ, and in a semiclassical limit, which provides paths, the PSA, the PGI and the electroweak charges have been derived. On that basis, the isospin symmetry (THM 8), and the isospin doublets (THM 9) have been derived. Moreover, on that basis, the **electroweak Lagrangian** can be derived (Eqs. 8.30, 8.31, 8.36).

(18) The electroweak Lagrangian in (17), combined with the phase transitions in (2.1), provide **masses of the bosons of the electroweak fields or potentials W_μ^-, W_μ^+ and Z_μ**: $M_{W,theo}$ and $M_{Z,theo}$. These masses are in accordance with the observed masses $M_{W,obs}$ and $M_{Z,obs}$. Hereby, the difference between theory and experiment is below 0.6%, whereby no fit has been executed, see THM (10).

(19) Altogether, the SQ provides the **essential results of the SMEWI, of GR and beyond**:

(19.1) Moreover, the SQ provides explanations and values for the following structures or quantities of the SMEWI: the $2D$ charge space, the values of the electroweak charges, the value of the weak angle, as well as the values of the VEV, $M_{W,theo}$ and $M_{Z,theo}$. Thus the SQ provides essential results beyond the traditional SMEWI.

(19.2) Similarly, the SQ provides a derivation of general relativity, GR, including the EFE, see THM (11).

(19.3) Moreover, the SQ provides solutions to three essential cases of incompleteness of GR, see chapter (9), in particular Fig. (9.4), PROP (5) and THM (12).

(20) Inherent to the above results are the answers to the questions in chapter (4).

10.2 Local derivation of global space

In this section, we summarize how global space forms on the basis of the local principles of SQ in my theory of vacuum.

(1) The SQ implies QP and QG, see Carmesin (2022).

(2) QG implies the following: curvature parameters k_j of pairs j of objects can be analyzed, the average $[k_j]$ is equal to the curvature parameter k, $[k_j]$ is equal to zero, or $k = 0$. Thus, space is flat at this average, see (Carmesin, 2020e, S. 4.8).

(3) According to the SQ, the present-day vacuum at Earth is constituted by vacuum that formed since the Big Bang at locations ranging from Earth towards the light horizon.

(4) The present-day vacuum in (3) has been derived on the basis of the average flatness of space in (2). Thereby, the density of the vacuum in a homogeneous universe has been derived in a semiclassical manner with the following result, see (Carmesin, 2022, THM 11) or (Carmesin, 2021d, THM 21):

$$\rho_{\Lambda,h.c.} = \frac{1}{4\pi G t_H^2}, \quad \text{whereby } t_H \text{ is the Hubble time} \qquad (10.1)$$

Note that the density of vacuum amounts to more than 66 % of the energy and mass of the present-day universe.

(5) The heterogeneity in the universe causes that the density ρ_Λ of the present-day vacuum is a slight modification of the vacuum in (4), see (Carmesin, 2021d, S. 7.5).

(6) Based on the SQ, local modifications of the vacuum have been derived with the rate gravity scalar, RS, a DEQ, see for instance Carmesin (2021d).

(7) Based on the SQ, and on the smoothness assumption, local modifications of the vacuum have been derived by deriving the EFE, see chapter (9).

(8) Based on the formed vacuum in the SQ, curvature described by the EFE has been derived and explained, Carmesin (2021d).

Altogether, averaged curvature, the density ρ_Λ of present-day vacuum, as well as local modifications of the vacuum have been derived on the basis of the SQ in my theory of vacuum.

10.3 Derivation of the spectrum of vacuum

In this section, we summarize how the spectrum of the vacuum has been derived on the basis of the local principles of SQ in my theory of vacuum.

(1) The SQ implies QP, including the Schrödinger equation, SEQ, see Carmesin (2022).

(2) The SQ implies QG, see Carmesin (2022).

(3) The SQ implies black holes and the Schwarzschild radius R_S, see e.g. Carmesin (2019d), Carmesin (2022).

(4) QG implies the Friedmann-Lemaître equation, FLE, about the expansion of space. Thereby, the FLE has been derived for

dimensions of space $D \geq 3$, in a completely natural manner[3], see Friedmann (1922), Lemaitre (1927) and e.g. Carmesin (2017b), Carmesin (2020f), Carmesin (2020e), Carmesin (2021d).

(5) The FLE in (4) combined with the observed present - day time after the Big Bang, see for instance Planck-Collaboration (2020), implies the present-day light horizon, R_{lh}, see Carmesin (2019d), Carmesin (2020f), Carmesin (2021a).

(6) The black holes in (3) combined with the SEQ in (1) imply that the Planck length L_P is the smallest length that can be observed by a single observation, see Carmesin (2019d), Carmesin (2020f), Carmesin (2021d), Carmesin (2021a).

(7) The Planck length L_P in (6), combined with the present-day light horizon in (4), further combined with the FLE in (3), imply a sequence of dimensional phase transitions as well as the dimensional horizon D_{hori}, see for instance Carmesin (2017b), Carmesin (2019d), Carmesin (2020f), Carmesin (2021d), or e.g. Carmesin (2021a).

(8) The SEQ in (1) describes the rate gravity waves, RGWs, of vacuum, see Carmesin (2022).

(9) The dimensional horizon D_{hori} in (7), combined with the RGWs in (8), imply the energy spectrum of the RGWs for dimensions ranging from $D = 3$ towards D_{hori}, see Figs. (2.8, 9.4, 2.6) and e.g. Carmesin (2017b), Carmesin (2019d), Carmesin (2020f), Carmesin (2021d), Carmesin (2021a).

Altogether, the SQ implies the solution of the SEQ, corresponding the solution of the DEQ of the RGWs. The energy spectrum of that solution is the spectrum of the zero-point energies $ZPE_{\Lambda,D}$ illustrated in Fig. (2.8) and presented in Eq. (2.90). According to the SQ, in addition to that energy spectrum $ZPE_{\Lambda,D}$, there are excitation states of vacuum caused

[3]Remind that physics at $D > 3$ has been observed, see Lohse et al. (2018), Zilberberg et al. (2018).

by a change of the (tensor) symmetry or by harmonic oscillations, see e.g. Carmesin (2021d), Carmesin (2021a), Carmesin (2021f).

10.4 Explanation of units in SMEWI

The elementary electric charge $\tilde{e}$ has the correct value in table (11.5), according to observation, see Millikan (1911), and according to our derivation, see Carmesin (2021f). Moreover, the couplings g, g' and g_z have been derived and explained on the basis of the elementary electric charge $\tilde{e}$, see chapters (5, 6). Thus g, g' and g_z represent **elementary charges of the electroweak interaction**. In particular, g, g' and g_z are determined on the basis of $\tilde{e}$, without the factor $\sqrt{4\pi}$ used in the SMEWI, see e.g. Weinberg (1996) or section (3.5).

Based on the fundamental structure of the unification of coupling constant and charge in $\tilde{e} = \sqrt{\alpha}$, the interaction force F of two elementary electric charges at a distance r is equal to $F = \tilde{e} \cdot [\tilde{e}/r^2]$, whereby the rectangular bracket represents the field, see e.g. Carmesin (2021f). Accordingly, the interaction force F of two elementary charges of the electroweak interaction g at a distance r is equal to $F = g \cdot [g/r^2]$. Using the SMEWI units, that energy is increased by the factor 4π. Accordingly, that factor 4π represents the integration of all angles. That integration represents the fact that all field lines remain at a very small region of interaction, as a result of very effective screening:

$$4\pi \cdot F = \int dA \cdot F = \int dAg \cdot [g/r^2] \quad \text{or} \quad (10.2)$$

$$4\pi \cdot F = 4\pi r^2 \cdot g \cdot [g/r^2] = 4\pi \cdot g^2 = g^2_{SMEWI} \quad \text{with} \quad (10.3)$$

$$g_{SMEWI} = g \cdot \sqrt{4\pi} \quad (10.4)$$

Analogously, we can derive the other SMEWI - couplings:

$$g'_{SMEWI} = g' \cdot \sqrt{4\pi} \quad \text{and} \quad g_{z,SMEWI} = g_z \cdot \sqrt{4\pi} \qquad (10.5)$$

The integration $\int dA$ is not essential in the analysis of the two-dimensional charge space in chapters (5, 6). However, it is essential in the formation of mass in chapter (8). That process takes place at very short distance, corresponding to the very effective screening that restricts the weak interaction to very short distances. At larger distances, the two components $\kappa_{emitted,\perp,+} = g'$ and $\kappa_{emitted,\perp,-}$ (parallel to g_z) combine, in order to minimize energy, see Carmesin (2021f). Thus $\kappa_{emitted,\perp,+} = g'$ and $\kappa_{emitted,\perp,-}$ form the elementary electric charge $\tilde{e}$, discovered at large distance by Millikan (1911).

10.5 Outlook

The SMEWI as well as the SMEP represent theories that are very successful at energies of the present-day accelerators of ca. 13 TeV, see e.g. Zyla (2020). In contrast, the SQ with its implication of quantum gravity represents a deeply founded theory ranging from the Planck scale L_P towards the light horizon, corresponding to energies ranging from 10^{-31} eV towards 10^{16} TeV. In that huge interval of energies, a series of 299 phase transitions has been derived and explained, see Figs. (2.6, 9.4) or e.g. Carmesin (2020f). These phase transitions took place in the early universe, they explain the era of 'cosmic inflation', they explain the dark energy, and they establish a present-day excitation spectrum underlying the formation of elementary particles and fundamental interactions. Thereby, essential parameters and mechanism are provided in precise accordance with observation, whereby no fit is executed.

Thus, the derived elementary particles and fundamental interactions provide a fundamental link between the early universe and elementary particle physics, as asked for in (Zyla, 2020, S. 11.8). Moreover, the detailed and huge energy spectrum corresponding to the 299 phase transitions, as well as the additional spectra based on tensor symmetries and harmonic oscillations, form the base for new physics to be discovered.

Hereby, the combined advanced experts and technologies of observation in elementary particles physics as well as in the space sciences constitute a promising basis. With it, the possible discoveries can be achieved, that have been outlined by the dynamics of the vacuum with its variety of excitation states, full of new properties and new physics.

Chapter 11

Appendix

11.1 Universal constants

In this section we present universal constants. Hereby, ε_0 is not a fundamental constant, as it can be derived from fundamental constants.

quantity	observed value	reference
G	$6.674\,08(31) \cdot 10^{-11}\ \frac{\mathrm{m}^3}{\mathrm{kg}\cdot\mathrm{s}^2}$	Tanabashi et al. (2018)
c	$299\,792\,458\ \frac{\mathrm{m}}{\mathrm{s}}$, exact	Tanabashi et al. (2018)
h	$6.626\,070\,15\ \cdot 10^{-34}$ Js, exact	Newell et al. (2018)
k_B	$1.380\,649\ \cdot 10^{-23}\ \frac{\mathrm{J}}{\mathrm{K}}$, exact	Newell et al. (2018)
ε_0	$8.854\,187\,817\ \cdot 10^{-12}\ \frac{\mathrm{F}}{\mathrm{m}}$	Tanabashi et al. (2018)

Table 11.1: Universal constants ((Newell et al., 2018, table 3), (Tanabashi et al., 2018, table 1.1)).

Additionally, in this section, we present used abbreviations.

abbreviation	full text	reference
DEQ	differential equation	C. (1)
EEP	Einstein equivalence principle	S. (2.4)
EFE	Einstein field Eq.	Eq. (9.36)
FV	formation of vacuum	S. (2.4)
GEP	Galileo's equivalence principle	S. (2.4)
GG	Gaussian gravity	S. (2.4)
GR	general relativity	S. (2.4)
LFV	locally formed vacuum	S. (2.4)
PFF	principles of free fall	S. (2.4)
PFP	principles of free propagation	S. (2.4)
PGI	principle of gauge invariance	S. (3.2)
PLA	principle of least action	S. (3.1)
PSA	principle of stationary action	S. (9.2)
PT	phase transition	S. (8.3)
QFT	quantum field theory	C. (7)
QG	quantum gravity	C. (2)
QP	quantum physics	C. (1)
SEQ	Schrödinger equation	S. (2.4.3)
SMC	SM of cosmology	C. (1)
SMEP	SM of elementary particles	C. (1)
SMEWI	SM of electroweak interaction	C. (1)
SM	standard model	C. (1)
SQ	spacetime-quadruple	Eq. (2.4)
SR	special relativity	C. (1)

Table 11.2: Abbreviations. Further abbreviations are represented in the glossary.

11.2 Natural units

Planck (1899) introduced Planck units. We mark quantities in natural units by a tilde, see Tab. 11.3 or Carmesin (2019d).

physical entity	Symbol	Term	in SI-Units
Planck length	L_P	$\sqrt{\frac{\hbar G}{c^3}}$	$1.616 \cdot 10^{-35}\,\mathrm{m}$
Planck time	t_P	$\frac{L_P}{c}$	$5.391 \cdot 10^{-44}\,\mathrm{s}$
Planck energy	E_P	$\sqrt{\frac{\hbar \cdot c^5}{G}}$	$1.956 \cdot 10^{9}\,\mathrm{J}$
Planck mass	M_P	$\sqrt{\frac{\hbar \cdot c}{G}}$	$2.176 \cdot 10^{-8}\,\mathrm{kg}$
Planck volume	$V_{D,P}$	L_P^D	
Planck volume, ball	$\bar{V}_{D,P}$	$V_D \cdot L_P^D$	
Planck density	ρ_P	$\frac{c^5}{G^2\hbar}$	$5.155 \cdot 10^{96}\,\frac{\mathrm{kg}}{\mathrm{m}^3}$
Planck density, ball	$\bar{\rho}_P$	$\frac{3c^5}{4\pi G^2\hbar}$	$1.2307 \cdot 10^{96}\,\frac{\mathrm{kg}}{\mathrm{m}^3}$
Planck density, ball	$\bar{\rho}_{D,P}$	$\frac{M_P}{\bar{V}_{D,P}}$	
Planck temperature	T_P	$T_P = \frac{E_P}{k_B}$	
scaled volume	$\tilde{V}_D$	$\frac{\bar{V}_{D,P}}{\bar{V}_D}$	
scaled energy	$\tilde{E}$	E/E_P	$E = \tilde{E} \cdot E_P$
scaled density	$\tilde{\rho}_D$	$\frac{\tilde{M}}{\tilde{r}^D} = \frac{\tilde{E}}{\tilde{r}^D}$	$\rho_D = \tilde{\rho}_D \cdot \bar{\rho}_{D,P}$
scaled length	$\tilde{x}$	x/L_P	$x = \tilde{x} \cdot L_P$
Planck charge	q_P	$\sqrt{4\pi\varepsilon_0 \cdot \hbar \cdot c}$	$11{,}71\,e$
scaled charge	$\tilde{q}$	$\tilde{q} = \frac{q}{q_P}$	

Table 11.3: Planck - units.

11.3 Observed macroscopic values

quantity	observed value	reference
H_0 in $\frac{\mathrm{km}}{\mathrm{s\cdot Mpc}}$	67.36 ± 0.54 (0.8 %)	[CMB]
Ω_Λ	0.6847 ± 0.0073 (1.1 %)	[CMB]
Ω_K	0.0007 ± 0.0019	[CMB]
z_{eq}	$3402 \pm 26(0.76\%)$	[CMB]
Ω_M	$0.3153 \pm 0.0073(2.3\%)$	[CMB]
Ω_r	$9.265^{+0.288}_{-0.283} \cdot 10^{-5}$ (3.1 %)	[CMB]
σ_8	$0.8057 \pm 0.008(1\%)$	[CMB]
ρ_{cr,t_0} in $\frac{kg}{m^3}$	$8.660^{+0.137}_{-0.137} \cdot 10^{-27}$ (1.6 %)	[CMB]
$\tilde{\rho}_{cr,t_0}$	$7.037 \cdot 10^{-123}$	[CMB]
$\tilde{\rho}_{v,t_0}$	$4.8181 \cdot 10^{-123}$	[CMB]
Ω_b	0.0493 ± 0.00032	[CMB]
Ω_c	0.2645 ± 0.0048	[CMB]
R_{lh}	$4.1412 \cdot 10^{26}$ m	[C2019]
T_{CMB}	$2.7255(6)(0.02\%)$ K	[T2018]
Ω_{CMB}	5.4501	[C2021]
Ω_ν	$3.8742 \cdot 10^{-5}(9.7\%)$	[C2021]
1 Mpc	$3.085\,677\,581\,49 \cdot 10^{22}$ m	[Z2020]

Table 11.4: Observations: [CMB] marks data based on the CMB ((Planck-Collaboration, 2020, table 2)), in particular based on the modes TT, TE, EE, the low energy and lensing. Quantities with a tilde are presented in natural units alias Planck units (see subsection 11.2). [Z2020], see (Zyla, 2020, table 2.1). [T2018], see Tanabashi et al. (2018). [C2019] is based on an evaluation in Carmesin (2019d). [C2021] is based on an evaluation in Carmesin (2021a).

11.4 Observed microscopic values

quantity	observed value	reference
m_H/c^2 in GeV	$124.51 - 126.02$	[Z2020, F. 11.4]
VEV, v in GeV	246.1965	[Z2020]
M_W in GeV/c^2	80.379 ± 0.0123	[T2018, p. 33]
M_W/M_Z	0.88153 ± 0.00017	[T2018, p. 33]
$\sin^2\theta_W$	$0.231\,22(4)$	[T2018, p. 127]
$\sin^2\theta_W(E)$		S. (3.5, 5.1.5)
$\tilde{e}$	$0.085\,424\,548$	[T2018]
$\alpha = \tilde{e}^2$	$7.297\,352\,5664(17) \cdot 10^{-3}$	[T2018]
$\tilde{e}_{SMEWI}$	$\sqrt{4\pi} \cdot \tilde{e}$	[W1996]
$\tilde{e}_{SMEWI,eff}$	$\sqrt{137/129} \cdot \tilde{e}_{SMEWI}$	[W1996]
coupling g'	$g' = \frac{\tilde{e}_{SMEWI,eff}(E)}{\cos\theta_W(E)}$	C. (6)
coupling g	$g = \frac{\tilde{e}_{SMEWI,eff}(E)}{\sin\theta_W(E)}$	C. (6)
y	hypercharge-number	[Z2020]
$g' \cdot y$	hypercharge	[Z2020]
$g \cdot \vec{\hat{\sigma}}/2$	isospin	[W1996]
$\hat{Y}_L, \hat{Y}_R$	Eqs. (8.3, 8.4, 8.5)	[W1996]

Table 11.5: Observations: [Z2020] is based on Zyla (2020). [T2018] is based on Tanabashi et al. (2018). [W1996] is based on Weinberg (1996).

11.5 Glossary

Words marked bold face can usually be found in the glossary.

Abbreviation: S. (section), C. (chapter), DEF. (definition), PROP. (proposition), THM. (theorem).

Big Bang: Start of time evolution of visible space

causal horizon: light horizon

two-dimensional charge space: see table (11.5) and Figs. (5.1, 6.1, 6.2)

CMB, Cosmic Microwave Background: Radiation emitted at $z \approx 1090$. (Tab. 11.4)

classical electrodynamics: see e.g. Landau and Lifschitz (1971)

complete time evolution of spacetime: Evolution of the light horizon $R_{lh}(t)$ ranging from the Planck - length L_P to the actual light horizon $R_{lh}(t_0)$

cosmic unfolding: It causes the **very rapid distance enlargement in the early universe**

cosmological constant: Λ corresponds to the dark energy with its density ρ_Λ (Tab. 11.4).

coupling constant α of electrodynamics: see table (11.5).

couplings g and g' of electroweak interaction: These couplings correspond to the charges of electroweak interaction, see table (11.5).

curvature parameter: the curvature parameter k describes the global curvature of space, see e.g. Carmesin (2021d)

dark energy: Energy of the cosmological density of the vacuum ρ_Λ (Tab. 11.4).

density, critical: ρ_{cr,t_0} or ρ_{cr} (Tab. 11.4 or for instance Carmesin (2021d))

density, critical, at a dimensional transition: $\tilde{\rho}_{D,c}$

density parameter: $\Omega_j = \rho_j/\rho_{cr,t_0}$ (Tab. 11.4)

density, vacuum: $\rho_\Lambda = \Omega_\Lambda \cdot \rho_{cr,t_0}$ (Tab. 11.4)

dimensional distance enlargement factor: A factor $Z_{D+s\to D}$ occurs at a dimensional phase transition from a dimension $D+s$ to a dimension D and describes the corresponding increase of distances, see e.g. Carmesin (2021d))

dimensional horizon D_{max} or $D_{horizon}$ or D_{hori}: It is the maximal dimension that the space within the actual light horizon can have achieved in the past. Thereby the following transformations of space are essential: the isotropic scale and the enlargement of distance caused by a dimensional phase transition, see e.g. Carmesin (2021d))

dimensional phase transition: Change of spatial dimension D, see e.g. Carmesin (2021d))

dimensional unfolding: Series of dimensional phase transitions in the early universe, see Figs. (2.6, 9.4) or e.g. Carmesin (2021d))

dynamical mass: $M = \frac{E}{c^2}$

elementary charge $\tilde{e}$:, see table (11.5) or Landau and Lifschitz (1971), Feynman (1985)

expansion of space: The expansion of the universe since the Big Bang is caused by an increase of the amount of vacuum, see for instance Carmesin (2021d).

very rapid distance enlargement in the early universe: Guth (1981) conjectured that factor, the factor has been explained by dimensional phase transitions in this book and by Carmesin (2017b), Carmesin (2019d)

forced oscillation: Forced oscillations are essential for the charge formation mechanism, see Carmesin (2021f), Landau and Lifschitz (1976).

frame: Each observation apparatus is localized in spacetime. That localization establishes a frame.

gamma matrices:

$$\gamma^0 = \begin{pmatrix} \mathbb{I} & 0 \\ 0 & -\mathbb{I} \end{pmatrix} \text{ and } \gamma^1 = \begin{pmatrix} 0 & \sigma_1 \\ -\sigma_1 & 0 \end{pmatrix} \tag{11.1}$$

$$\gamma^2 = \begin{pmatrix} 0 & \sigma_2 \\ -\sigma_2 & 0 \end{pmatrix} \text{ and } \gamma^3 = \begin{pmatrix} 0 & \sigma_3 \\ -\sigma_3 & 0 \end{pmatrix} \tag{11.2}$$

$$\gamma^5 = \begin{pmatrix} \mathbb{I} & 0 \\ 0 & \mathbb{I} \end{pmatrix} \text{ and } \mathbb{I} = \begin{pmatrix} 1 & 0 \\ 0 & 1 \end{pmatrix} \tag{11.3}$$

gravitational field: G^*, see e.g. Carmesin (2021d))

Higgs boson: see C. (8)

Higgs mechanism: see C. (8)

horizon: Global limit of visibility, see e.g. Carmesin (2021d))

Hubble - parameter: $H = \frac{\dot{a}}{a}$, see e.g. Carmesin (2021d))

Hubble - constant: $H_0 = H(t_0)$ Hubble parameter at t_0, for details see Carmesin (2021d), Carmesin (2021c)

hypercharge: see table (11.5) and Figs. (5.1, 6.1, 6.2)

incomplete: A theory that does not describe the physically known objects or properties is incomplete

isospin: see table (11.5) and Figs. (5.1, 6.1, 6.2)

light horizon, actual: $R_{lh} = 4.142 \cdot 10^{26}$ m (Tab. 11.4)

natural units: Planck - units (Tab. 11.3)

Planck scale: At that scale there occurs the **length limit** and the **density limit** in nature. Accordingly, natural units or Planck units have been introduced (Tab. 11.3).

quantum electrodynamics, QED: see e.g. Feynman (1985), Landau and Lifschitz (1982)

very rapid enlargement of distances: see for instance Carmesin (2021d))

RGW, rate gravity wave: Carmesin (2021d)

rate of the formation of vacuum: see for instance Carmesin (2022)

scaled emitted transverse field: C. (1)

Schwarzschild radius R_S: At this radius the escape velocity is equal to c

SMEP, Standard Model of Elementary Particles: (C. 1)

spacetime: Combination of space and time, see e.g. Carmesin (2021d)

time evolution of the vacuum: C. (1)

transverse emitted field: C. (1)

unfolding, dimensional: Space unfolds when the dimension decreases, see Figs. (2.6, 9.4)

vacuum: The vacuum has a volume, a density and the velocity c. (C. 1 or Carmesin (2021d))

vacuum expectation value, VEV: see table (11.5) and C. (8)

weak angle Θ_W: The weak angle characterizes the structure of the charges of the electroweak interaction in the two-dimensional charge space, see Figs. (6.1, 6.2). The value has been derived from the SQ, see Fig. (5.2).

Acknowledgement

I thank Matthias Carmesin and Johannes Carmesin for helpful discussions. I thank Paul Sawitzki, Philipp Schöneberg, Jörn Kankelfitz, Dennis Feldmann and Jonas Lieber for interesting discussions. I am especially grateful to I. Carmesin for many helpful discussions and for proofreading the manuscript.

Bibliography

Aharonov, Y. and Bohm, D. (1959). Significance of electromagnetic potentials in the quantum theory. *Physical Review*, 115:485–490.

Archimedes (1897). *The Sand-Reckoner, In: The Works of Archimedes (230 BC), translated by T. L. Heath in 1897*. Cambridge University Press, Cambridge.

ATLAS, C. (2021). Search for Higgs boson pair production in the two bottom quarks plus two photons final state in pp collisions at $\sqrt{s} = 13$ TeV with the ATLAS detector. *arXiv*, 2112.11876v1[hep-ex]:1–53.

Ballentine, L. E. (1998). *Quantum Mechanics*. World Scientific Publishing, London and Singapore.

Bialynicki-Birula, I. and Bialynicki-Birula, Z. (1975). *Quantum Electrodynamics*. Pergamon Press, Oxford, 1 edition.

Blokhintsev, D. I. and Galperin, F. M. (1934). Neutrino hypothesis and conservation of energy. *Pod Znamenem Marxisma*, 6:147–157.

Born, M. and Wolf, E. (1980). *Principles of Optics*, volume 1. Pergamon Press, Oxford New York, 6 edition.

Bos, H. J. M. (1974). Differentials, higher-order differentials and the derivative in the Leibnizian calculus. *Archive for History of Exact Sciences*, 14:1–90.

Brahe, T. (1588). *De mundi aetherei recentioribus phaenomenis.* Brahe, Uraniborg.

Brahe, T. and Kepler, J. (1627). *Tabulae Rudolphinae.* Auftraggeber Rudolph und Ferdinand, Ulm.

Carmeli, M. (1982). *Classical Fields: General Relativity and Gauge Theory.* John Wiley and Sons, New York - Chichester - Brisbane - Toronto - Singapore.

Carmesin, H.-O. (1996). *Grundideen der Relativitätstheorie.* Verlag Dr. Köster, Berlin.

Carmesin, H.-O. (2006). Entdeckungen im Physikunterricht durch Beobachtungen des Himmels. In Nordmeier, V. and Oberländer, A., editors, *Tagungs-CD Fachdidaktik Physik, ISBN 978-386541-190-7*, Berlin. Deutsche Physikalische Gesellschaft, Deutsche Physikalische Gesellschaft.

Carmesin, H.-O. (2012). Schüler entdecken die Einstein-Geometrie mit dem Beschleunigungssensor. *PhyDid B Internetzeitschrift*, ISSN 2191-379X.

Carmesin, H.-O. (2016). Mit dem Zwillingsparadoxon zur speziellen und allgemeinen Relativitätstheorie. *PhyDid B Internetzeitschrift.*

Carmesin, H.-O. (2017a). Quantum Gravity: Discoveries about the Early Universe Including Big Bang, Big Bounce and a Critical Discussion of these. German Astronomical Society Conference at University Göttingen.

Carmesin, H.-O. (2017b). *Vom Big Bang bis heute mit Gravitation: Model for the Dynamics of Space.* Verlag Dr. Köster, Berlin.

Carmesin, H.-O. (2018a). A Model for the Dynamics of Space - Expedition to the Early Universe. *PhyDid B, FU Berlin, hal-02077596*, pages 1–9.

Carmesin, H.-O. (2018b). *Entstehung der Raumzeit durch Quantengravitation - Theory for the Emergence of Space, Dark Matter, Dark Energy and Space-Time.* Verlag Dr. Köster, Berlin.

Carmesin, H.-O. (2018c). *Entstehung dunkler Energie durch Quantengravitation - Universal Model for the Dynamics of Space, Dark Matter and Dark Energy.* Verlag Dr. Köster, Berlin.

Carmesin, H.-O. (2018d). *Entstehung dunkler Materie durch Gravitation - Model for the Dynamics of Space and the Emergence of Dark Matter.* Verlag Dr. Köster, Berlin.

Carmesin, H.-O. (2019a). A Novel Equivalence Principle for Quantum Gravity. *PhyDid B Internet Journal*, pages 1–9.

Carmesin, H.-O. (2019b). A Novel Equivalence Principle for Quantum Gravity. *PhyDid B - Didaktik der Physik - Beiträge zur DPG - Frühjahrstagung - Aachen - Germany - hal-02511998*, pages 1–9.

Carmesin, H.-O. (2019c). A Novel Equivalence Principle for Quantum Gravity. *Verhandl. DPG (VI)*, 54(3):42.

Carmesin, H.-O. (2019d). Die Grundschwingungen des Universums - The Cosmic Unification - With 8 Fundamental Solutions based on G, c and h. In Carmesin, H.-O., editor, *Universe: Unified from Microcosm to Macrocosm - Volume 1.* Verlag Dr. Köster, Berlin.

Carmesin, H.-O. (2019e). Equivalence Principle of Quantum Gravity. *Verhandl. DPG (VI)*, 54(2):74.

Carmesin, H.-O. (2019f). Kontroverse Konstante. *Physik Journal*, 18(7):14.

Carmesin, H.-O. (2020a). Density Parameter Ω_Λ of the Dark Energy is a function of g, c and h, and it Evolves with Time. *Verhandl. DPG*, DPG Tagung Bonn GR18.1.

Carmesin, H.-O. (2020b). Explanation of the Rapid Enlargement of Distances in the Early Universe. *PhyDid B*, pages 9–17.

Carmesin, H.-O. (2020c). Explanation of the Rapid Enlargement of Distances in the Early Universe. *Verhandl. DPG*, DPG Tagung Bonn DD4 Astronomie Location P-HS 5.

Carmesin, H.-O. (2020d). Explanation of the Rapid Enlargement of Distances in the Early Universe and Comparison with Inflaton Models. *Verhandl. DPG*, DPG Tagung Bonn GR6.12.

Carmesin, H.-O. (2020e). The Universe Developing from Zero-Point Energy: Discovered by Making Photos, Experiments and Calculations. In Carmesin, H.-O., editor, *Universe: Unified from Microcosm to Macrocosm - Volume 3*. Verlag Dr. Köster, Berlin.

Carmesin, H.-O. (2020f). Wir entdecken die Geschichte des Universums mit eigenen Fotos und Experimenten. In Carmesin, H.-O., editor, *Universe: Unified from Microcosm to Macrocosm - Volume 2*. Verlag Dr. Köster, Berlin.

Carmesin, H.-O. (2021a). Cosmological and Elementary Particles Explained by Quantum Gravity. In Carmesin, H.-O., editor, *Universe: Unified from Microcosm to Macrocosm - Volume 5*. Verlag Dr. Köster, Berlin.

Carmesin, H.-O. (2021b). Lernende erkunden die Raumzeit. *Der Mathematik Unterricht*, 2.:47–56.

Carmesin, H.-O. (2021c). Physical Explanation of the H_0-Tension. *International Journal of Engineering and Science Invention*, 10(8,II):34–38.

Carmesin, H.-O. (2021d). Quanta of Spacetime Explain Observations, Dark Energy, Graviton and Nonlocality. In Carmesin, H.-O., editor, *Universe: Unified from Microcosm to Macrocosm - Volume 4*. Verlag Dr. Köster, Berlin.

Carmesin, H.-O. (2021e). Solution of the H_0 Tension. *Verhandl. DPG*, DPG Tagung SMuK GR13.1.

Carmesin, H.-O. (2021f). The Elementary Charge Explained by Quantum Gravity. In Carmesin, H.-O., editor, *Universe: Unified from Microcosm to Macrocosm - Volume 6*. Verlag Dr. Köster, Berlin.

Carmesin, H.-O. (2021g). The Origin of the Energy. *PhyDid B, FU Berlin*, pages 29–34.

Carmesin, H.-O. (2022). Quantum Physics Explained by Gravity and Relativity. In Carmesin, H.-O., editor, *Universe: Unified from Microcosm to Macrocosm - Volume 7*. Verlag Dr. Köster, Berlin.

Carmesin, H.-O. and Brüning, P. (2018). A Monte Carlo Simulation of Cosmic Inflation. *Verhandl. DPG*, page DD27(3).

Carmesin, H.-O. and Carmesin, M. (2018a). Explanation of Cosmic Inflation by Gravitation. *Verhandl. DPG*, page GR16(7).

Carmesin, H.-O. and Carmesin, M. (2018b). Explanation of Cosmic Inflation by Quantum Gravity. *Verhandl. DPG*, page EP14(5).

Carmesin, H.-O., Emse, A., Conrad, U., and Pröhl, I. K. (2021). *Universum Physik Sekundarstufe II Nordrhein-Westfalen Einführungsphase*. Cornelsen Verlag, Berlin.

Carmesin, H.-O., Emse, A., Piehler, M., Pröhl, I. K., Salzmann, W., and Witte, L. (2020). *Universum Physik Sekundarstufe II Niedersachsen Qualifikationsphase*. Cornelsen Verlag, Berlin.

Carmesin, H.-O., Emse, A., Piehler, M., Pröhl, I. K., Salzmann, W., and Witte, L. (2022). *Universum Physik Sekundarstufe II Gesamtband Qualifikationsphase*. Cornelsen Verlag, Berlin.

Carmesin, H.-O. and Schöneberg, P. (2022). Droplet Model Used to Analyze the Early Universe. *International Journal of Engineering and Science Invention*, 11(II)1:58–66.

Carmesin, M. and Carmesin, H.-O. (2020). Quantenmechanische Analyse von Massen in ihrem eigenen Gravitationspotenzial. *PhyDid B, FU Berlin*, pages 19–27.

Cavendish, H. (1798). Experiments to determine the density of the earth. *Phil. Trans. R. Soc. Lond.*, 88:469–516.

Chambre, M. C. d. l. (1662). *Lumiere*. Jacques Dallin, Paris.

Christenson, J. H., Cronin, J. W., Fitch, V. L., and Turlay, R. (1964). Evidence for the 2π Decay of the K_2^0 Meson. *Phys. Rev. Lett.*, 13.

Corry, L., Renn, J., and Stachel, J. (1997). Belated decision in the hilbert-einstein priority dispute. *Science*, 278:1270–1273.

Cottingham, W. and Greenwood, D. (2007). *An Introduction to the Standard Model of Particle Physics*. Cambridge University Press, Cambridge, 2 edition.

Coulomb, C.-A. (1785). Construction et usage d'une balance electrique etc. *Histoire de l'Academie des sciences avec les memoires de mathematique et de physique*, 1788:569–577.

Dalton, J. (1808). *A New System of Chemical Philosophy Part I*. Bickerstaff, London.

de Sitter, W. (1913). Ein astronomischer Beweis für die Konstanz der Lichgeschwindigkeit. *Pysik. Zeitschr.*, 14:429.

Einstein, A. (1905). Zur Elektrodynamik bewegter Körper. *Annalen der Physik*, 17:891–921.

Einstein, A. (1911). Über den Einfluss der Schwerkraft auf die Ausbreitung des Lichts. *Annalen der Physik*, 35:898–908.

Einstein, A. (1915a). Die Feldgleichungen der Gravitation. *Sitzungsberichte der Königlich Preußischen Akademie der Wissenschaften*, pages 844–847.

Einstein, A. (1915b). Erklärung der Perihelbewegung des Merkur aus der allgemeinen Relativitätstheorie. *Sitzungsberichte der Königlich Preußischen Akademie der Wissenschaften*, pages 831–839.

Einstein, A. (1917). Kosmologische Betrachtungen zur allgemeinen Relativitätstheorie. *Sitzungsberichte der Königlich Preußischen Akademie der Wissenschaften*, pages 142–152.

Einstein, A., Podolski, B., and Rosen, N. (1935). Can the quantum-mechanical description of physical reality be considered complete? *Phys. Rev.*, 47:777–780.

Englert, F. and Brout, R. (1964). Broken Symmetry and the mass of gauge vector mesons. *Phys. Rev. Lett.*, 13(9):321–323.

Erb, R. (1992). Geometrische Optik mit dem Fermat-Princip. *Physik in der Schule*, 30:291–295.

Erler, J. and Schott, M. (2019). Electroweak Precision Tests of the Standard Model after the Discovery of the Higgs Boson. *Arxiv*, page 1902.05142v2.

Euklid (BC325). *Elements.* Cambridge University Press, Cambridge.

Faraday, M. (1852). On the physical character of the lines of magnetic force. *The London, Edinburgh and Dublin Philo-*

sophical Magazine and Journal of Science, Taylor and Francis, 4(3):401–428.

Fermat, P. (1657). *OEuvres, translated by Tannery*. Gauthier-Villars, Paris.

Fermi, E. (1933). Versuch einer Theorie der beta-Strahlen. *Zeitschrift f. Physik A*, 88:161–177.

Fewster, C. and Rejzner, K. (2019). Algebraic Quantum Field Theory - an introduction. *arXiv*, 1904p04051v2:1–47.

Feynman, R. P. (1967). *The Character of Physical Law*. MIT Press, Boston.

Feynman, R. P. (1985). *QED - The Strange Theory of Light and Matter*. Princeton University Press, Princton.

Fock, W. (1926). Über die invariante Form der Wellen- und Bewegungsgleichungen für einen geladenen Massenpunkt. *Z. f. Physik*, 39:226–232.

Friedmann, A. (1922). Über die Krümmung des Raumes. *Z. f. Physik*, 10:377–386.

Galileo, G. (1638). *Dialogues concerning two new sciences (translated)*. Elfevirii, Leida.

Gauss, C. F. (1809). *Theoria motus corporum coelestium in sectionibus conicis solem ambientium*. Perthes und Besser, Hamburg.

Gauss, C. F. (1827). *Disquisitiones Generales circa Superficies Curvas*. Typis Dieterichianis, Göttingen.

Gauss, C. F. (1833). *Intensitas vis Magneticae Terrestris ad Mensarum Absolutam Revocata*. Sumtibus Dieterichianis, Göttingen.

Gell-Mann, M. (1964). A Schematic Model of Baryons and Mesons. *Phys. Lett.*, 8:214–215.

Giesel, K., Hofmann, S., Thiemann, T., and Winkler, O. (2009). Manifestly Gauge-Invariant General Relativistic Perturbation Theory: I. Foundations. *arXiv*, 0711.0115v2:1–80.

Glashow, Sheldon, L. (1959). The renormalizability of vector meson interactions. *Nuclear Physics*, 10:107–117.

Goldhaber, M., Grodzins, L., and Sunyar, A. W. (1957). Helicity of Neutrinos. *Phys. Rev.*, 109:1015–1017.

Griffiths, D. (2008). *Introduction to Elementary Particles*. Wiley-VCH, Weinheim, 2 edition.

Guericke, O. v. (1672). *EXPERIMENTA Nova (ut vocantur) Magdeburgica DE VACUO SPATIO*. Amsterdam.

Guralnik, G. S., Hagen, C. R., and Kibble, T. W. B. (1964). Global conservation laws and massless particles. *Phys. Rev. Lett.*, 13(20):585–587.

Guth, A. H. (1981). Inflationary universe: A possible solution to the horizon and flatness problems. *Physical Review D*, 23:347–356.

Heeren, L., Sawitzki, P., and Carmesin, H.-O. (2020). Comprehensive Derivation of a Density Limit of the Evolution of Space. *PhyDid B, FU Berlin*, pages 39–42.

Herren, L., Carmesin, H.-O., and Sawitzki, P. (2020). Density Limit in the Evolution of Space According to General Relativity. *Verhandl. DPG*, DPG Tagung Bonn GR6.15.

Higgs, P. W. (1964). Broken Symmetries, Massless Particles and Gauge Fields. *Phys. Lett.*, pages 132–133.

Hilbert, D. (1915). Die Grundlagen der Physik. *Nachrichten von der Königlichen Gesellschaft der Wissenschaften zu Göttingen, Math-Physik. Klasse, November.*, pages 395–407.

Hobson, M. P., Efstathiou, G. P., and Lasenby, A. N. (2006). *General Relativity*. Cambridge University Press, Cambridge.

Hubble, E. (1929). A relation between distance and radial velocity among extra-galactic nebulae. *Proc. of National Acad. of Sciences*, 15:168–173.

Huygens, C. (1673). De vi centrifuga. *Ouvres completes*, XVI:255–301.

Huygens, C. (1690). *Traite de la lumiere*. Chez Pierre van der Aa, Leide.

Jackson, J. D. (1975). *Classicla Electrodynamics*. John Wiley, New York.

Jegerlehner, F. (2001). The effective fine structure constant at TESLA energies. *arXiv*, 0105283v1:1–21.

Jegerlehner, F. (2011). Electroweak effective couplings for future precision experiments. *IL NUOVE CIMENTO*, 34C(5)Suppl. 1:31–40.

Jegerlehner, F. (2019). The effective fine structure constant and other SM running couplings. Humboldt University Berlin.

Jormakka, J. (2020). Quantization of gravitation. *ResearchGate*, pages 1–12.

Kepler, J. (1619). Harmonice Mundi - Linz - Libri Verlag. In Caspar, M., editor, *Gesammelte Werke - 1940*, volume 6, pages 1–563. Clarendon Press, Oxford.

Kepler, J. (1627). *Tabulae Rudolphinae*. Jonae Saurii, Ulm.

Kobel, M., Bilow, U., Lindenau, P., and Schorn, B. (2017). *Teilchenphysik*. Joachim Herz Stiftung, Hamburg.

Kumar, A. (2018). *Fundamentals of Quantum Mechanics*. Cambridge University Press, Cambridge.

Landau, L. (1937). On the Theory of Phase Transitions. *Zh. Eksp. Toer. Fiz.*, 7:19–32.

Landau, L. and Lifschitz, J. (1960). *Course of Theoretical Physics - Mechanics*. Pergamon Press, Oxford.

Landau, L. and Lifschitz, J. (1965). *Course of Theoretical Physics III - Quantum Mechanics*. Pergamon Press, Oxford, 2. revised edition.

Landau, L. and Lifschitz, J. (1971). *Course of Theoretical Physics II - The Classical Theory of Fields*. Pergamon Press, Oxford, 3. edition.

Landau, L. and Lifschitz, J. (1975). *Course of Theoretical Physics VII - Theory of Elasticity*. Pergamon Press, Oxford, 2. edition.

Landau, L. and Lifschitz, J. (1976). *Course of Theoretical Physics I - Mechanics*. Pergamon Press, Oxford, 3. edition.

Landau, L. and Lifschitz, J. (1982). *Course of Theoretical Physics IV - Quantum Electrodynamics*. Pergamon Press, Oxford, 2. edition.

Lasenby, A., Doran, C., and Gull, S. (1998). Gravity, gauge theories and geometric algebra. *Phil. Trans. of the Royal Soc. A*, 356:487–582.

Lee, J. M. (1997). *Riemannian Manifolds: An Introduction to Curvature*. Springer Verlag, New York.

Lee, T. D. and Yang, C. N. (1956). Question of Parity Conservation in Weak Interaction. *Phys. Rev.*, 104.

Leibniz, G. W. (1684). Nova methodus pro maximis et minimis. *Acta Eruditorum*, pages 467–473.

Lemaitre, G. (1927). Un univers homogene de masse constante et de rayon croissant rendant compte de la vitesse radiale des nebuleuses extra-galactiques. *Annales de la Societe Scientifique de Bruxelles*, A47:49–59.

Lieber, J. and Carmesin, H.-O. (2021). Dynamics in the Early Universe. *PhyDid B, FU Berlin*, pages 49–52.

Lohse, M. et al. (2018). Exploring 4D Quantum Hall Physics with a 2D Topological Charge Pump. *Nature*, 553:55–58.

Maxwell, J. C. (1865). A dynamical theory of the electromagnetic field. *Philosophical Transactions of the Royal Society of London*, 155:459–512.

Millikan, R. A. (1911). The Isolation of an Ion, a Precision Measurement of its Charge, and the Correction of Stokes's Law. *Physica Review*, 32:349–397.

Moore, T. A. (2013). *A General Relativity Workbook*. University Science Books, Mill Valley, CA.

Newell, D. B. et al. (2018). The CODATA 2017 values of h, e, k, and N_A for the revision of the SI. *Metrologia*, 55:L13–L16.

Newton, I. (1686). *Newton's Principia - first American Edition - English 1729*. Daniel Adee, New York.

Oersted, H. C. (1820). Experimente circa effectum conflictus electrici in acum magneticam. *Publisher Oerstedt at University of Copenhagen*, pages 1–5.

Oldershaw, Robert, L. (1998). Democritus - scientific wizard of the 5th century bc. *Speculations in Science and Technology*, 21:37–44.

Pearle, P. (2017). Feynman's lecture utilizing the Aharonov-Bohm effect. *Quantum Studies: Mathematics and Foundations*, ISSN21965609:1–11.

Perlmutter, S. et al. (1998). Discovery of a supernova explosion at half the age of the universe. *Nature*, 391:51–54.

Peskin, Michael, E. (2015). On the Trail of the Higgs Boson. *Annalen der Physik*, 528:20–34.

Pich, A. (2007). The Standard Model of Electroweak Interactions. In Fleischer, R., editor, *European School of High-Energy Physics*, volume Report CERN-2007-005. CERN.

Planck, M. (1899). Über irreversible Strahlungsvorgänge. *Verlag der Königlich Preußischen Akademie der Wissenschaften*, pages 440–480.

Planck, M. (1900). On the theory of the energy distribution law of the normal spectrum. *Verhandl. Dtsch. Phys. G.*, 2:237.

Planck-Collaboration (2020). Planck 2018 results. VI. Cosmological parameters. *Astronomy and Astrophysics*, pages 1–73.

Ratzinger, W. and Schwaller, P. (2021). Whispers from the dark side: Confronting light new physics with NANOGrav data. *SciPost Phys.*, 10:1–11.

Riess, A. G. et al. (2000). Tests of the Accelerating Universe with Near-Infrared Observations of a High-Redshift Type Ia Supernova. *The Astrophysical Journal*, 536:62–67.

Riess, A. G. et al. (2021). Cosmic Distances Calibrated at 1 % Precision with Gaia EDR3 Parallaxes and Hubble Space

Telescope Photometry of 75 Milky Way Cepheids Confirm Tension with ΛCDM. *The Astrophys. J. Lett.*, 908:L6:1 – 11.

Rojo, A. and Bloch, A. (2018). *The Principle of Least Action*. Cambridge University Press, Cambridge.

Rutherford, E. (1911). The scattering of alpha and beta particles by matter and the structure of atoms. *Philosophical Magazine*, 6/21:669–688.

Sakurai, J. J. and Napolitano, J. (1994). *Modern Quantum Mechanics*. Addison-Wesley, New York - London - Delhi.

Salam, A. and Ward, J. C. (1959). Weak and electromagnetic interactions. *Il Nuovo Cimento*, 11:568–577.

Santos, d. W. C. (2019). Introduction of Gauge Theory of Gravitation. *arXiv*, 1905.08113v1:1–23.

Sawitzki, P. and Carmesin, H.-O. (2021). Dimensional transitions in a Bose gas. *PhyDid B, FU Berlin*, pages 53–59.

Schlichting, H.-J. (1999). Zum Fall des freien Falls. In Sumfleth, E., editor, *Chemiedidaktik im Wandel - Gedanken zu einem neuen Chemieunterricht*. Literatur - Verlag, Münster.

Schöneberg, P. and Carmesin, H.-O. (2020a). Density Problem in the Early Universe and Solution with Quantum Gravity. *Verhandl. DPG*, DPG Tagung Bonn GR6.14.

Schöneberg, P. and Carmesin, H.-O. (2020b). Solution of a Density Problem in the Early Universe. *PhyDid B, FU Berlin*, pages 43–46.

Schöneberg, P. and Carmesin, H.-O. (2021a). Solution of the horizon problem. *PhyDid B, FU Berlin*, pages 61–64.

Schöneberg, P. and Carmesin, H.-O. (2021b). Solution of the horizon problem. *Verhandl. DPG*, DPG Tagung SMuK GR13.2.

Schwartz, M. D. (2014). *Quantum Field Theory and the Standard Model.* Cambridge University Press, Cambridge.

Smoot, G. F. (2007). Nobel Lecture: Cosmic microwave background radiation anisotropies: Their discovery and utilization. *Review of Modern Physics*, 79:1347–1379.

Sommerfeld, A. (1978). *Mechanik der deformierbaren Medien.* Verlag Harri Deutsch, Frankfurt, 6. edition.

Spergel, D. N. et al. (2007). Three-Year Wilkinson Microwave Anisotropy Probe (WMAP) Observations: Implications for Cosmology. *Astrophys. Journal*, 170:377–408.

Sprenger, L. and Carmesin, H.-O. (2018). A Computer Simulation of Cosmic Inflation. *PhyDid B*, pages 61–64.

Stephani, H. (1980). *Allgemeine Relativitätstheorie.* VEB Deutscher Verlag der Wissenschaften, Berlin, 2. edition.

Straumann, N. (2013). *General Relativity* . Springer, Dordrecht - Heidelberg - New York - London, 2. edition.

Swanson, N. (2017). A philosopher's guide to the foundations of quantum field theory. *Philosophy Compass*, 12:1–15.

Tanabashi, M., Particle-Data-Group, et al. (2018). Review of particle physics. *Phys. Rev. D*, 98:1–1898.

Teschl, G. (2014). *Mathematical Methods in Quantum Mechanics.* American Mathematical Society, Providence, 2. edition.

Tsoucalas, G., Laios, K., Karamanou, M., and Androutsos, G. (2013). The atomic theory of Leucippus and its impact on medicine before Hippocrates. *Hellenic Journal of Nuclear Medicine*, 16:68–69.

Weinberg, S. (1967). A Model of Leptons. *Phys. Rev. Lett.*, 19:1264–1266.

Weinberg, S. (1972). *Gravitation and Cosmology: Principles and Applications of the General Theory of Relativity*, volume 2. Cambridge University Press, Cambridge.

Weinberg, S. (1996). *The Quantum Theory of Fields.* John Wiley and Sons, New York - London - Sydney - Toronto.

Weyl, H. (1919). Eine neue Erweiterung der Relativitätstheorie. *Annalen der Physik*, 59:101–133.

Weyl, H. (1929). Elektron und Gravitation. *Z. f. Physik*, 56:330–352.

Wigner, E. (1931). *Gruppentheorie und ihre Anwendung auf die Quantenmechanik der Atomspektren.* Friedrich Vieweg und Sohn Verlag, Braunschweig.

Wigner, E. (1959). *Group Theory and its Applications to Quantum Mechanics of Atomic Spectra.* Academic Press, New York.

Will, C. M. (2014). The Confrontation between General Relativity and Experiment. *arXiv*, 1403.7377v1:1–113.

Wirtz, C. (1922). Radialbewegung der Gasnebel. *Astronomische Nachrichten*, 215:281–286.

Wu, C. S. et al. (1957). Experimental Test of Parity Conservation in Beta Decay. *Phys. Rev. Lett.*, 105:1413–1415.

Yang, C. N. and Mills, R. L. (1954). Conservation of isotopic spin and isotopic gauge invariance. *Phys. Rev.*, 96:191–195.

Zilberberg, O. et al. (2018). Photonic topological pumping through the edges of a dynamical four-dimensional quantum Hall system. *Nature*, 553:59–63.

Zyla, P. A. e. a. P. D. G. (2020). Review of Particle Physics (by Particle Data Group). *Progr. Theor. Exp. Phys.*, 083C01:1–2092.